

University of Windsor

Scholarship at UWindor

Electronic Theses and Dissertations

Theses, Dissertations, and Major Papers

2006

Nonlinear instabilities in photochemical oxidations of 1,4-cyclohexanedione and its derivatives.

Bei Zhao

University of Windsor

Follow this and additional works at: <https://scholar.uwindsor.ca/etd>

Recommended Citation

Zhao, Bei, "Nonlinear instabilities in photochemical oxidations of 1,4-cyclohexanedione and its derivatives." (2006). *Electronic Theses and Dissertations*. 2868.

<https://scholar.uwindsor.ca/etd/2868>

This online database contains the full-text of PhD dissertations and Masters' theses of University of Windsor students from 1954 forward. These documents are made available for personal study and research purposes only, in accordance with the Canadian Copyright Act and the Creative Commons license—CC BY-NC-ND (Attribution, Non-Commercial, No Derivative Works). Under this license, works must always be attributed to the copyright holder (original author), cannot be used for any commercial purposes, and may not be altered. Any other use would require the permission of the copyright holder. Students may inquire about withdrawing their dissertation and/or thesis from this database. For additional inquiries, please contact the repository administrator via email (scholarship@uwindsor.ca) or by telephone at 519-253-3000ext. 3208.

Nonlinear Instabilities in Photochemical Oxidations of
1,4-Cyclohexanedione and its derivatives

By

Bei Zhao

A Thesis

Submitted to the Faculty of Graduate Studies and Research
through the Department of Chemistry and Biochemistry
in Partial Fulfillment of the Requirements for
the Degree of Master of Science at the
University of Windsor

Windsor, Ontario, Canada
2006

© 2006 Bei Zhao



Library and
Archives Canada

Bibliothèque et
Archives Canada

Published Heritage
Branch

Direction du
Patrimoine de l'édition

395 Wellington Street
Ottawa ON K1A 0N4
Canada

395, rue Wellington
Ottawa ON K1A 0N4
Canada

Your file *Votre référence*
ISBN: 978-0-494-17120-2
Our file *Notre référence*
ISBN: 978-0-494-17120-2

NOTICE:

The author has granted a non-exclusive license allowing Library and Archives Canada to reproduce, publish, archive, preserve, conserve, communicate to the public by telecommunication or on the Internet, loan, distribute and sell theses worldwide, for commercial or non-commercial purposes, in microform, paper, electronic and/or any other formats.

The author retains copyright ownership and moral rights in this thesis. Neither the thesis nor substantial extracts from it may be printed or otherwise reproduced without the author's permission.

AVIS:

L'auteur a accordé une licence non exclusive permettant à la Bibliothèque et Archives Canada de reproduire, publier, archiver, sauvegarder, conserver, transmettre au public par télécommunication ou par l'Internet, prêter, distribuer et vendre des thèses partout dans le monde, à des fins commerciales ou autres, sur support microforme, papier, électronique et/ou autres formats.

L'auteur conserve la propriété du droit d'auteur et des droits moraux qui protègent cette thèse. Ni la thèse ni des extraits substantiels de celle-ci ne doivent être imprimés ou autrement reproduits sans son autorisation.

In compliance with the Canadian Privacy Act some supporting forms may have been removed from this thesis.

Conformément à la loi canadienne sur la protection de la vie privée, quelques formulaires secondaires ont été enlevés de cette thèse.

While these forms may be included in the document page count, their removal does not represent any loss of content from the thesis.

Bien que ces formulaires aient inclus dans la pagination, il n'y aura aucun contenu manquant.


Canada

Abstract

In the closed 1,4-cyclohexanedione(CHD) bromate oscillatory reaction, we discovered that stirring can induce transitions between simple and period-doubled oscillations. When illumination was employed to characterize the importance of microfluctuations of concentrations, the threshold stirring rate for inducing a bifurcation was found to increase proportionally to the intensity of the applied light. Numerical simulations with an existing model illustrate that the experimental phenomena could be qualitatively reproduced by considering effects of mixing on diffusion-limited radical reactions, namely, the disproportion reaction of hydroquinone radicals.

A novel light-mediated chemical oscillator, i.e. 1,4-benzoquinone(Q)-bromate oscillator, was uncovered and investigated systematically in a batch reactor. Dependence of the oscillatory dynamics on the intensity of illumination was characterized. Quenching experiments suggest that the bromate - 1,4-Q oscillator is not only Br^- controlled, but also radical-controlled. Oscillations were also investigated in a CSTR system. A mechanism was proposed, which successfully reproduced the experimental phenomena.

Acknowledgements

I would like to express my sincere appreciation to my supervisor Dr. Jichang Wang for his guidance and help on my studies and research during my graduate term at the University of Windsor. His scientific intelligence and attitude had a big influence on my academic training. I am deeply indebted to him for his great effort to support and encourage me, which will be remembered forever.

I would also like to express my gratitude to Dr. Aroca Ricardo and Dr. David Ting for being my committee members with all my heart.

I am also very grateful to our group members, Mr. Mohammad Harati and Ms. Nan Li for their help and advice and to faculty and staff in the department of Chemistry and Biochemistry for their support and kind help.

Especially, I would like to give my special thanks to my parents and my dear friends for their encouragement to enable me to complete this work.

Table of Contents

Abstract	III
Acknowledgements	IV
List of Tables	VII
List of Figures	VIII
Chapter 1. Introduction	1
1.1 A brief history	1
1.2 FKN mechanism and 1,4-cyclohexanedione-bromate reaction	2
1.3 External factors that influence the oscillatory dynamics.	7
1.4 Outlook of the study in chemical oscillatory system.	9
Chapter 2. Cooperative effects of stirring and illumination in the 1, 4-cyclohexanedione and bromate reaction	11
2.1 Introduction	11
2.2 Experimental procedure	12
2.3 Experimental results	14
2.4 Numerical simulations	33
2.5 Conclusions	41
Chapter 3. Nonlinear Phenomena in light-mediated 1, 4-Benzoquinone - bromate reaction	43

3.1 Introduction	43
3.2 Experimental procedure	45
3.3 Experimental Results in a closed system	53
3.3.1 Behavior at Different Compositions	53
3.3.2 The influence of $[\text{Br}^-]$	65
3.3.3 The study of a pulse-light perturbation	72
3.3.4 Perturbations with radical scavenger	78
3.3.5 Perturbations with Q	80
3.4 The study in an open system.	82
3.5 UV/Visible spectrophotometric measurements	86
3.6 H_2Q and H_2Q -Q-Bromate Oscillation	96
3.7 Simulations of the Q-Bromate Oscillations.	101
3.8 Conclusions	113
Chapter 4. Summary and Perspectives	116
Appendix	118
Reference	122
Vita Auctoris	127
Publications and Presentations (2003-2006)	128

List of Tables

Chapter 1. Introduction

Table 1.1 Abbreviated FKN Mechanism governing the BZ reaction.	3
Table 1.2 Abbreviated model for uncatalyzed 1,4-CHD-bromate reaction	6

Chapter 2. Cooperative effects of stirring and illumination in the 1,4-cyclohexanedione and bromate reaction

Table 2.1 Mechanistic model of the CHD-bromate-acid oscillatory system	36
---	----

Chapter 3. Nonlinear phenomena in light-mediated 1,4-benzoquinone - bromate reaction

Table 3.1 The light intensity correspondence between the control panel of the lamp and intensity measured by the optical photometer	51
Table 3.2 The peak number and amplitude of the oscillations at different wavelength.	76
Table 3.3 Mechanism of 1,4-Benzoquinone-bromate-acid photo oscillator	102
Table 3.4 Results summary of Figure 3.42	107

List of Figures

Chapter 1. Introduction

Figure 1.1 Mechanism of the formation of 1, 4-dihydroxybenzene. 5

Chapter 2. Cooperative effects of stirring and illumination in the 1, 4-cyclohexanedione and bromate reaction

Figure 2.1 A schematic illustration of the experimental set-up 14

Figure 2.2 Time series obtained under different stirring rates (a) 400 RPM and (b) 1200 RPM. Other reaction conditions are: $[\text{H}_2\text{SO}_4] = 0.9\text{M}$, $[\text{1,4-CHD}] = 0.06\text{M}$, and $[\text{BrO}_3^-] = 0.14\text{M}$. 15

Figure 2.3 Time series obtained under different stirring rates in one reaction process. The reaction conditions are: $[\text{H}_2\text{SO}_4] = 0.9\text{M}$, $[\text{1,4-CHD}] = 0.06\text{M}$, and $[\text{BrO}_3^-] = 0.14\text{M}$. 16

Figure 2.4 Time series obtained under different stirring rates (a) 400 RPM, (b) 600RPM and (c) 1000 RPM. Other reaction conditions are: $[\text{H}_2\text{SO}_4] = 0.9\text{M}$, $[\text{1,4-CHD}] = 0.06\text{M}$, $[\text{BrO}_3^-] = 0.15\text{M}$, and $[\text{H}_2\text{Q}] = 0.03\text{M}$. The total volume of the solution is 41 ml, which reduced the free surface to minimum. 17

Figure 2.5 Time series obtained under the protection of different inert gases (a) N₂ and (b) Ar. Other reaction conditions are: [H₂SO₄] = 0.9M, [1,4-CHD] = 0.03M, and [BrO₃⁻] = 0.14M, [H₂Q]=0.01M. The stirring rate is 400 RPM protected by argon or N₂ at the flow rate of 1.0 ml/min. 18

Figure 2.6 Time series showing the dependence of oscillation pattern on different stirring rates. Reaction conditions are [H₂SO₄] = 0.9M, [1,4-CHD] = 0.06M, [H₂Q] = 0.03M and [BrO₃⁻] = 0.14M. 20

Figure 2.7 Time series showing the dependence of oscillation pattern on stirring rates. (a) 500 RPM, (b) 700RPM and (c) 800 RPM. Other reaction conditions are [H₂SO₄] = 0.9M, [1,4-CHD] = 0.06M, [H₂Q] = 0.03M and [BrO₃⁻] = 0.14M. 21

Figure 2.8 Time series obtained under different stirring rates in one reaction (a) [H₂Q] = 0.01M, (b) [H₂Q] = 0.02M, (c) [H₂Q] = 0.03M Other reaction conditions are: [H₂SO₄] = 0.9M, [1,4-CHD] = 0.03M, and [BrO₃⁻] = 0.14M. Protected by Argon at the flow rate of 1.0 ml/min. 23

Figure 2.9 Time series obtained under different stirring rates (a) 100 RPM, (b) 400RPM and (c)800 RPM. Other reaction conditions are: [H₂SO₄] = 0.9M, [1,4-CHD] = 0.03M, and [BrO₃⁻] = 0.14M, [H₂Q] = 0.01M. Protected by argon at the flow rate of 1.0 ml/min. 24

Figure 2.10 Effects of stirring on the reaction behavior in the presence of

illumination, in which the intensity of the applied light is $I_1 = 25\text{mW/cm}^2$, $I_2 = 10\text{mW/cm}^2$, and $I_3 = 35\text{mW/cm}^2$. Other reaction conditions are $[\text{H}_2\text{SO}_4] = 0.9\text{M}$, $[\text{1,4-CHD}] = 0.06\text{M}$, $[\text{H}_2\text{Q}] = 0.03\text{M}$ and $[\text{BrO}_3^-] = 0.14\text{M}$. 25

Figure 2.11 Effects of stirring on the reaction behavior in the presence of illumination, in which the intensity of the applied light is $I_1 = 35\text{mW/cm}^2$ and $I_2 = 50\text{mW/cm}^2$ using protocol 1. Other reaction conditions are $[\text{H}_2\text{SO}_4] = 0.9\text{M}$, $[\text{1,4-CHD}] = 0.06\text{M}$, $[\text{H}_2\text{Q}] = 0.03\text{M}$ and $[\text{BrO}_3^-] = 0.14\text{M}$. 27

Figure 2.12 Effects of illumination on the reaction behavior under the constant stirring rate, in which the intensity of the applied light is $I_1 = 30\text{mW/cm}^2$ and $I_2 = 40\text{mW/cm}^2$, $I_3 = 50\text{mW/cm}^2$ using protocol 1. Other reaction conditions are $[\text{H}_2\text{SO}_4] = 0.9\text{M}$, $[\text{1,4-CHD}] = 0.06\text{M}$, $[\text{H}_2\text{Q}] = 0.03\text{M}$ and $[\text{BrO}_3^-] = 0.14\text{M}$. The stirring rate is 400RPM. 29

Figure 2.13 Effects of illumination with a single fiber or dual fibers. Other reaction conditions are $[\text{H}_2\text{SO}_4] = 0.9\text{M}$, $[\text{1,4-CHD}] = 0.06\text{M}$, $[\text{H}_2\text{Q}] = 0.03\text{M}$ and $[\text{BrO}_3^-] = 0.14\text{M}$. The stirring rate is 800 RPM. 29

Figure 2.14 Summary of the minimum light intensity requested to revive the oscillation in the reaction of Figure 2.13. 31

Figure 2.15 Effects of stirring on the reaction behavior in the presence of illumination, using protocol 1. Other reaction conditions are $[\text{H}_2\text{SO}_4] = 0.9\text{M}$, $[\text{1,4-CHD}] = 0.03\text{M}$, $[\text{H}_2\text{Q}] = 0.03\text{M}$ and $[\text{BrO}_3^-] = 0.14\text{M}$. A Br^- selective

electrode is used in this measurement.

31

Figure 2.16 Stirring sensitivity of the 1,4-CHD-bromate reaction investigated by (a) a small Pt electrode and (b) a gold electrode. Other reaction conditions are $[\text{H}_2\text{SO}_4] = 0.9\text{M}$, $[\text{1,4-CHD}] = 0.06\text{M}$, $[\text{H}_2\text{Q}] = 0.03\text{M}$ and $[\text{BrO}_3^-] = 0.14\text{M}$.

33

Figure 2.17 Simulated time series of the 1,4-CHD-Bromate Acid Reaction.

(a) and (b), $[\text{BrCHD}]_0 = 1 \times 10^{-8} \text{ M}$; (c) and (d) $[\text{BrCHD}]_0 = 0.01 \text{ M}$. Other reaction conditions are $[\text{H}_2\text{SO}_4] = 0.9\text{M}$, $[\text{1,4-CHD}] = 0.06\text{M}$, and $[\text{BrO}_3^-] = 0.14\text{M}$.

37

Figure 2.18 Stirring sensitivity of the 1,4-CHD-bromate reaction calculated with the model listed in Table 2.1. Different stirrings correspond to the following values of k_{10} , stir1: $k_{10} = 8.8 \times 10^8 \text{ M}^{-1}\text{s}^{-1}$; stir2: $k_{10} = 2.0 \times 10^{11} \text{ M}^{-1}\text{s}^{-1}$; and stir3: $k_{10} = 2.0 \times 10^{12} \text{ M}^{-1}\text{s}^{-1}$. Other reaction conditions are $[\text{H}_2\text{SO}_4] = 0.9\text{M}$, $[\text{1,4-CHD}] = 0.06\text{M}$, $[\text{H}_2\text{Q}] = 0.03\text{M}$ and $[\text{BrO}_3^-] = 0.14\text{M}$.

39

Figure 2.19 Cooperative effects of stirring and illumination in the 1,4-CHD-bromate reaction calculated from the model listed in table 1 and reaction R20 listed in context. Other reaction conditions are $[\text{H}_2\text{SO}_4] = 0.9\text{M}$, $[\text{1,4-CHD}] = 0.06\text{M}$, $[\text{H}_2\text{Q}] = 0.03\text{M}$ and $[\text{BrO}_3^-] = 0.14\text{M}$. Rate constants in the three time series are: (a) $k_{10} = 6 \times 10^{11} \text{ M}^{-1}\text{s}^{-1}$, $k_{20} = 6 \times 10^{-7} \text{ M}^{-1}\text{s}^{-1}$; (b) $k_{10} = 2 \times 10^{12} \text{ M}^{-1}\text{s}^{-1}$, $k_{20} = 6 \times 10^{-7} \text{ M}^{-1}\text{s}^{-1}$; and (c) $k_{10} = 2 \times 10^{12} \text{ M}^{-1}\text{s}^{-1}$, $k_{20} = 2 \times 10^{-6}$

XI

$M^{-1}s^{-1}$. 40

Figure 2.20 Simulation of photo effects on spontaneous oscillations. Other reaction conditions are $[H_2SO_4] = 0.9M$, $[1,4-CHD] = 0.06M$, $[H_2Q] = 0.03M$ and $[BrO_3^-] = 0.14M$. $k_{10} = 8.8 \times 10^8 M^{-1}s^{-1}$, light off corresponds to $k_{20} = 0$ and light on corresponds to $k_{20} = 3.1 \times 10^{-6} M^{-1}$. 41

Chapter 3. Nonlinear Phenomena in light-mediated 1,4-benzoquinone-bromate reaction

Figure 3.1 Equipment setup of batch reactor 46

Figure 3.2 Equipment setup of UV-Visible spectrophotometer 47

Figure 3.3 Equipment set up for study with CSTR method. 48

Figure 3.4 The spectrum of the halogen light source measure by UV- Visible spectrophotometer. (a) When light intensity is $30\%I_0$, (b) When the light intensity is $45\%I_0$, (c) When the light intensity is $60\%I_0$. 49

Figure 3.5 The relationship of the percentage tuner and the light intensity. (a) from a single fiber through double layer glass filled with water, (b) from the light bulb 3cm away through double layer water circulating glass. (c) The scheme of the control panel of the halogen lamp. 52

Figure 3.6 Reaction behavior at different illumination intensity, (a) $100\%I_0$, (b) $90\%I_0$, (c) $80\%I_0$, (d) $75\%I_0$ and (e) $0\%I_0$. The other conditions are: $[Q]$

= 0.02M, $[\text{H}_2\text{SO}_4] = 1.8\text{M}$, $[\text{NaBrO}_3] = 0.05\text{M}$, total volume of the reaction is 30ml, stirring rate 700 RPM, N_2 protection and $T = 25^\circ\text{C}$. 54

Figure 3.7 The potential curve at the beginning of the reaction in a batch reactor under the condition of $[\text{Q}] = 0.02\text{M}$, $[\text{H}_2\text{SO}_4] = 1.8\text{M}$, $[\text{NaBrO}_3] = 0.05\text{M}$, total volume of the reaction is 30ml, stirring rate 700 RPM, N_2 protection, $T = 25^\circ\text{C}$, light intensity 100% I_0 . 55

Figure 3.8 Comparison of oscillations at different light intensities. (a) 90% I_0 , (b) 100% I_0 . The other reaction conditions are $[\text{Q}] = 0.02\text{M}$, $[\text{H}_2\text{SO}_4] = 1.8\text{M}$, $[\text{NaBrO}_3] = 0.05\text{M}$, total volume 30ml, stirring rate 700 RPM, N_2 protection and $T = 15^\circ\text{C}$. 56

Figure 3.9 Time series obtained at different light intensity. (a) 100% I_0 , (b) 75% I_0 , (c) 50% I_0 , Reaction conditions are $[\text{Q}] = 0.02\text{M}$, $[\text{H}_2\text{SO}_4] = 1.8\text{M}$, $[\text{NaBrO}_3] = 0.03\text{M}$, total volume 30ml, stirring rate 700 RPM, N_2 protection and $T = 25^\circ\text{C}$. 57

Figure 3.10 Changes of the oscillation behavior with respect to varying the concentration of H_2SO_4 : (a) 1.0M, (b) 1.4M, (c) 1.8M, (d) 1.9M. The other conditions are $[\text{Q}] = 0.02\text{M}$, $[\text{NaBrO}_3] = 0.05\text{M}$, total volume 30ml, stirring rate 700 RPM, N_2 protection and $T = 25^\circ\text{C}$ 58

Figure 3.11 Oscillatory behavior under different concentrations of Q: (a) 0.015M, (b) 0.02M, (c) 0.025M, (d) 0.03M. The other reaction conditions

are $[\text{H}_2\text{SO}_4] = 1.8\text{M}$, $[\text{NaBrO}_3] = 0.05\text{M}$, total volume 30ml, stirring rate 700 RPM, N_2 protection and $T = 25^\circ\text{C}$. 59

Figure 3.12 Changes of oscillation behavior with respect to varying the concentration of $[\text{NaBrO}_3]$: (a) 0.03M, (b) 0.04M, (c) 0.05M, (d) 0.06M, Other reaction conditions are $[\text{Q}] = 0.02\text{M}$, $[\text{H}_2\text{SO}_4] = 1.8\text{M}$, 100% I_0 total volume 30ml, stirring rate 700 RPM, N_2 protection and $T = 25^\circ\text{C}$. 60

Figure 3.13 Changes of Oscillation behavior with respect to varying the temperature. (a) 10°C , (b) 15°C , (c) 20°C , (d) 25°C , (e) 30°C . Other conditions are $[\text{Q}] = 0.02\text{M}$, $[\text{H}_2\text{SO}_4] = 1.8\text{M}$, $[\text{NaBrO}_3] = 0.05\text{M}$, 100% I_0 total volume 30ml, stirring rate 700 RPM, N_2 protection. 61

Figure 3.14 Oscillations at different volume of solution. (a) 44ml, (b) 30ml, (c) 20ml, (d) 10ml. Other reaction conditions are $[\text{Q}] = 0.02\text{M}$, $[\text{H}_2\text{SO}_4] = 1.8\text{M}$, $[\text{NaBrO}_3] = 0.05\text{M}$, 100% I_0 , stirring rate 700 RPM, N_2 protection and $T = 25^\circ\text{C}$. 62

Figure 3.15 The influence of N_2 /Air purging on the reaction behavior. (a) air bubbling 1.0 Reaction conditions are $[\text{Q}] = 0.02\text{M}$, $[\text{H}_2\text{SO}_4] = 1.8\text{M}$, $[\text{NaBrO}_3] = 0.05\text{M}$, 100% I_0 , total volume 30ml, stirring rate 700 RPM, N_2 or Air, $T = 20^\circ\text{C}$. 64

Figure 3.16 The influence of stirring on the oscillations. (a) 700rpm, (b) 500rpm and (c) 300rpm. Reaction conditions are $[\text{Q}] = 0.02\text{M}$, $[\text{H}_2\text{SO}_4] =$

1.8M, $[\text{NaBrO}_3] = 0.05\text{M}$, 100% I_0 , total volume 30ml, stirring rate 700 RPM, N_2 protection and $T = 25^\circ\text{C}$. 65

Figure 3.17 Oscillations monitored simultaneously by Pt electrode (a) and by Br^- selective electrode (b). Reaction conditions are $[\text{Q}] = 0.02\text{M}$, $[\text{H}_2\text{SO}_4] = 1.8\text{M}$, $[\text{NaBrO}_3] = 0.05\text{M}$, 100% I_0 , stirring rate 700 RPM, N_2 protection and $T = 25^\circ\text{C}$. 66

Figure 3.18 Reaction behavior in the presence of different concentrations of Br_2 initially. (a) $[\text{Br}_2] = 0.001\text{M}$, induction time 11266s, (b) $[\text{Br}_2] = 0.005\text{M}$, induction time 14217s, (c) $[\text{Br}_2] = 0.01\text{M}$, induction time 20334s, (d) $[\text{Br}_2] = 0.001\text{M}$, extra $[\text{Q}] = 0.002\text{M}$, induction time 11197s, (e) $[\text{Br}_2] = 0.005\text{M}$, extra $[\text{Q}] = 0.01\text{M}$, induction time 12763s. Other reaction conditions are $[\text{Q}] = 0.02\text{M}$, $[\text{H}_2\text{SO}_4] = 1.8\text{M}$, $[\text{NaBrO}_3] = 0.05\text{M}$, 100% I_0 , stirring rate 700 RPM, N_2 protection and $T = 25^\circ\text{C}$. 68

Figure 3.19 The study of influence of adding malonic acid (a) $[\text{MA}] = 0.01\text{M}$, (b) $[\text{MA}] = 0.02\text{M}$, (c) $[\text{MA}] = 0.05\text{M}$, (d) $[\text{MA}] = 0.06\text{M}$. Other reaction conditions are $[\text{Q}] = 0.02\text{M}$, $[\text{H}_2\text{SO}_4] = 1.8\text{M}$, $[\text{NaBrO}_3] = 0.05\text{M}$, 100% I_0 , stirring rate 700 RPM, N_2 protection and $T = 25^\circ\text{C}$. 69

Figure 3.20 Perturbation study by adding Br^- at different phase angles using a syringe (Hamilton 25 μL); the first three perturbations are the addition of 2 μL 0.01M NaBr each time; the last three perturbations are 4 μL 0.001M

NaBr each time, (a) monitored by Pt electrode, (b) monitored by Br selective electrode. The reaction conditions are $[Q] = 0.02\text{M}$, $[\text{H}_2\text{SO}_4] = 1.8\text{M}$, $[\text{NaBrO}_3] = 0.05\text{M}$, $100\%I_0$, stirring rate 700 RPM, and $T = 25^\circ\text{C}$. 71

Figure 3.21 Perturbation study by adding (a) 10 μL and (b) 25 μL 0.01M NaBr at different phase angles at the condition of $[Q] = 0.02\text{M}$, $[\text{H}_2\text{SO}_4] = 1.8\text{M}$, $[\text{NaBrO}_3] = 0.05\text{M}$, $100\%I_0$, stirring rate 700 RPM, and $T = 25^\circ\text{C}$. 72

Figure 3.22 Oscillation is revived by reducing light intensity at the end of the oscillation window. Reaction conditions are $[Q] = 0.02\text{M}$, $[\text{H}_2\text{SO}_4] = 1.8\text{M}$, $[\text{NaBrO}_3] = 0.05\text{M}$, $100\%I_0$, total volume 30ml, stirring rate 700 RPM, and $T = 25^\circ\text{C}$. 73

Figure 3.23 Oscillations under different light intensities. Other reaction conditions are $[Q] = 0.02\text{M}$, $[\text{H}_2\text{SO}_4] = 1.8\text{M}$, $[\text{NaBrO}_3] = 0.05\text{M}$, $100\%I_0$, total volume 30ml, stirring rate 700 RPM, and $T = 25^\circ\text{C}$. 74

Figure 3.24 Oscillation with additional illumination at different wavelength range (a) using four light fibers to illuminate. The illumination for others are using two light fibers illuminate directly and another two fiber filtered with a narrow band filter which allows the light to pass through at the wavelength of: (b) 400nm, (c) 450nm, (d) 500nm, (e) 550nm, (f) 600nm, (g) 650nm. Other reaction conditions are $[Q] = 0.02\text{M}$, $[\text{H}_2\text{SO}_4] = 1.8\text{M}$, $[\text{NaBrO}_3] = 0.05\text{M}$, $100\%I_0$, total volume 30ml, stirring rate 700 rpm, and $T = 25^\circ\text{C}$. 75

Figure 3.25 Results analysis for Figure 3.24. (a) The relation of the number of peak vs the central wavelength of the band filters. (b) The relation of the amplitude vs the central wavelength of the narrow band filters. (c) The relation of the amplitude vs the peak number. (d) The relation of amplitude/peak number vs the wavelength of the narrow band filters. 76

Figure 3.26 Response of the reaction behavior to the addition of 1%(V/V) ethanol. monitored by Pt electrode, Reaction conditions are $[Q] = 0.02M$, $[H_2SO_4] = 1.8M$, $[NaBrO_3] = 0.05M$, $100\%I_0$, total volume 30ml, stirring rate 700 RPM, and $T = 25^\circ C$. 79

Figure 3.27 Different reaction behaviors with the different addition of 1%(V/V) ethanol at the beginning.(a) 10uL, (b) 25uL, (c) 75uL. Other reaction conditions are $[Q] = 0.02M$, $[H_2SO_4] = 1.8M$, $[NaBrO_3] = 0.05M$, $100\%I_0$, total volume 30ml, stirring rate 700 RPM, and $T=25^\circ C$. 80

Figure 3.28 The response of the oscillatory system to the addition of Q. The reaction conditions are $[Q] = 0.02M$, $[H_2SO_4] = 1.8M$, $[NaBrO_3] = 0.05M$, $100\%I_0$, total volume 30ml, stirring rate 700 RPM, and $T = 25^\circ C$. 81

Figure 3.29 CSTR study of 1,4-benzoquinone-bromate-acid photo chemical oscillatory system at the condition of $[Q] = 0.02M$, $[H_2SO_4] = 1.8M$, $[NaBrO_3] = 0.05M$, $100\%I_0$, stirring rate 700RPM, $T = 25^\circ C$, flow rate 30uL/min. (a) Time series plotted over extended time period.(b) Time series

within a short time frame.

83

Figure 3.30 CSTR study of 1,4-Benzoquinone-bromate-acid photo chemical Oscillatory System at different flow rates. (a) 20uL/min, the average amplitude is 35mV, (b) 16uL/min, the average amplitude is 30mV, (c) 14uL/min. Other reaction conditions are $[Q] = 0.02M$, $[H_2SO_4] = 1.8M$, $[NaBrO_3] = 0.05M$, $100\%I_0$, stirring rate 700RPM, $T = 25^\circ C$.

84

Figure 3.31 Light perturbation in a CSTR at the condition of $[Q] = 0.02M$, $[H_2SO_4] = 1.8M$, $[NaBrO_3] = 0.05M$, $100\%I_0$, stirring rate 700RPM, $T = 25^\circ C$, and flow rate 30uL/min.

85

Figure 3.32 Br^- perturbation in a CSTR at the condition of $[Q] = 0.02M$, $[H_2SO_4] = 1.8M$, $[NaBrO_3] = 0.05M$, $100\%I_0$, stirring rate 700RPM, $T = 25^\circ C$, flow rate 30uL/min. (a) monitored by Pt electrode, (b) monitored by Br^- selective electrode.

86

Figure 3.33 UV-visible Spectra of diluted solution of Q and H_2Q . (a) UV-visible of spectra of Q and H_2Q at $1 \times 10^{-4}M$, (b) The comparison of the spectra plot of Q at the concentration of $1 \times 10^{-4}M$ and approximately $2 \times 10^{-5}M$, (c) The comparison of the spectra plot of H_2Q at the concentration of $1 \times 10^{-4}M$ and approximately $2 \times 10^{-5}M$.

87

Figure 3.34 UV-visible Spectra of (a) mixed solution of 0.02M H_2Q and 1.8M H_2SO_4 , (b) mixed solution of 0.02M Q and 1.8M H_2SO_4 .

90

Figure 3.35 UV-visible spectra collected at different reaction time. (a) $t = 0s$, (b) $t = 727s$, (c) $t = 3245s$, (d) $t = 5502s$, (e) the comparison of above spectrums. (f) The fast reaction at the beginning. The reaction conditions are $[Q] = 0.02M$, $[H_2SO_4] = 1.8M$, $[NaBrO_3] = 0.05M$, illumination method using Protocol C, $100\%I_0$, stirring rate 700RPM, $T = 23^\circ C$. 92

Figure 3.36 Time series of the Q-bromate oscillation monitored by UV-visible spectrophotometer at different wavelength. (a) Time series at the 289nm, 312nm, 360nm, 428nm, (b) The zoom-in window of the oscillation at 312nm and 360nm. The reaction conditions are $[Q] = 0.02M$, $[H_2SO_4] = 1.8M$, $[NaBrO_3] = 0.05M$, illumination method using Protocol C, $100\%I_0$, stirring rate 700RPM, $T = 23^\circ C$. 95

Figure 3.37 Time series H_2Q -bromate Oscillation. The reaction conditions are $[H_2Q] = 0.02M$, $[NaBrO_3] = 0.05M$, $[H_2SO_4] = 1.8M$, Light $100\%I_0$, stirring rate 700RPM, and $T = 25^\circ C$. 96

Figure 3.38 Time series of H_2Q -bromate system at different concentration of H_2SO_4 . (a) $[H_2SO_4] = 0.1M$, (b) $[H_2SO_4] = 0.2M$, (c) $[H_2SO_4] = 0.3M$, (d) $[H_2SO_4] = 0.5M$. Other reaction conditions are $[H_2Q] = 0.005M$, $[NaBrO_3] = 0.06M$, Light $100\%I_0$, stirring rate 700RPM, and $T = 25^\circ C$. 98

Figure 3.39 Time series of the H_2Q -Q-bromate system with different light illumination. (a) $0\%I_0$, (b) $40\%I_0$, (c) $60\%I_0$, (d) $75\%I_0$, (e) $100\%I_0$ Other

reaction conditions are $[\text{H}_2\text{Q}] = 0.005\text{M}$, $[\text{Q}] = 0.01\text{M}$, $[\text{NaBrO}_3] = 0.06\text{M}$, $[\text{H}_2\text{SO}_4] = 0.1\text{M}$, Light $100\%I_0$, stirring rate 700RPM, and $T = 25^\circ\text{C}$. 100

Figure 3.40 Time series of H_2Q -bromate and Q -bromate reaction system. (a) $[\text{H}_2\text{Q}] = 0.015\text{M}$, (b) $[\text{Q}] = 0.015\text{M}$. Other reaction conditions are $[\text{H}_2\text{SO}_4] = 0.1\text{M}$, $[\text{NaBrO}_3] = 0.06\text{M}$, Light $75\%I_0$, stirring rate 700RPM, and $T = 25^\circ\text{C}$.

101

Figure 3.41 Simulations of Q -bromate photochemical oscillator in terms of (a) $[\text{QBr}]$ (b) $[\text{Br}^-]$, and (c) $[\text{Br}^-]$ with additional 0.005M QBr . Other concentrations are $[\text{Q}] = 0.02\text{M}$, $[\text{H}_2\text{SO}_4] = 1.8\text{M}$, $[\text{NaBrO}_3] = 0.05\text{M}$. The rate constant $k_{13} = 2.2 \times 10^{-4} \text{M}^{-1}\text{s}^{-1}$. 104

Figure 3.42 Simulation of Q -bromate oscillation under different light intensity. (a) $[\text{Q}]$ at $k_{13} = 1.0 \times 10^{-5} \text{M}^{-1}\text{s}^{-1}$, (b) $[\text{Br}^-]$ at $k_{13} = 1.0 \times 10^{-5} \text{M}^{-1}\text{s}^{-1}$, (c) $[\text{Br}^-]$ at $k_{13} = 9.0 \times 10^{-5} \text{M}^{-1}\text{s}^{-1}$, (d) $[\text{Br}^-]$ at $k_{13} = 1.5 \times 10^{-4} \text{M}^{-1}\text{s}^{-1}$, (e) $[\text{Br}^-]$ at $k_{13} = 2.2 \times 10^{-4} \text{M}^{-1}\text{s}^{-1}$, (f) $[\text{Br}^-]$ at $k_{13} = 3.2 \times 10^{-4} \text{M}^{-1}\text{s}^{-1}$. The reaction conditions are $[\text{Q}] = 0.02\text{M}$, $[\text{H}_2\text{SO}_4] = 1.8\text{M}$, $[\text{NaBrO}_3] = 0.05\text{M}$. 106

Figure 3.43 Simulation of Br^- perturbation in the Q -bromate oscillation. (a) $[\text{Br}^-] = 3 \times 10^{-4}\text{M}$, (b) $[\text{Br}^-] = 5 \times 10^{-4}\text{M}$. The reaction conditions are $[\text{Q}] = 0.02\text{M}$, $[\text{H}_2\text{SO}_4] = 1.8\text{M}$, $[\text{NaBrO}_3] = 0.05\text{M}$. 108

Figure 3.44 Simulation of the oscillation revival with the addition of Q at

the end of the oscillation. The reaction conditions are $[Q] = 0.02\text{M}$, $[\text{H}_2\text{SO}_4] = 1.8\text{M}$, $[\text{NaBrO}_3] = 0.05\text{M}$. 109

Figure 3.45 Simulation of ethanol perturbation by controlling the reaction $R14 \text{BrO}_2^* \rightarrow \text{final product}$ and $R15 \text{HQ}^* \rightarrow \text{final product}$, (a) $k_{14} = 30 \text{ M}^{-1}\text{s}^{-1}$, (b) $k_{14} = 70 \text{ M}^{-1}\text{s}^{-1}$, (c) $k_{15} = 1 \times 10^5 \text{ M}^{-1}\text{s}^{-1}$, (d) $k_{15} = 1 \times 10^6 \text{ M}^{-1}\text{s}^{-1}$. 110

Figure 3.46 Simulations of Q-bromate oscillation under different $[\text{H}_2\text{SO}_4]$ (a) 2.0M, (b) 1.8M, (c) 1.6M, (d) 1.4M. The other reaction conditions are $[Q] = 0.02\text{M}$, $[\text{NaBrO}_3] = 0.05\text{M}$. 111

Figure 3.47 Simulation of Q-bromate oscillation under different $[\text{NaBrO}_3]$ (a) 0.06M, (b) 0.05M, (c) 0.04M, (d) 0.03M. The other reaction conditions are $[Q] = 0.02\text{M}$, $[\text{H}_2\text{SO}_4] = 1.8\text{M}$. 113

Chapter 1. Introduction

1.1 A brief history

Oscillatory behaviors are ubiquitous in nature, such as circadian rhythms, heart beat and neural oscillators. Understanding the onset of oscillations has caught great attention in the potential application in biology, engineering, and physics. Concentrating on chemical systems, the first report of an oscillatory chemical reaction was published in 1828, in which Fechner described the potential oscillation generated by an iron electrode in a weak acidic solution.¹ In 1899 Ostwald observed that the rate of chromium dissolution in acid periodically increased and decreased.² The above two oscillatory systems are inhomogeneous. The first homogeneous isothermal chemical oscillator was the reaction of iodine and hydrogen peroxide which was reported as early as in 1921 by Bray et al.³ However, chemical oscillations were considered to be impossible since scientists thought it conflicted with the second law of thermodynamics.^{4,5}

The Belousov-Zhabotinsky reaction, which has become one of the most extensively studied chemical oscillators, was discovered in 1950s. It was not well accepted until the early 1970s, which also indicates the beginning of modern nonlinear chemical dynamics. Field, Noyes and Körös developed the FKN mechanism to qualitatively characterize the behavior of the BZ reaction.⁶

1.2 FKN mechanism and 1,4-cyclohexanedione-bromate Reaction

The BZ reaction is a chemical oscillator which has been most extensively studied in both homogenous isothermal aqueous systems and in reaction-diffusion media. A typical initial composition for the BZ reaction in a well-stirred batch reactor could be: Malonic Acid, sodium bromate, ammonium ceric nitrate, sulphate acid at 20°C and with 1-2ml of 0.025M ferrion as indicator. After a short induction period, the reaction enters its oscillatory phase, where color changes between red and blue periodically. There are corresponding oscillations in the potential of a platinum electrode and a bromide ion selective electrode.⁷

The mechanism of the BZ reaction is rather complicated: a recent improved model for the Ce(IV)/Ce(III)-catalyzed reaction contains 80 elementary steps and 26 variable species concentrations. The skeleton FKN mechanism which contains the most important parts of the kinetic mechanism is presented in Table 1.1.

Table 1.1 Abbreviated FKN Mechanism governing the BZ reaction.

No.	Elementary steps
<i>R1</i>	$Br^- + HOBr + H^+ \leftrightarrow Br_2 + H_2O$
<i>R2</i>	$HBrO_2 + Br^- + H^+ \leftrightarrow 2HOBr$
<i>R3</i>	$Br^- + BrO_3^- + 2H^+ \leftrightarrow HOBr + HBrO_2$
<i>Process A</i>	$BrO_3^- + 2Br^- + 3H^+ \rightarrow 3HOBr$
<i>R4</i>	$2HBrO_2 \leftrightarrow BrO_3^- + HOBr + H^+$
<i>R5</i>	$BrO_3^- + HBrO_2 + H^+ \leftrightarrow 2BrO_2^* + H_2O$
<i>R6</i>	$BrO_2^* + M_{red} + H^+ \leftrightarrow HBrO_2 + M_{ox}$
<i>Process B</i>	$BrO_3^- + HBrO_2 + 2M_{red} + 3H^+ \rightarrow 2HBrO_2 + 2M_{ox} + H_2O$
<i>R7</i>	$MA + Br_2 \rightarrow BrMA + Br^- + H^+$
<i>R8</i>	$2M_{ox} + MA + BrMA \rightarrow fBr^- + 2M_{red} + other\ products$
<i>Process C</i>	$2M_{ox} + MA + BrMA \rightarrow fBr^- + 2M_{red} + other\ products$

Process A is obtained from (R3) + (R2) +3(R1). It removes bromide ions in the process by reducing bromate to bromine. As the concentration of bromide ion decreases, the rates of R2 and R3 slow down. After the concentration of bromide falls below some critical level $[Br^-]_{cr}$, the intermediate $HBrO_2$ can begin to compete with bromide as a reducing agent for bromate, which initiates process B. R₅ produces two molecules of the radical species BrO_2^* which react rapidly via R₆ returning to $HBrO_2$ and oxidizing the

catalyst. From the total stoichiometric equation of Process B, one molecule HBrO_2 leads to the production of two molecules of HBrO_2 , thus the rate of increase of $[\text{HBrO}_2]$ becomes proportional to its own concentration. This is an autocatalytic reaction step, which is the core of nonlinear dynamics. The autocatalytic process is further limited by R4, the self-disproportionation reaction involving HBrO_2 . Process C resets the conditions by reducing the catalyst formed from Processes A and B and by producing bromide ion. When the concentration of bromide ion reaches a high level, Process B is inhibited. Therefore, the concentration of bromide ion is a key factor to drive process A and B to cycle back and forth.^{4,6,7}

This control effect of bromide ion in the BZ system has been confirmed by, for example, experiments conducted by Noszticzius and coworkers.⁸ They observed the lengthening of induction time with the addition of bromide ion initially. Peter Ruoff performed a series of experiments by perturbing the BZ system with the solution of KBr , AgNO_3 and HOBr and found that the phase shift observed in the experiments agreed well with the mechanism based on the bromide-control assumption.⁹

In addition, Forsterling, Venkataraman and Sorensen also observed significant influence of radicals in the BZ system, in which the presence of oxygen, a radical scavenger to malonyl radicals could quench the oscillation.¹⁰

Despite that the BZ media have been extensively studied to gain insight into pattern formation, the production of carbon dioxide will potentially affect the formation of chemical waves if the reaction time is too long. Because of this disadvantage, another

oscillator, 1,4-cyclohexanedione(CHD)-bromate reaction which was uncovered in the early 1980s, has attracted increasing attention in the last decade.¹¹⁻²⁰

The uncatalyzed 1,4-CHD-bromate oscillation was first reported by Farage and Janjic in 1982.^{11,12} With the presence of ferrion as indicator, it was soon applied in the study of chemical waves in reaction-diffusion media.^{14,15} The detailed mechanisms of the uncatalyzed and ferrion-catalyzed system were promoted by Szalai and Körös on the basis of spectrophotometric studies.^{16,17} The simulation agrees with the experimental results very well. The mechanism is demonstrated in Figure 1.1, which suggests that 1,4-CHD in its reaction with acidic bromate undergoes aromatization and one of its main product 1,4-dihydroxybenzene(H₂Q) is further oxidized and brominated to 1,4-benzoquinone and bromoorganics. They pointed out that the oscillatory behavior can be attributed to H₂Q which was generated continuously. A simplified three viable model for the uncatalyzed 1,4-CHD-bromate reaction is listed in Table 1.2.

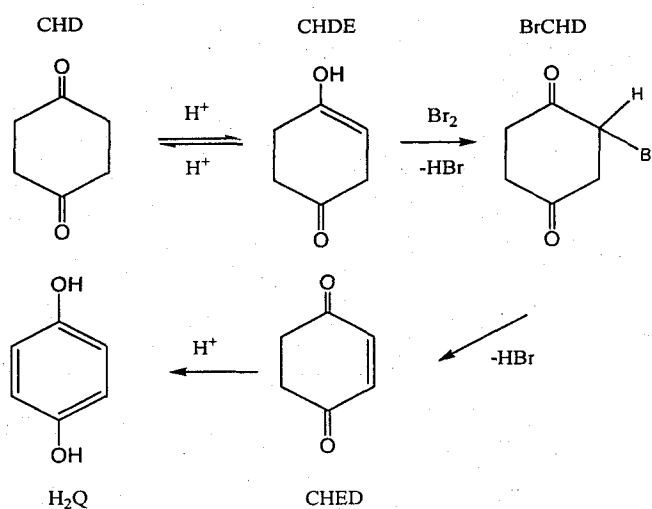


Figure 1.1 Mechanism of the formation of 1,4-dihydroxybenzene.¹⁷

Table 1.2 Abbreviated model for the uncatalyzed 1,4-CHD-bromate reaction¹⁷

No.	Elementary steps
<i>M1</i>	$Br^- + HBrO_2 + H^+ \rightarrow 2HOBr$
<i>M2</i>	$Br^- + BrO_3^- + 2H^+ \rightarrow HOBr + HBrO_2$
<i>M3</i>	$2HBrO_2 \rightarrow HOBr + BrO_3^- + H^+$
<i>M4</i>	$HBrO_2 + H_2Q + BrO_3^- + H^+ \rightarrow 2HOBr_2 + Q + H_2O$
<i>M5</i>	$BrCHD \rightarrow CHED + Br^- + H^+$
<i>M6</i>	$CHED + H^+ \rightarrow H_2Q + H^+$
<i>M7</i>	$H_2Q + BrO_3^- + H^+ \rightarrow Q + HBrO_2 + H_2O$

According to the mechanism in Table 1.2, the rate of Br^- production is faster than the rate of H_2Q production, thus bromide ion reach the high steady-state concentration rapidly and wins the competition for $HBrO_2$ (M1) over H_2Q (M4), which results in the slow accumulation of H_2Q . When H_2Q is accumulated high enough to a threshold value while $[Br^-]$ drops below the critical value, the autocatalytic reaction M4 is triggered; however, after that, the concentration of H_2Q rapidly decreases. When $[H_2Q]$ drops below a critical level, the autocatalytic step M4 is terminated. At the same time, M1 and M3 slowly consume $HBrO_2$ and reset the condition back. M5 and M6 reproduce bromide ion and H_2Q to make the oscillation continues. Therefore, both bromide ion and H_2Q are critical for the control of the oscillation.

1.3. External factors that influence the oscillatory dynamics.

Besides internal concentration fluctuations of the species in the reaction system, external factors such as the presence of oxygen, mechanical stirring, temperature and light illumination could sometimes significantly affect the oscillatory behavior. Therefore these parameters could be applied to control the oscillation dynamics.

In the BZ reaction, the influence of oxygen was first reported by Barkin et al. They found that the presence of oxygen could enhance the reduction of ceric ions by malonic acid.²¹ De-Kepper observed that the flux of oxygen could change phase diagram of the BZ oscillation system.²¹ Roux and Rossi found that varying the concentration of MA under the bubbling of oxygen could start or inhibit the BZ oscillations at different conditions.²¹ Bar-Eli and Haddad discovered that under the bubbling of oxygen, the BZ reaction had longer induction time and shorter oscillation duration, and the frequency was also increased.²¹ Wang and co-workers observed that the presence of oxygen in the gas phase above a closed, stirred BZ system can induce complexity.²² They further managed to use the flow rate of oxygen to control the complexity of the oscillation and observed oxygen oscillation in the reaction system with an oxygen electrode. Moreover they attribute the stirring rate as a primary factor that influences the rate of oxygen transport into the reaction mixture. The simulation work was also successfully conducted by considering the effect of oxygen to the free radical BrMA*. Steinbock et al discovered that the oxygen influences in the BZ reaction depend on the compositions, at low acid, low bromate but high [MA], the oxygen inhibition to the oscillation is pronounced.²³

From the study of Farage and Janjic, the oxygen influence to the 1,4-CHD-bromate system is not as obvious as that seen in the BZ reaction.¹²

Stirring effects were observed, on the other hand, in both the BZ reaction and the 1,4-CHD-bromate reaction. There are many explanations about how the stirring rate influences the system. Detailed introduction on stirring effects was presented in first part of the chapter 2.

Temperature has pronounced effects on bromate-based oscillations. The general phenomena is that an increase in temperature leads to an increase in the frequency of oscillation. The temperature dependence of the BZ reaction has been characterized by Nagy et. al.²⁴ They reported that the temperature dependence of the BZ reaction is related to the initial compositions of the reaction. Masia et al showed that temperature is a bifurcation parameter of the closed unstirred BZ reaction. In the 1,4-CHD-bromate reaction.²⁵ Szalai and Körös observed that increasing temperature shortens the induction period.¹⁶ This is because CHD reacts with bromate slowly at room temperature, which is a key step to influence the induction time. Elevating temperature could speed up this reaction.

Photosensitive oscillations have caught great attention in the last two decades since light provides a convenient approach to explore interactions between intrinsic dynamics and external forcing. Various experiments and mechanistic study have been performed, especially in the Ruthenium-catalyzed BZ reaction. Those investigations suggested that the photochemical production of bromous acid and bromide ion by the interaction

between the photo excited $\text{Ru}(\text{bpy})_3^{2+}$ and BrMA is responsible to the observed unique photo sensitivity.²⁶⁻³³ Mechanism of the photo response for the 1,4-CHD-bromate system appear to be different from that of the BZ reaction. A series of study indicate that the photosensitive intermediate species H_2Q may be a critical factor.³⁴⁻³⁷ Our group found that the final product 1,4-benzoquinone (Q) also plays an important role in the photochemical 1,4-CHD-bromate reaction.^{36,37}

1.4. Outlook of the study in chemical oscillatory system.

The study of nonlinear chemical kinetics has blossomed in the last three decades and has made significant contribution to the understanding of various complexities in nature. While a variety of chemical and biochemical systems have recently been found to be capable of exhibiting oscillatory behavior under suitable conditions, bromate-based oscillating reactions, especially the Belousov-Zhabotinsky (BZ) system, are still the most extensively studied chemical oscillators. For example, due to the easy implementation of external perturbation, the photosensitive $\text{Ru}(\text{bpy})_3^{2+}$ -BZ medium has been investigated by researcher working in different areas to understand pattern formation as well as to gain insights into interactions between intrinsic dynamics and external forcing.³⁸ Notably, various nonlinear phenomena which do not exist in perturbation free environment had been discovered in perturbed nonlinear media.³⁹

While significant amounts of effort had been dedicated to understanding mechanisms of these known chemical oscillators such as the BZ reaction, searching for new chemical

oscillators remains to be an active topic and attracts a great deal of attention in the study of nonlinear chemical dynamics.^{39, 40} For example, Farage and Janjic reported that 1,4-cyclohexanedione (CHD) reacted with acidic bromate in an oscillatory manner in 1982.¹¹ As opposed to most of the uncatalyzed bromate oscillators in which only a few, highly damped temporal redox-potential and bromide-ion-concentration oscillations could be obtained under batch conditions, 200-300 high frequency oscillations were recorded in the CHD-bromate reaction under optimal chemical conditions. Due to the absence of production of gases, which is a particular advantage in studying chemical waves, 1,4-CHD-bromate reaction in the presence of ferroin has attracted increasing attention in the last decade.¹⁴⁻¹⁵ In 2002, Horvath and co-workers reported oscillatory photochemical decomposition of tetrathionate ions.⁴¹ Recently, Kurin-Csörgei et. al. reported systematic design of chemical oscillators using complexation and precipitation equilibria.⁴²

The design and development of new oscillatory chemical reactions not only supplied dynamicists with new and different systems for characterization, but a great deal of new chemistry has been developed in the process.

Chapter 2. Cooperative effects of stirring and illumination in the 1,4-cyclohexanedione and bromate reaction

2.1 Introduction

Bromate-based oscillators using 1,4-cyclohexanedione(1,4-CHD) as the organic substrate have attracted increasing attention in the past decade.^{11-21, 34-37} The subtle response of the 1,4-CHD-bromate reaction to illumination has made it an attractive model system for exploring perturbed spatiotemporal dynamics.⁴³ The bubble-free, uncatalyzed 1,4-CHD-bromate oscillator was first reported by Farage and Janjic in 1982.¹¹⁻¹² They also observed strong influences of mechanical stirring in this system, which showed that the amplitude of oscillation was amplified by increasing the stirring rate. Notably, when spontaneous oscillations stopped at a higher stirring rate, decreasing the stirring rate could revive the oscillatory behavior. In this chapter, we explore the possibility of using stirring as a control parameter to induce bifurcations in the 1,4-CHD-bromate reaction.

Stirring effects on nonlinear chemical dynamics have motivated many experimental and theoretical studies in a variety of chemical systems, conducted either in continuously flow stirred tank reactors (CSTR) or in batch reactors.⁴⁴⁻⁷² These observed effects include changes both in the frequency and the amplitude of oscillation, and quenching of spontaneous oscillations.⁴⁴⁻⁵¹ Most of these observed effects can be explained on the basis of concentration fluctuations. In a CSTR system, for example, incomplete mixing of fresh reactants flowing into the bulk solution led to concentration fluctuations.⁵²⁻⁵⁴ In a batch

reactor, despite there is no inflow of fresh, concentrated chemicals, concentration fluctuations may result from interactions between fast chemical reactions and turbulent transports of substances.⁵⁵⁻⁵⁹ Numerical investigations with cellular mixing models and probabilistic cellular automaton models, carried out independently by several research groups, have shed light on the significance of inhomogeneity in observed stirring effects.⁶¹⁻⁶³

Depending on the properties of each reacting system, observed stirring effects had also been explained in terms of other sources other than fluctuations in local concentrations. For example, gas exchange such as O₂ absorption and/or Br₂ loss in bromate-oscillators with an open surface has been considered as an important factor.^{45,47,56,63-67} Absorptions of intermediate reagents onto the hydrophobic walls of the reactor, Pt-electrode, or stirring bar once were also considered as a possible reason.^{64,68} In addition, Noszticzius and co-workers demonstrated that different stirring effects in the BZ reaction could also be modeled semi-quantitatively by a diffusion-controlled radical-radical reaction step in a radicalator model.⁶⁹ In the following, we demonstrate that effects of stirring in the 1,4-CHD-bromate reaction can also be qualitatively described by considering influences of mixing on diffusion-limited radical reactions.

2.2 Experimental procedure

All reactions were carried out in batch conditions under the protection of inert gases (Nitrogen or Argon). A schematic plot of our apparatus is presented in Figure 2.1. The

internal diameter of the jacketed reaction beaker (purchased from ChemGlass) is 37mm. Reaction temperature was kept at $(25.0 \pm 0.1)^\circ\text{C}$ by a circulating water bath (Thermo NesLab RTE 7). The reaction solution was stirred with an octagonal magnetic stirring bar (diameter 8mm and length 16mm) driven by a magnetic stirrer (Fisher isotemp, speed ranges from 60 to 1200RPM). The reaction was monitored by coupling a $\text{Hg}|\text{Hg}_2\text{SO}_4|\text{K}_2\text{SO}_4$ reference electrode (Radiometer Analytical XR200) with either a regular platinum electrode (Length/Diameter 140/1 mm) or a small platinum electrode (Length/Diameter 2/1 mm). A bromide selective electrode was also employed to follow the evolution of bromide ions. To examine the influence of absorption of intermediates on Pt, a gold electrode (Radiometer, P201) was also employed. All measurements were recorded through a pH/potential meter (Radiometer PHM220) connected to a personnel computer via personal Daq(USB Data Acquisition Modules, IOtech).

Stock solutions NaBrO_3 (Aldrich, 99%), 1.0M, and sulfuric acid (Aldrich, 98%), 3M, were prepared with double-distilled water. 1,4-CHD (98% , Aldrich) and 1,4-hydroquinone (99%, Aldrich) were directly dissolved in the reaction mixture. The volume of the reaction mixture was fixed at 30.0cm^3 in all experiments. A flow meter (Cole Parmer) was used to control the flow of inert gases. A fiber optic halogen lamp (Fisher Scientific, Model DLS-100HD, 150W) with continuous variable light intensity was used as the light source and the light perturbation was implemented by placing two bifurcated fibers to illuminate the glass beaker either from opposite sides or from one side. The light intensity was measured with an optical photometer from Newport(model

1815c).

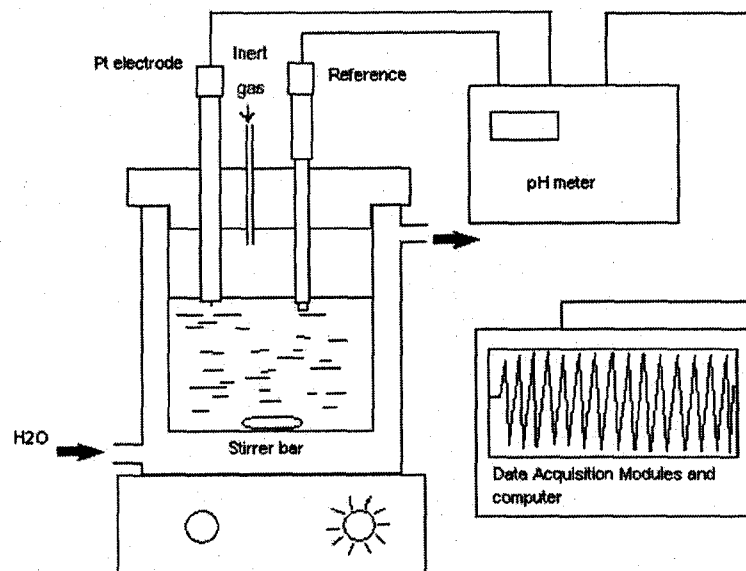


Figure 2.1 A schematic illustration of the experimental set-up

2.3 Experimental results

Figure 2.2 presents two time series obtained under different stirring rates: (a) 400 RPM, and (b) 1200 RPM. Other reaction conditions are $[\text{H}_2\text{SO}_4] = 0.9\text{M}$, $[\text{1,4-CHD}] = 0.06\text{M}$, and $[\text{BrO}_3^-] = 0.14\text{M}$. The frequency of oscillation decreases in responding to the increasing stirring rate. Meanwhile, as shown in the figure, spontaneous oscillations last for a shorter period of time under higher stirring rate. Notably, there is no visible change in the induction time, which is about 8200 seconds under the conditions studied here. When stirring rate was switched periodically between 300 and 1200 RPM during one reaction process as shown in Figure 2.3, increasing the stirring rate to 1200 RPM at the

earlier stage of the oscillatory window resulted in a significant amplification of the amplitude of oscillation. If the stirring rate was restored to 300RPM, the amplitude of oscillation became smaller again. Similar effects of stirring on the amplitude and frequency of oscillation were also reported by Farage and co-workers in 1982.¹² Interestingly, if the stirring rate was switched to 1200RPM at the later stage of the oscillatory window, quenching phenomenon was observed, where spontaneous oscillations could be restored by decreasing the stirring rate back to 300RPM. We would like to note that the above stirring-induced transitions between oscillatory and stationary states have only been seen at the end of the oscillatory window.

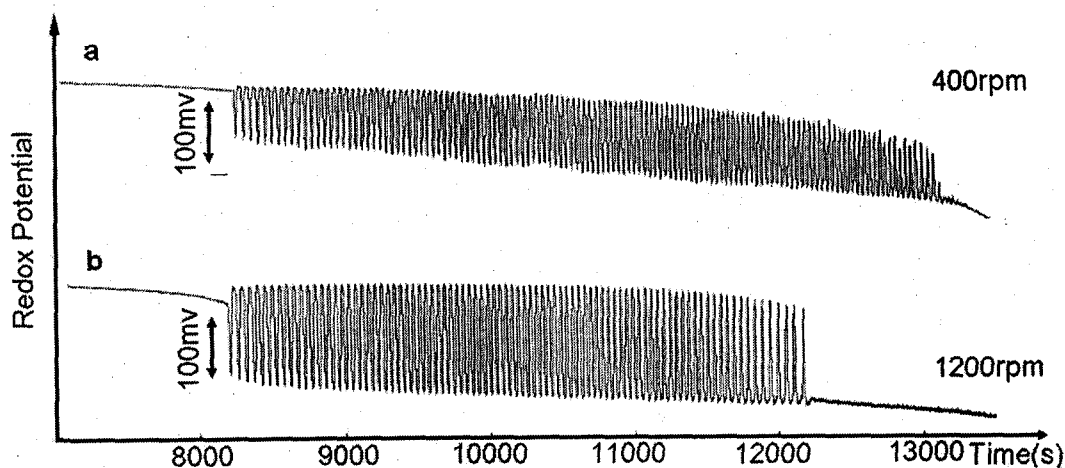


Figure 2.2 Time series obtained under different stirring rates (a) 400 RPM and (b) 1200 RPM. Other reaction conditions are: $[\text{H}_2\text{SO}_4] = 0.9\text{M}$, $[\text{1,4-CHD}] = 0.06\text{M}$, and $[\text{BrO}_3^-] = 0.14\text{M}$.

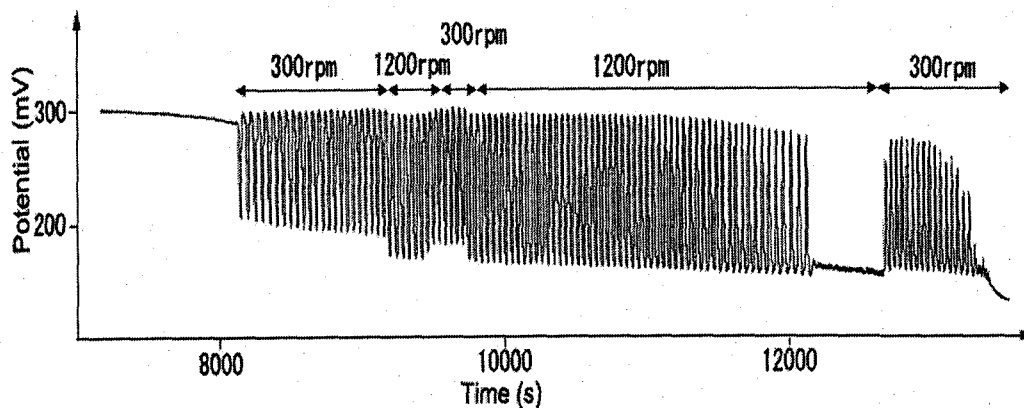


Figure 2.3 Time series obtained under different stirring rates in one reaction process. The reaction conditions are: $[\text{H}_2\text{SO}_4] = 0.9\text{M}$, $[\text{1,4-CHD}] = 0.06\text{M}$, and $[\text{BrO}_3^-] = 0.14\text{M}$.

When the flow of argon was adjusted from 1.0 to 2.0 ml/min and then to 3.0 ml/min, no variations in the above observed behavior (such as the induction time, quenching phenomenon, etc.) were recorded. These results suggest that the loss of volatile species, if there is any, does not play an important role in the above observed stirring effects because increasing the flow of gas above the solution surface at a constant stirring or increasing stirring rate at a constant gas flow would result in the same influence on the loss of volatile species. This conclusion is further supported by experiments conducted in the absence of free solution surface (i.e., the reaction mixture filled up the reactor), where same stirring effects as presented above were observed (see Figure 2.4). The increasing of the oscillation duration and the enhancement of the oscillation amplitude at higher stirring rate were observed as well in these figures. One thing I should note here is the addition of $\text{H}_2\text{Q}(0.03\text{M})$ in this series wouldn't influence the stirring effects on the

duration and the amplitude of oscillation. However, H_2Q affects to occurrence of the complex behavior and their response to the stirring variation. These phenomena are to be discussed later in detail.

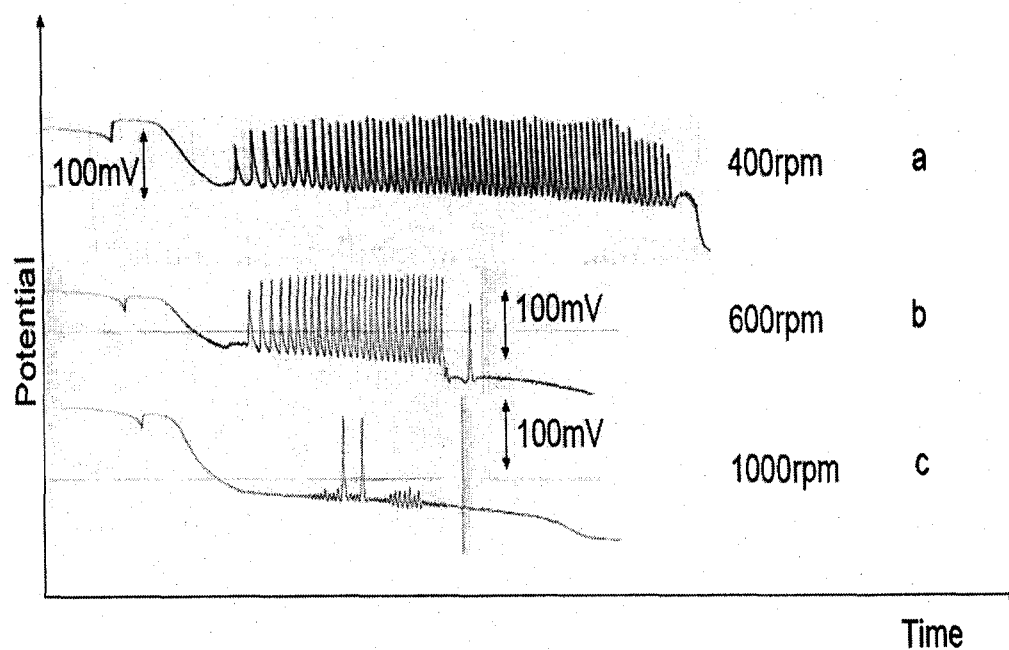


Figure 2.4 Time series obtained under different stirring rates (a) 400 RPM, (b) 600RPM, and (c) 1000 RPM. Other reaction conditions are: $[H_2SO_4] = 0.9M$, $[1,4-CHD] = 0.06M$, $[BrO_3^-] = 0.15M$, and $[H_2Q]=0.03M$. The total volume of the solution is 41 ml, which reduced the free surface to minimum.

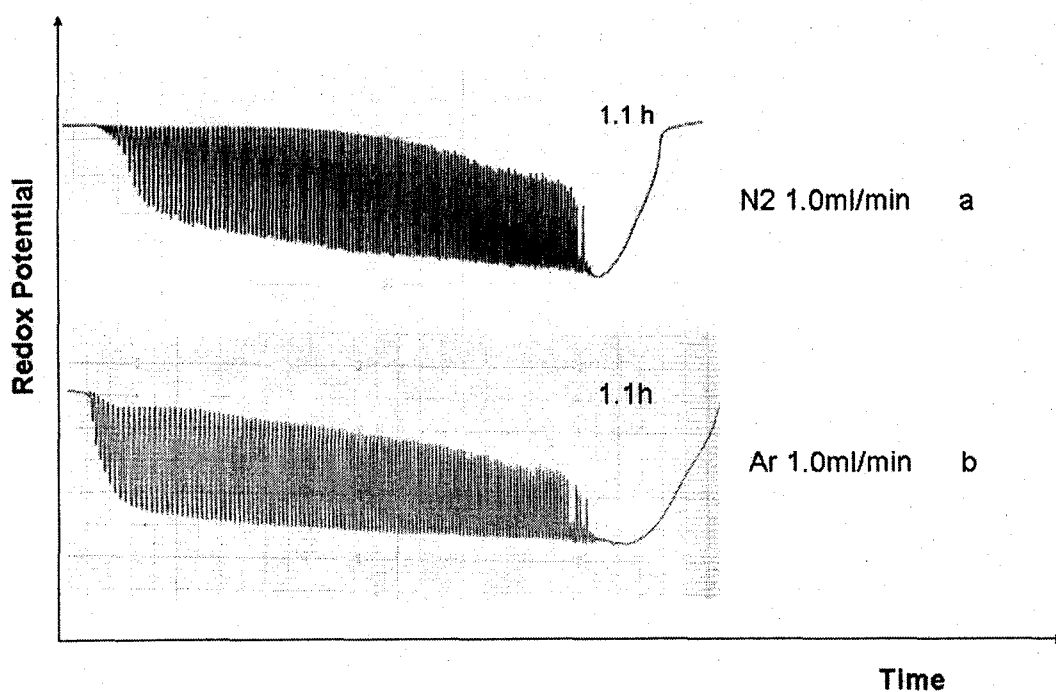


Figure 2.5 Time series obtained under the protection of different inert gases (a) N₂ and (b) Ar. Other reaction conditions are: [H₂SO₄] = 0.9M, [1,4-CHD] = 0.03M, and [BrO₃⁻] = 0.14M, [H₂Q] = 0.01M. The stirring rate is 400 RPM, the flow rate of Ar or N₂ is 1.0 ml/min.

Both argon and nitrogen are inert gas; however, as we know, argon is heavier than nitrogen and the air, so that argon could stay close to the surface of the reacting solution stably due to the gravity and thus offers a better protection. In concern of the prices of the experiment, we prefer to use nitrogen to replace Argon as the protection gas. Under the sufficient flow rate such as 1.0 ml/min, our experiments shown in Figure 2.5 indicate that there is no obvious difference in the induction time and oscillation duration when either N₂ or Ar is used. Therefore, we assume it's acceptable to use nitrogen to replace argon in

the experiments. Moreover, we examined both PVC and Teflon lids and did not observe any difference in the overall reaction behavior.

In complementing to transitions between stationary and oscillatory states, which had been observed in the BZ reaction by Ruoff,⁷⁰ our experiments further showed that increasing stirring rate in the 1,4-CHD-bromate reaction could induce consecutive bifurcations, leading to more complicated oscillations. An example of such a scenario is presented in Figure 2.6a, where reaction conditions are $[H_2SO_4] = 0.9M$, $[1,4-CHD] = 0.06M$, $[BrO_3^-] = 0.14M$ and $[H_2Q] = 0.03M$. As shown in the figure, as soon as the stirring rate was increased from 400 RPM to 600 RPM, two period-doubled oscillations appeared and then the system returned to simple oscillations of one peak per period. The reverse transition from period-2 to period-1 oscillations could be simply due to continuous variations in the reaction conditions since no fresh reactants were supplied in a batch reactor. When the stirring rate was increased further to 700 RPM, complex oscillations were revived, in which oscillations started with one large and two small peaks per period (1^2) and then evolved to patterns of one large and one small peak per period (1^1). Later, simple oscillations were restored after the stirring rate was changed back to 400RPM. The fact that higher stirring rates led to complicated oscillatory phenomena implicates that, in addition to micro fluctuations in concentrations, there are other nontrivial mechanisms responsible for the observed stirring sensitivity in the 1,4-CHD-bromate reaction. Furthermore, in the earlier stage of the reaction in Figure 2.6b, when the stirring rate is increased from 400 RPM to 700 RPM, the 1^1 and 1^2

oscillations were observed, while in the later stage of the reaction, increasing stirring from 400 RPM to 600 RPM, 1^1 oscillations continue. It confirmed the connection between stirring rate and complex phenomena in this reaction system. It also indicates that at the different reaction stages, effects of the stirring rate on the reaction behavior is different, presumably due to the consumption of reactants in the batch reactor.

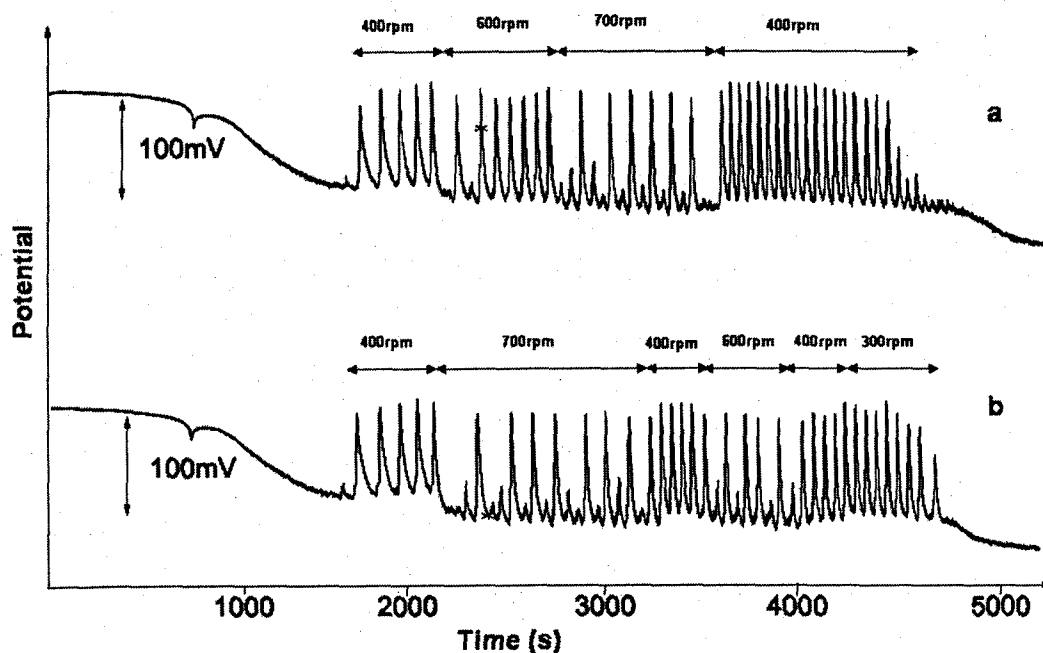


Figure 2.6 Time series showing the dependence of oscillation pattern on different stirring rates. Reaction conditions are $[\text{H}_2\text{SO}_4] = 0.9\text{M}$, $[\text{1,4-CHD}] = 0.06\text{M}$, $[\text{H}_2\text{Q}] = 0.03\text{M}$ and $[\text{BrO}_3^-] = 0.14\text{M}$.

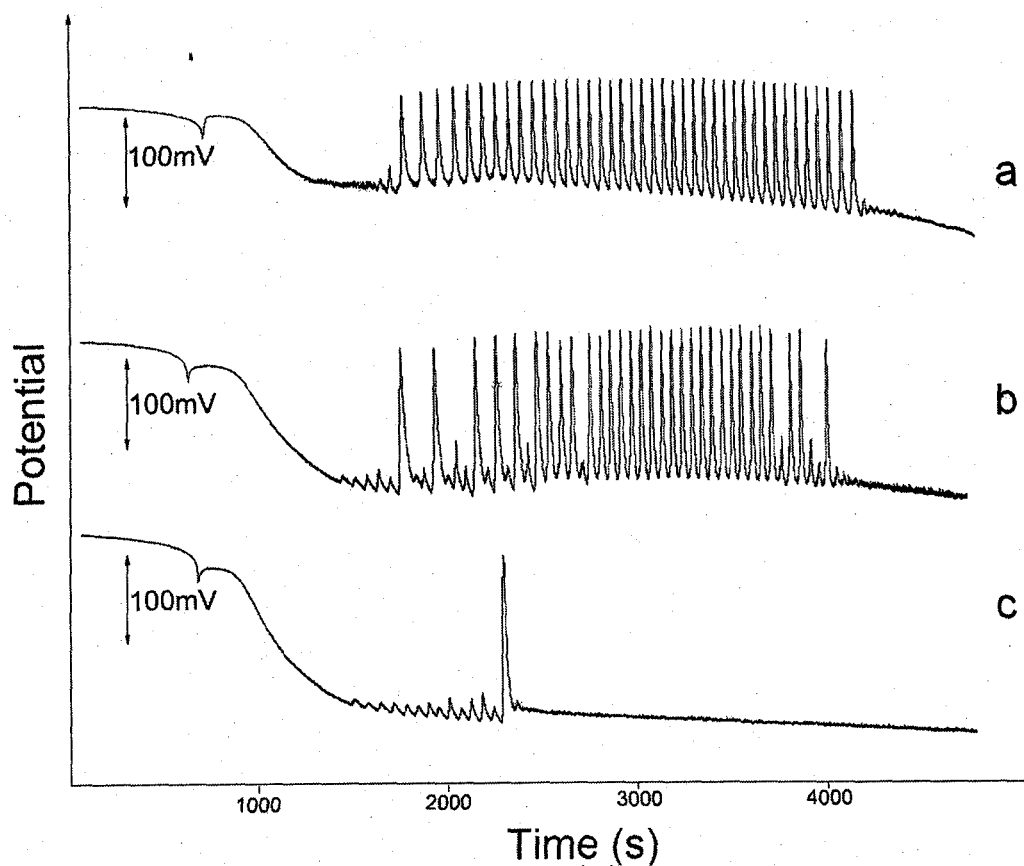


Figure 2.7 Time series showing the dependence of oscillation pattern on stirring rates. (a) 500 RPM, (b) 700RPM and (c) 800 RPM. Other reaction conditions are $[\text{H}_2\text{SO}_4] = 0.9\text{M}$, $[\text{1,4-CHD}] = 0.06\text{M}$, $[\text{H}_2\text{Q}] = 0.03\text{M}$ and $[\text{BrO}_3^-] = 0.14\text{M}$.

Figure 2.7 presents three time series conducted respectively at different, but constant stirring rates. At the stirring rate 500 RPM (Figure 2.7a) only simple period-1 oscillations were obtained. Here, the frequency of oscillation appeared to increase in time, which could be explained by the influence of BrCHD. The detailed discussion is shown in simulation part (see in Figure 2.17). When the stirring was increased to 700RPM in

Figure 2.7b, transient complex oscillations took place.

In contrary to transient complex oscillations reported in closed BZ reaction systems, which typically started from simple and then gradually evolved to more complicated patterns,^{74,75} here spontaneous oscillations started with the most complicated mode (1^3) and then gradually evolved to simple oscillations. When stirring rate was further increased to 800 RPM in Figure 2.7c, only one large peak, preceded by a number of small amplitude oscillations, was observed. In comparison to the results shown in Figure 2.2, here stirring appears to have more dramatic effects on the reaction behavior. Recall that the only difference between experiments shown in Figure 2.2 and Figure 2.7 is that 0.03M H_2Q , an intermediate product in the studied chemical system, is added in Figure 2.7. It thus implicates that H_2Q may have played an important role in the observed stirring sensitivity. More specifically, effects of stirring on the collective behavior of the 1,4-CHD-bromate reaction may take place through processes involving H_2Q and/or products of H_2Q . Figure 2.8 displays the response of the system to the stirring switched periodically between 400RPM and 1200 RPM, in which different concentrations of H_2Q are used. In Figure 2.8a, the oscillation amplitude was amplified by increasing stirring from 400RPM to 1200RPM; however, oscillation wasn't quenched even at the end of the oscillation stage. Increase the concentration of H_2Q to 0.02M and 0.03M (Figure 2.8b and c), allows the occurrence of quenching phenomenon by 1200RPM stirring in both experiments. Moreover, at the end of the experiment in Figure 2.8c, complex reaction behavior was observed. All of these phenomena in Figure 2.8 again indicated that H_2Q

concentration has significant effect on the stirring sensitivity.

With the addition of 0.01M H_2Q , in Figure 2.9, the amplitude of oscillation is increased and the oscillation duration is reduced by raising the stirring rate. The trend on the variation of the amplitude and oscillation duration with respect to stirring rate is similar with the trend seen in earlier experiments. The higher concentration of H_2Q added the better possibility to observe complex behavior (e.g. Figure 2.6, Figure 2.7). The detailed explanation to the complex behavior in mechanistic point of view is still unaccomplished with the current model.

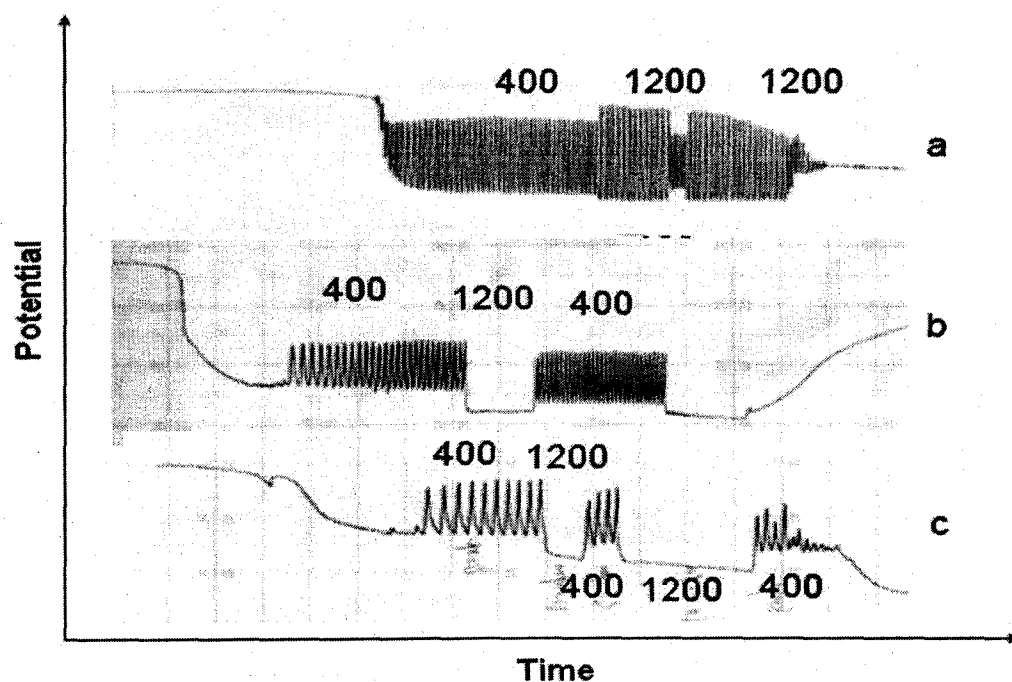


Figure 2.8 Time series obtained under different stirring rates in one reaction (a) $[H_2Q] = 0.01M$, (b) $[H_2Q] = 0.02M$ (c) $[H_2Q] = 0.03M$ Other reaction conditions are: $[H_2SO_4] =$

0.9M, [1,4-CHD] = 0.03M, and $[\text{BrO}_3^-]$ = 0.14M. Protected by argon at the flow rate of 1.0 ml/min.

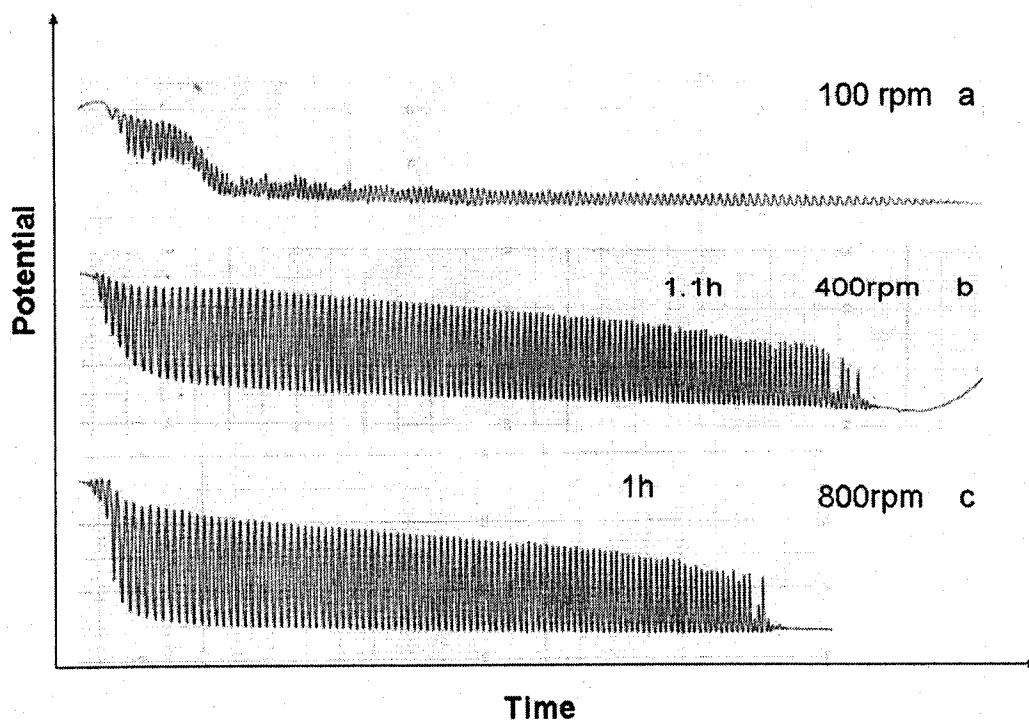


Figure 2.9 Time series obtained under different stirring rates (a) 100 RPM, (b) 400RPM and (c) 800 RPM. Other reaction conditions are: $[\text{H}_2\text{SO}_4]$ = 0.9M, [1,4-CHD] = 0.03M, and $[\text{BrO}_3^-]$ = 0.14M, $[\text{H}_2\text{Q}]$ = 0.01M. Protected by argon at the flow rate of 1.0 ml/min.

To shed light on the importance of concentration fluctuations in the observed stirring sensitivity, illumination was introduced in the following experiments as a means to manifest the inhomogeneity in local reaction dynamics. Two protocols were investigated here: (1) a single fiber was employed to illuminate the reaction solution from one side of

the reactor; (2) two bifurcated fibers were used to illuminate the solution from opposite sides of the reactor. Considering the facts that (1) the light intensity is stronger at the central of the light beam, and (2) light intensity decreases along the light path due to absorption, scattering, etc., the first illumination protocol is expected to generate much stronger spatial inhomogeneity inside the reactor.

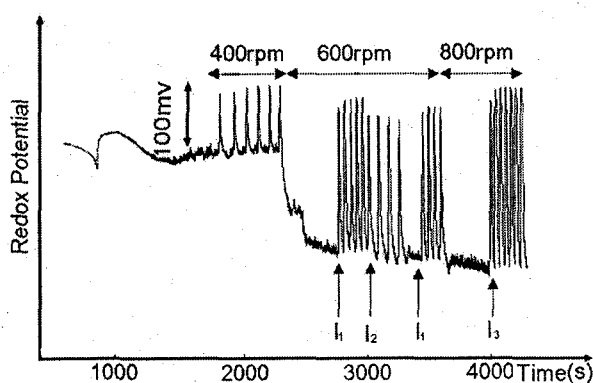


Figure 2.10 Effects of stirring on the reaction behavior in the presence of illumination, in which the intensity of the applied light is $I_1 = 25\text{mW/cm}^2$, $I_2 = 10\text{mW/cm}^2$, and $I_3 = 35\text{mW/cm}^2$. Other reaction conditions are $[\text{H}_2\text{SO}_4] = 0.9\text{M}$, $[\text{1,4-CHD}] = 0.06\text{M}$, $[\text{H}_2\text{Q}] = 0.03\text{M}$ and $[\text{BrO}_3^-] = 0.14\text{M}$.

Figure 2.10 presents effects of stirring on the collective reaction behavior in the presence of illumination. Other reaction conditions are identical to those used in Figure 2.6, except a small Pt electrode is employed here to follow the reaction. In consistent with earlier observation, when stirring was increased, spontaneous oscillations stopped. However, illuminating the system with a 25mW/cm^2 light revived the oscillatory behavior. Decreasing the light intensity to 10mW/cm^2 reduced both the frequency and

amplitude of these light-revived oscillations. After the 10mW/cm^2 illumination became incapable of sustaining oscillations at the stirring rate 600RPM, adjusting light to 25mW/cm^2 was able to revive spontaneous oscillations. Significantly, if the stirring was increased to a higher value (800RPM), these light-induced oscillations disappeared again; but, a further increase in the light intensity (35mW/cm^2) was able to bring oscillatory behavior back. This experiment illustrates that the threshold stirring rate for stopping spontaneous oscillations increases proportionally to the intensity of the applied light. Such a cooperative interaction of light and stirring could arise from illumination-enhanced fluctuations in local concentrations (kinetics), which obviously requires higher stirring rate to homogenize the solution. A recent numerical study reported spontaneous oscillations induced by inhomogeneous local kinetics in an excitable BZ medium.⁷⁵ Our further experiments showed that, however, despite that illumination protocol 1 generated stronger spatial inhomogeneity, the light intensity required to induce oscillations with a single fiber was exactly twice as much as that of using dual fibers in protocol 2 (shown in Figure 2.14 and Figure 2.15). Such a result indicates that fluctuations in local kinetics (e.g. concentrations) are not the primary reason for the behavior seen in Figure 2.10.

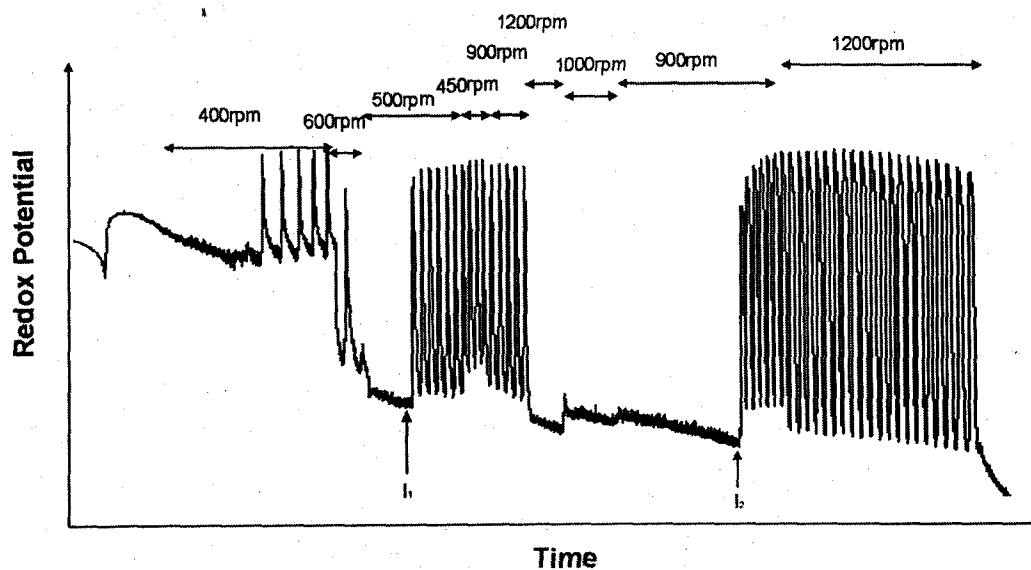


Figure 2.11 Effects of stirring on the reaction behavior in the presence of illumination, in which the intensity of the applied light is $I_1 = 35\text{mW/cm}^2$ and $I_2 = 50\text{mW/cm}^2$ using protocol 1. Other reaction conditions are $[\text{H}_2\text{SO}_4] = 0.9\text{M}$, $[\text{1,4-CHD}] = 0.06\text{M}$, $[\text{H}_2\text{Q}] = 0.03\text{M}$ and $[\text{BrO}_3^-] = 0.14\text{M}$.

In Figure 2.11, the sudden switch from 400RPM to 600RPM caused a dramatic potential decrease. The general trend of the potential level at different stirring rates concluded from all the above experiments is that a higher stirring rate leads the Pt potential base line to a lower Pt potential value. The illumination effect on the potential level is that the higher intensity the illumination is the higher potential level it is. After 35mW/cm^2 light illumination, i.e. I_1 brought the oscillation back at 500RPM, a small decrease of the stirring rate to 450RPM led to the potential bottom rise and the oscillation

amplitude decreases. Keeping the illumination intensity constant and bringing up the stirring rate to 900RPM, the potential bottom is lowered again, but the oscillation amplitude increases. Further increasing the stirring rate to 1200RPM, the oscillation disappeared. At the quenched stage from 1200RPM to 900 RPM, the potential change also followed the rule that higher stirring rate lowers the potential. When the light intensity is increased to 50 mW/cm^2 , the oscillation came back, similar to the I_3 induced oscillation in Figure 2.10. Increasing the stirring rate from 900RPM to 1200RPM again causes the significant increase of the oscillation amplitude

Figure 2.12 demonstrates that, keeping the stirring rate at 400RPM, when the reaction is illuminated with $I_1=30 \text{ mW/cm}^2$, the oscillation continues, but the amplitude is reduced and the frequency is increased. In addition, the average potential rose to a higher level. When the illumination was removed, the oscillation amplitude increased and the frequency was reduced; however, the reaction behavior couldn't restore to the original mode and the bottom potential was still higher than the potential level before the illumination. This indicates that the illumination has substantially changed the composition of the reaction system. With higher illumination intensity $I_2 = 40\text{mW/cm}^2$, similar phenomena are observed again, in which, the amplitude of the oscillation is slightly smaller and the frequency and bottom potential are slightly higher than the ones with I_1 respectively. Replacing I_2 with even more intense illumination $I_3 = 50 \text{ mW/cm}^2$, the bottom potential jumped up and oscillation disappeared. Remove I_3 , the oscillation comes back, indicating that strong illumination could quench the oscillation.

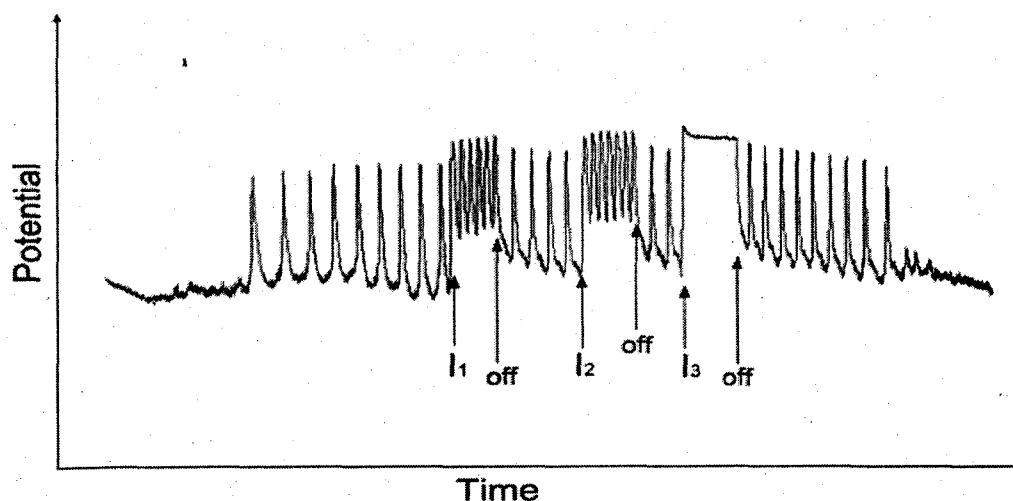


Figure 2.12. Effects of illumination on the reaction behavior under a constant stirring rate, in which the intensity of the applied light is $I_1=30\text{mW}/\text{cm}^2$, and $I_2=40\text{mW}/\text{cm}^2$, and $I_3=50\text{mW}/\text{cm}^2$ using protocol 1. Other reaction conditions are $[\text{H}_2\text{SO}_4] = 0.9\text{M}$, $[\text{1,4-CHD}] = 0.06\text{M}$, $[\text{H}_2\text{Q}] = 0.03\text{M}$ and $[\text{BrO}_3^-] = 0.14\text{M}$. The stirring rate is 400RPM.

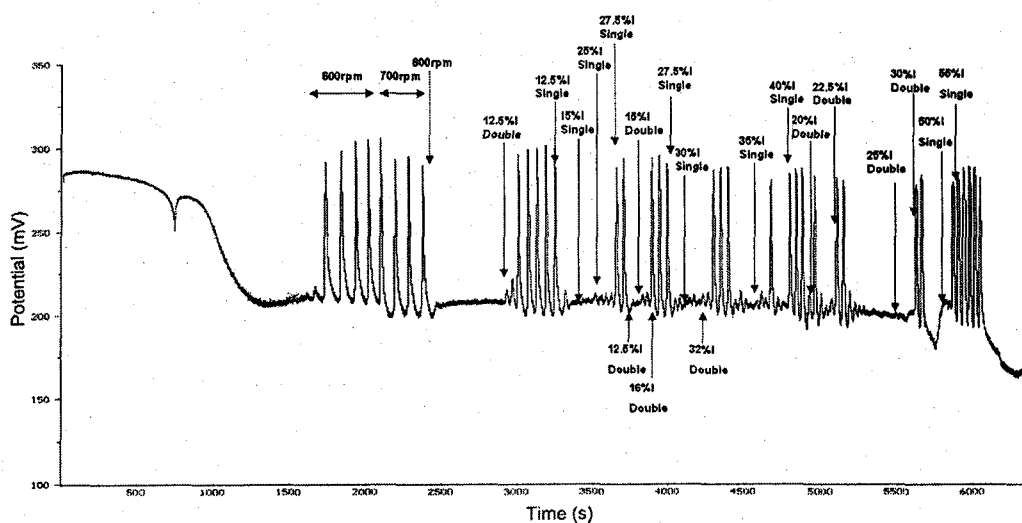


Figure 2.13 Effects of illumination with a single fiber or dual fibers. Other reaction conditions are $[\text{H}_2\text{SO}_4] = 0.9\text{M}$, $[\text{1,4-CHD}] = 0.06\text{M}$, $[\text{H}_2\text{Q}] = 0.03\text{M}$ and $[\text{BrO}_3^-] =$

0.14M. The stirring rate is 800 RPM.

Figure 2.13 and Figure 2.14 present the equivalence of protocol 1 and protocol 2. In Figure 2.13, at a considerably high stirring rate 800 RPM, where the oscillation was quenched, the protocol 1 and protocol 2 of illumination was applied alternatively. The light intensity was increased gradually to find out the minimum light intensity which could bring the oscillation back. Considering that this minimum light intensity changes in time, in order to compare the protocol 1 and protocol 2 at the same moment, the time series of the minimum light intensity for each protocol were drawn separately shown in Figure 2.14. It clearly indicated that the minimum light intensity of protocol 1 is approximately twice of the minimum light intensity of the protocol 2 at about the same time. That means if the illumination of protocol 1 at 40mW/cm^2 light intensity could just bring the oscillation back, then the illumination of protocol 2 at 20 mW/cm^2 could work in the same way.

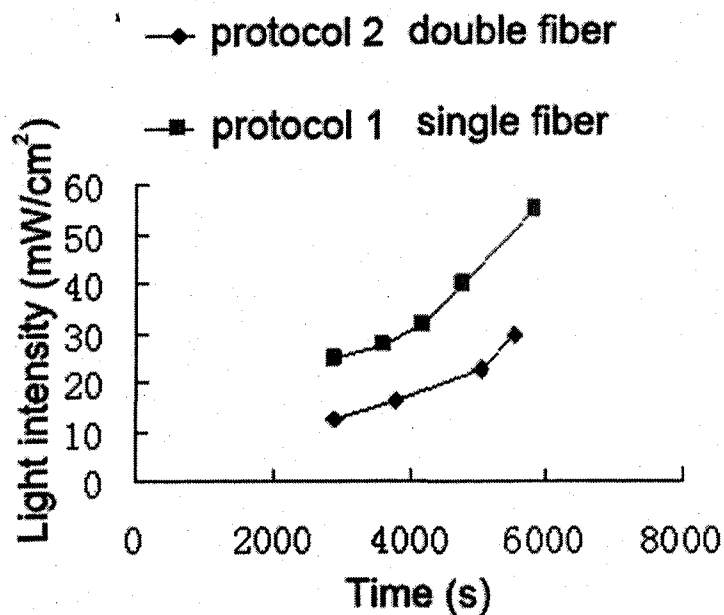


Figure 2.14 Summary of the minimum light intensity requested to revive the oscillation in the reaction of Figure 2.13.

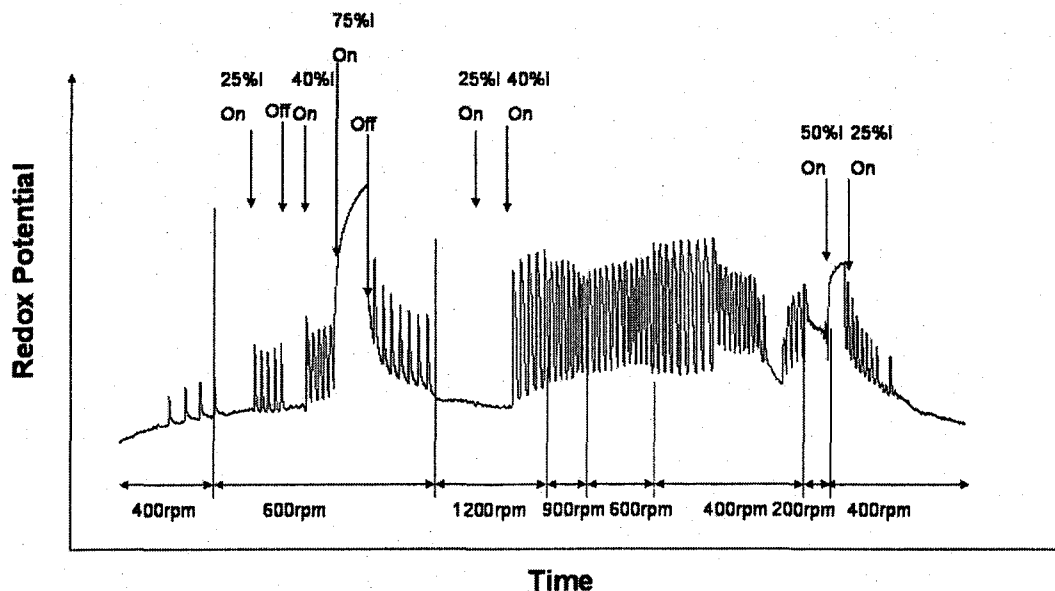


Figure 2.15 Effects of stirring on the reaction behavior in the presence of illumination,

using protocol 1. Other reaction conditions are $[\text{H}_2\text{SO}_4] = 0.9\text{M}$, $[1,4\text{-CHD}] = 0.03\text{M}$, $[\text{H}_2\text{Q}] = 0.03\text{M}$ and $[\text{BrO}_3^-] = 0.14\text{M}$. A Br^- selective electrode is used in this measurement.

The lower potential corresponds to the higher Br^- concentration and the higher potential corresponds to the lower Br^- concentration.

Figure 2.15 demonstrates the similar phenomena with a bromide ion selective electrode as shown in Figure 2.10 and Figure 2.11. It again confirmed that the effect of the stirring rate and the illumination is due to the internal reaction kinetics. From the figure we can find out that a lower stirring rate corresponds to the lower potential, that is, higher Br^- concentration, i.e. the reduced state. While intensive illumination corresponds to the high potential and lower Br^- concentration, i.e. an oxidative state.

The cooperative interaction of stirring and illumination may result from their opposite kinetic influences on the reaction dynamics: the above experiments have showed that higher stirring rates drove the system toward a reduced steady state; In contrast, illumination in the 1,4-CHD-bromate reaction quenched spontaneous oscillations to an oxidized state.⁷⁶ Therefore, the apparent effects of stirring on oscillations shall be weakened or even cancelled out by the presence of illumination. As a result, oscillations were retained even after the stirring rate was increased to beyond the critical value in which oscillations would otherwise have disappeared in the absence of light. In other words, the critical stirring rate is pushed up to a higher value. This hypothesis is supported by the following numerical simulations.

Figure 2.16 presents two results recorded respectively with a small Pt electrode and a gold electrode. Reaction conditions used here are the same as those in Figure 2.6, i.e., $[\text{H}_2\text{SO}_4] = 0.9\text{M}$, $[\text{1,4-CHD}] = 0.06\text{M}$, $[\text{BrO}_3^-] = 0.14\text{M}$ and $[\text{H}_2\text{Q}] = 0.03\text{M}$. Oscillation patterns in Figures 2.16a and 2.16b are qualitatively the same, suggesting that adsorption of intermediates on Pt electrode does not play any role in the observed stirring effects.

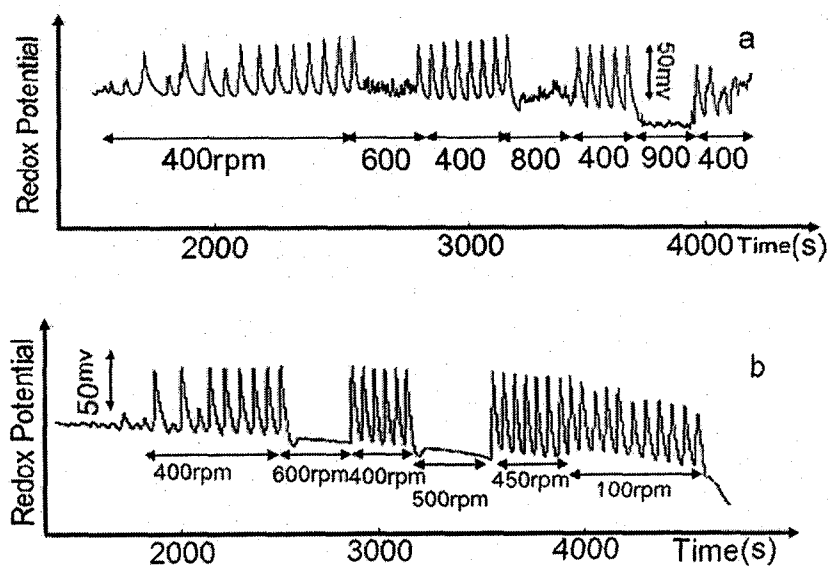


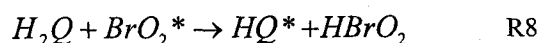
Figure 2.16 Stirring sensitivity of the 1,4-CHD-bromate reaction investigated by (a) a small Pt electrode and (b) a gold electrode. Other reaction conditions are $[\text{H}_2\text{SO}_4] = 0.9\text{M}$, $[\text{1,4-CHD}] = 0.06\text{M}$, $[\text{H}_2\text{Q}] = 0.03\text{M}$ and $[\text{BrO}_3^-] = 0.14\text{M}$.

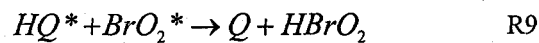
2.4 Numerical simulations

Micro fluctuations in bromide ion concentrations have been suggested by Ruoff to play a leading role in the occurrence of spontaneous oscillations in a closed anaerobic classical BZ reaction.⁶⁷ Since the 1,4-CHD-bromate oscillator is also bromide-controlled,

mechanism of micro-fluctuations in Br^- concentration shall also be capable of explaining the transition from oscillatory to stationary states observed above. On the other hand, our perturbation experiments with inhomogeneous light source suggest that in addition to micro-fluctuations, which cannot be avoided in a mechanistically stirred reaction system, there could also be other nontrivial mechanisms responsible for the observed stirring effects. Such a speculation is further supported by the fact that transitions between oscillatory and stationary states only appears at the end of the oscillatory window, even though at the beginning of the oscillation window the system is also at the neighborhood of a bifurcation point and thus is equally susceptible to fluctuations in concentrations of Br^- . To explore other explanations, we turned our attention to the possible influence of mixing on those diffusion-controlled radical reactions, in particular those processes involving hydroquinone and/or products of hydroquinone, suggested by comparing experiments shown in Figures 2.2 and 2.7.

The 1,4-CHD-bromate reaction mechanism has been developed by Szalai and co-workers^{19,20}. The mechanism, listed in Table 2.1, contains 19 reaction steps and is closely related to the FKN mechanism proposed by Field, Noyes and Körös for the BZ reaction.⁵ According to the above mechanism, H_2Q reacts with bromine dioxide radicals to produce bromous acid and hydroquinone radicals (see R8), and hydroquinone radicals then undertake two different reactions as shown by R9 and R10.





Whether a hydroquinone radical is going to take R9 or R10 is determined by the availability of its counter parts. Within the scope of a cellular model, in which the reaction solution is divided into an infinite number of small cells with each cell being governed by the same mechanism as listed in Table 2.1, only one hydroquinone radical is produced within each cell after the system undergoes an autocatalytic cycle (R6 + R7 +R8). Therefore, the fast disproportion of a hydroquinone radical relies on transportations which allow it to meet with another hydroquinone radical from neighboring sites. Consequently, increasing stirring rate would effectively result in an increase in the reaction R10. Working out from this perspective, in the following simulations rate constant k_{10} was simply adjusted to account for the influence of stirring.

Table 2.1. Mechanistic Model of the 1,4-CHD-Bromate-Acid Oscillatory System

No.	Reaction steps	Rate constant	
R1	$Br^- + HOBr + H^+ \leftrightarrow Br_2 + H_2O$	$k_1=8 \times 10^9 M^2 s^{-1}$	$k_{-1}=80 s^{-1}$
R2	$Br^- + HBrO_2 + H^+ \leftrightarrow 2HOBr$	$k_2=2.5 \times 10^6 M^2 s^{-1}$	$k_{-2}=2 \times 10^5 M^1 s^{-1}$
R3	$Br^- + BrO_3^- + 2H^+ \leftrightarrow HOBr + HBrO_2$	$k_3=1.2 M^3 s^{-1}$	$k_{-3}=3.2 M^2 s^{-1}$
R4	$HBrO_2 + H^+ \leftrightarrow H_2BrO_2^+$	$k_4=2 \times 10^6 M^1 s^{-1}$	$k_{-4}=1 \times 10^8 s^{-1}$
R5	$HBrO_2 + H_2BrO_2^+ \rightarrow HOBr + BrO_3^- + 2H^+$	$k_5=1.7 \times 10^5 M^1 s^{-1}$	
R6	$HBrO_2 + BrO_3^- + H^+ \leftrightarrow Br_2O_4 + H_2O$	$k_6=48 M^2 s^{-1}$	
R7	$Br_2O_4 \leftrightarrow 2BrO_2^*$	$k_7=7.5 \times 10^4 s^{-1}$	$k_{-7}=1.4 \times 10^9 M^1 s^{-1}$
R8	$H_2Q + BrO_2^* \rightarrow HQ^* + HBrO_2$	$k_8=8 \times 10^5 M^1 s^{-1}$	
R9	$HQ^* + BrO_2^* \rightarrow Q + HBrO_2$	$k_9=8 \times 10^9 M^1 s^{-1}$	
R10	$2HQ^* \leftrightarrow H_2Q + Q$	$k_{10}=8.8 \times 10^8 M^1 s^{-1}$	$k_{-10}=7.7 \times 10^4 M^1 s^{-1}$
R11	$CHD + H^+ \leftrightarrow CHDE + H^+$	$k_{11}=7.0 \times 10^4 M^1 s^{-1}$	$k_{-11}=5.2 \times 10^2 M^1 s^{-1}$
R12	$CHDE + Br_2 \rightarrow BrCHD + H^+ + Br^-$	$k_{12}=2.8 \times 10^9 M^1 s^{-1}$	
R13	$CHDE + HOBr \rightarrow BrCHD + H_2O$	$k_{13}=2.8 \times 10^9 M^1 s^{-1}$	
R14	$BrCHD \rightarrow CHED + Br^- + H^+$	$k_{14}=5 \times 10^5 M^1 s^{-1}$	
R15	$CHED + H^+ \rightarrow H_2Q + H^+$	$k_{15}=1.94 \times 10^4 M^1 s^{-1}$	
R16	$H_2Q + Br_2 \rightarrow Q + 2Br^- + 2H^+$	$k_{16}=3 \times 10^4 M^1 s^{-1}$	
R17	$H_2Q + BrO_3 + H^+ \rightarrow Q + Br^- + H^+ + H_2O$	$k_{17}=2 \times 10^2 M^2 s^{-1}$	
R18	$H_2Q + HOBr \rightarrow Q + Br^- + H^+ + H_2O$	$k_{18}=6 \times 10^5 M^1 s^{-1}$	
R19	$CHD + BrO_3 + H^+ \rightarrow H_2Q + HBrO_2 + H_2O$	$k_{19}=1 \times 10^5 M^2 s^{-1}$	

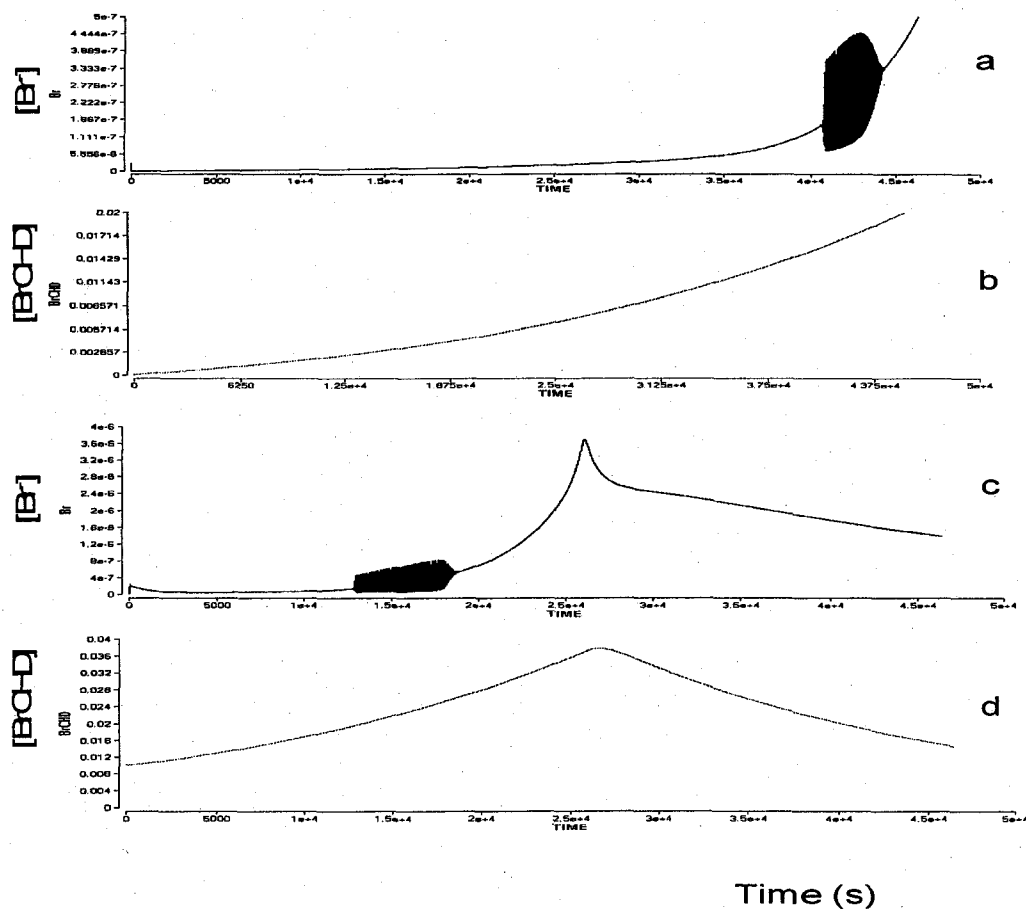


Figure 2.17 Simulated time series of the 1,4-CHD-Bromate Acid Reaction. (a) and (b), $[\text{BrCHD}]_0 = 1 \times 10^{-8} \text{ M}$; (c) and (d) $[\text{BrCHD}]_0 = 0.01 \text{ M}$. Other reaction conditions are $[\text{H}_2\text{SO}_4] = 0.9\text{M}$, $[\text{1,4-CHD}] = 0.06\text{M}$, and $[\text{BrO}_3^-] = 0.14\text{M}$.

According to the mechanism proposed by Szalai and co-workers, spontaneous oscillations in the 1,4-CHD-bromate reaction do not commence until the concentration of BrCHD, a precursor of Br^- , has reached a threshold level where sufficient amount of

inhibitor Br^- can be produced. This mechanism could be described by the Figure 2.17. Figure 2.17a and b indicated the accumulation of BrCHD lead to the oscillation. Figure 2.17d and a indicated that with the addition of BrCHD initially, the induction time was shortened significantly. Because BrCHD concentration increases in time, the production of Br^- is also accelerated accordingly, which consequently lead to an increase in the oscillation frequency (see in Figure 2.7a).

Figure 2.18 presents a time series calculated from the model listed in Table 2.1. Same as observed in experiments, there was a long induction time. After spontaneous oscillations began, stirring rate was increased slightly, which was implemented via increasing rate constant k_{10} . Similar to what took place in experiments, the amplitude of oscillation was increased while the frequency of oscillation was decreased. If stirring rate was increased still, which was again achieved by further increasing rate constant k_{10} , quenching phenomenon was seen there. After the system has stayed at the non-oscillatory period for a while, adjusting the rate constant k_{10} back to its original value (i.e., restoring the stirring rate) revived spontaneous oscillations. The above scenario is the same as what happened in experiments (see Figure 2.3), illustrating that effects of stirring in the 1,4-CHD-bromate reaction could arise from impacts of mixing on diffusion-limited radical reactions. So far, no complex oscillations have been seen in the modeling.

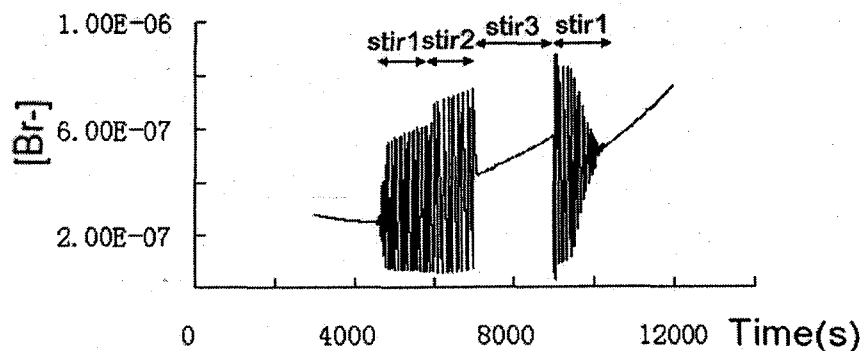
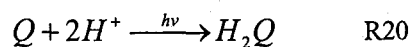


Figure 2.18 Stirring sensitivity of the 1,4-CHD-bromate reaction calculated with the model listed in Table 2.1. Different stirrings correspond to the following values of k_{10} , stir1: $k_{10} = 8.8 \times 10^8 \text{ M}^{-1}\text{s}^{-1}$; stir2: $k_{10} = 2.0 \times 10^{11} \text{ M}^{-1}\text{s}^{-1}$; and stir3: $k_{10} = 2.0 \times 10^{12} \text{ M}^{-1}\text{s}^{-1}$. Other reaction conditions are $[\text{H}_2\text{SO}_4] = 0.9\text{M}$, $[\text{1,4-CHD}] = 0.06\text{M}$, $[\text{H}_2\text{Q}] = 0.03\text{M}$ and $[\text{BrO}_3^-] = 0.14\text{M}$.

To simulate the cooperative effects of stirring and illumination on oscillatory behavior, the following schematic reaction has been added to the above model to account for the kinetic influences of light.



The above process was suggested by Görner in a recent study on photoprocesses of *p*-Benzoquinone in aqueous solution.⁷⁶ In our simulation, rate constant k_{20} was adjusted arbitrarily to reflect the influence of light, in which increasing k_{20} corresponds to an increase in the intensity of the applied light. The only difference between Figures 2.19a and 2.19b was the rate constant k_{10} , which was higher in Figure 2.19b to account for an increase in stirring rate. Again, same as observed in experiments, oscillatory behavior

was quenched there. Then, increasing the intensity of illumination (accomplished by merely increasing rate constant k_{20}) in Figure 2.19c revived spontaneous oscillations. Such a scenario is qualitatively the same as the cooperative interaction of stirring and illumination seen in experiments, suggesting that the opposite kinetic influences of light and stirring could be responsible of the phenomena seen in Figure 2.11.

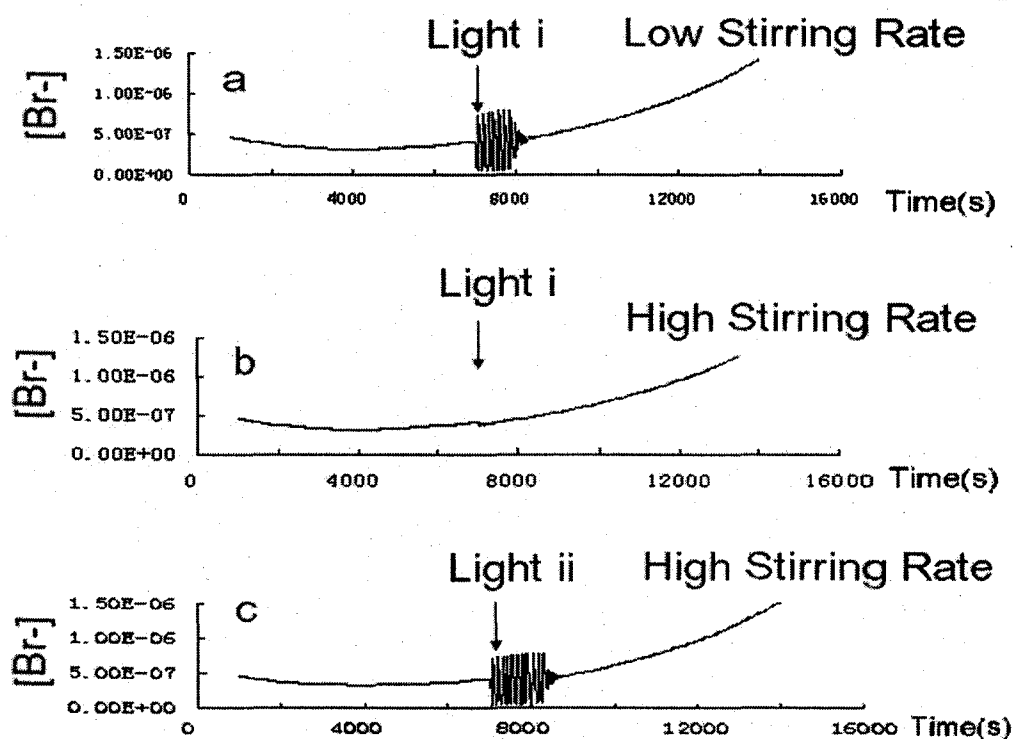


Figure 2.19 Cooperative effects of stirring and illumination in the 1,4-CHD-bromate reaction calculated from the model listed in Table 2.1 and reaction R20 listed in context. Other reaction conditions are $[\text{H}_2\text{SO}_4] = 0.9\text{M}$, $[\text{1,4-CHD}] = 0.06\text{M}$, $[\text{H}_2\text{Q}] = 0.03\text{M}$ and $[\text{BrO}_3^-] = 0.14\text{M}$. Rate constants in the three time series are: (a) $k_{10} = 6 \times 10^{11} \text{ M}^{-1}\text{s}^{-1}$, $k_{20} = 6 \times 10^{-7} \text{ M}^{-1}\text{s}^{-1}$; (b) $k_{10} = 2 \times 10^{12} \text{ M}^{-1}\text{s}^{-1}$, $k_{20} = 6 \times 10^{-7} \text{ M}^{-1}\text{s}^{-1}$; and (c) $k_{10} = 2 \times 10^{12} \text{ M}^{-1}\text{s}^{-1}$, $k_{20} = 2 \times 10^{-6} \text{ M}^{-1}\text{s}^{-1}$.

Using the same model as above, Figure 2.20 successfully simulated the phenomena observed in Figure 2.13. $k_{10} = 8.8 \times 10^8 \text{ M}^{-1}\text{s}^{-1}$, corresponds to the low stirring rate when the oscillation exists. When k_{20} was adjusted to $3.1 \times 10^{-6} \text{ M}^{-1}\text{s}^{-1}$ from 0, it indicated certain illumination was applied. At this moment the squeezed oscillation appeared in the simulation which coincident with the phenomena observed in Figure 2.13.

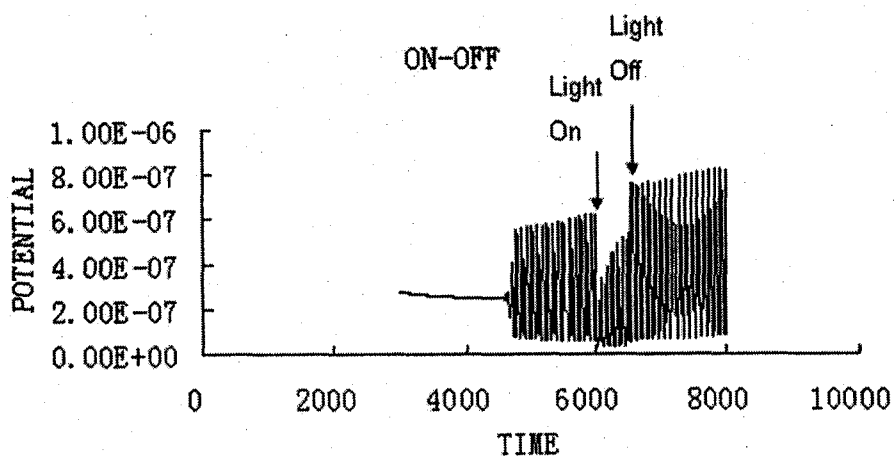


Figure 2.20 Simulation of photo effects on spontaneous oscillations. Other reaction conditions are $[\text{H}_2\text{SO}_4] = 0.9\text{M}$, $[\text{1,4-CHD}] = 0.06\text{M}$, $[\text{H}_2\text{Q}] = 0.03\text{M}$ and $[\text{BrO}_3^-] = 0.14\text{M}$. $k_{10} = 8.8 \times 10^8 \text{ M}^{-1}\text{s}^{-1}$, light off correspond to $k_{20} = 0$ and light on corresponds to $k_{20} = 3.1 \times 10^{-6} \text{ M}^{-1}$.

2.5 Conclusions

In complementing to existing investigations on stirring effects in nonlinear reaction systems, which have showed stirring-induced transitions between stationary and oscillatory states,^{11,12,70} this study demonstrates that stirring could induce consecutive

bifurcations, leading to more complicated oscillatory behavior. Notably, the transition from simple to complex oscillations occurs as a result of increasing stirring rate, where faster mixing is supposed to lead to a more homogeneous medium and thus suppress fluctuation-caused irregular behavior. The occurrence of complex behavior at higher stirring rates therefore implicates that in addition to micro-fluctuations there are other nontrivial mechanisms being responsible of the observed effects of stirring. Numerical simulations with an existing model illustrate that effects of mixing on radical reactions could be a source of the observed stirring effects.

When the 1,4-CHD-bromate reaction is exposed to light, the stirring rate required to quench spontaneous oscillations is found to increase proportionally with respect to the intensity of the applied light. Our experiments with two different illumination protocols indicate that inhomogeneous local kinetics does not play a leading role in the cooperative interaction of stirring and light. Simulations by accounting for the kinetic effects of light on the production of hydroquinone from 1,4-benzoquinone qualitatively reproduce experimental results. In summary, although one cannot preclude the presence of micro-fluctuations in concentrations, this study illustrates that the observed stirring effects as well as the cooperative interaction of stirring and light could arise from the influence of mixing on chemical processes such as diffusion-limited hydroquinone radical reactions. These information are important for future investigations of 1,4-CHD-bromate-(ferroin) oscillators.

Chapter 3. Nonlinear Phenomena in light-mediated 1,4-Benzoquinone-bromate reaction

3.1 Introduction

Photochemical reactions extensively exist and play vital roles in nature and industrial production. For instance, photosynthesis is the basis of the primary production of the food chain, and it depends on the photoreactions of some pigments such as chlorophyll and carotene etc.⁷⁷

Photochemical effects have been also studied in nonlinear chemical systems. Thirty years ago, Vavilin et al first reported the effect of light on the BZ reaction. The oscillations in the cerium-catalyzed BZ system were either modified or completely suppressed depending on the light intensity and chemical composition under the illumination of ultraviolet light.⁷⁸ Later, Gáspár et al discovered that the ferriin- and ruthenium-catalyzed systems responded more significantly to the influence of visible light while the cerium-catalyzed system seemed to be unaffected.⁷⁸ Since then, Ruthenium-catalyzed BZ reaction has been considered as a typical oscillatory system that response to light illumination and has been studied extensively in both stirred and reaction-diffusion system.²⁶⁻³³ These investigations have made significant contributions to the understanding of a variety of complex behaviors in nature including stochastic resonance and synchronizations. In the CO₂ free 1,4-CHD-bromate system, Kurin-Csörgei et al⁷⁶ and Huh et al^{34,35} have observed the photosensitivity of the ferriin-

catalyzed reaction in both stirred and reaction diffusion system. Our group has carried out a series of studies on the photo effects to the uncatalyzed 1,4-CHD-bromate system and proposed that intermediate products hydroquinone and benzoquinone may be the key species in these photo effected phenomena.^{36,37}

Quinones, a kind of aromatic dicarbonyl compounds, have the unique photochemical properties, and are considered as important photochemical substances in both industry and in physiology.⁸⁰⁻⁸³ For example, quinone is a common component of biologically relevant molecules (e.g. Vitamin K1 is phyloquinone) that serve as electron acceptors in electron transport chains such as those in Photosystems I & II of photosynthesis, and aerobic respiration. In industry, quinones may act as tanning agents.

1,4-hydroquinone (H₂Q) has broad applications in both industries and household products.^{80,81} It is used, for example, as corrosion inhibitors in boilers, process regulators in polystyrene manufacture, and photochemical developers, stabilizers in printing and has a typical application in hyperpigmentation removal & skin bleaching . The broad application of H₂Q arises from its strong reducing ability, in which H₂Q itself is sacrificed to produce 1,4-benzoquinone (Q). Therefore, exploring the conversion of Q back to H₂Q has tremendous potential in applications, in addition to their scientific interests. It motivates us to explore light-mediated recycling of Q/H₂Q in acidic environment.

3.2 Experimental procedure

Stock solutions NaBrO_3 (Aldrich, 99%), 0.06M, and sulfuric acid (Aldrich, 98%), 3 M, were prepared with double-distilled water. 1,4-Benzoquinone (98%, Aldrich) and 1,4-hydroquinone (99%, Aldrich) were directly dissolved in the reaction mixture.

For the study in a batch reactor, most reactions were carried out under the protection of nitrogen which was controlled with a flow meter (Cole Parmer). A schematic plot of our apparatus is presented in Figure 3.1. The reaction temperature was well controlled by a circulating water bath (Thermo NesLab RTE 7). The reaction solution was stirred with an octagonal magnetic stirring bar (diameter 8 mm and length 16 mm) driven by a magnetic stirrer (LabTech, Daihan labtech co.ltd, speed ranges from 1 to 9 roughly 100 to 900RPM). The reaction was monitored by coupling a $\text{Hg}|\text{Hg}_2\text{SO}_4|\text{K}_2\text{SO}_4$ reference electrode (Radiometer Analytical XR200) with a platinum electrode. A bromide ion selective electrode was also employed to follow the evolution of bromide ions. All measurements were recorded either through VoltaLab (PGZ 100) or Powerlab/4SP, and connected to a personal computer.

A fiber optic halogen lamp (Fisher Scientific, Model DLS-100HD, 150 W) with continuous variable light level was used as the light source, and the light illumination was implemented by using two bifurcated fibers to illuminate the glass beaker from opposite sides. The light intensity was measured with an optical photometer from Newport (model 1815C).

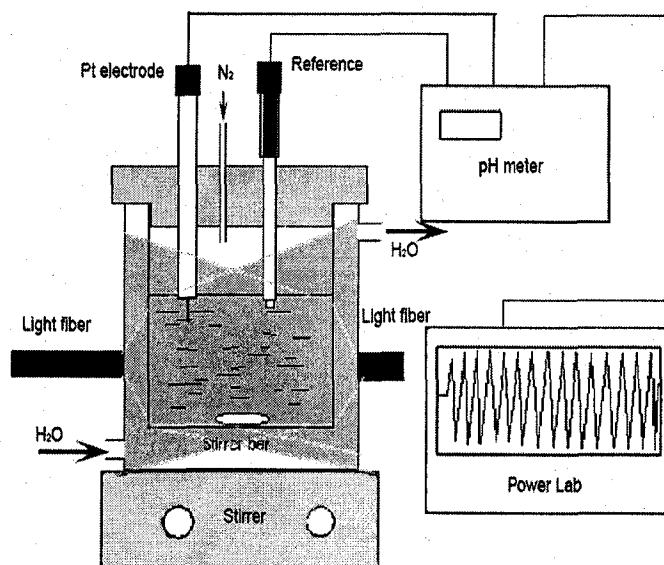


Figure 3.1 Equipment setup of batch reactor

For absorption spectra measured with an UV-Visible spectrophotometer (Ocean Optics), the equipment setup is demonstrated in Figure 3.2. The quartz glass cuvette (10mm light path, allowing 200-2500nm light pass, HELLMA) containing 2.5ml sample mixture was placed in a CUV sample holder (Ocean Optics) which has two water jacket connected to a circulating water bath (Thermo NesLab RTE 7). The Deuterium light (wavelength from about 200nm- 900nm) supplied by the lightsource UV-VIS-NIR(DH-2000, Mikropack) went through the sample via an optic fiber (Ocean Optics). The absorption time series was measured by USB 2000 (Ocean Optics) and plotted by the software OOIBase332 via a personal computer. We control the temperature at 20°C, but the actual temperature in cuvette is 23-24°C, due to the direct illumination. The solution is stirred by a small magnetic bar. A single light fiber from the halogen lamp

(Fisher Scientific, Model DLS-100HD, 150 W) was placed on top of the cuvette to supply the illumination (see Figure 3.2.)

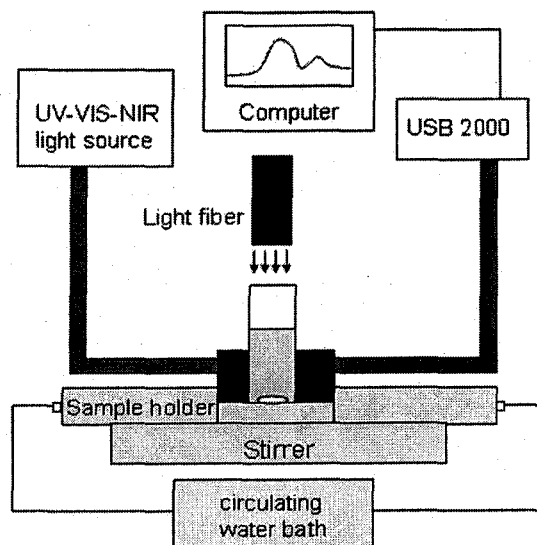


Figure 3.2 Equipment setup of UV-Visible spectrophotometer

For the study in a CSTR system, 20ml mixture (Q 0.02M, H_2SO_4 1.8M, NaBrO_3 0.05M) was initially prepared in the batch reactor. Through the cover of the batch reactor, two syringe pumps (KD scientific Infusion /Withdrawal Pumps) were connected to serve as an input and output driver. From the input syringe, the mixed solution (Q 0.02M, H_2SO_4 1.8M NaBrO_3 0.05M) was slowly injected into the batch reactor. On the other hand, the output syringe pump keeps on drawing the solution out of the batch reactor at the same speed. The equipment was shown in Figure 3.3.

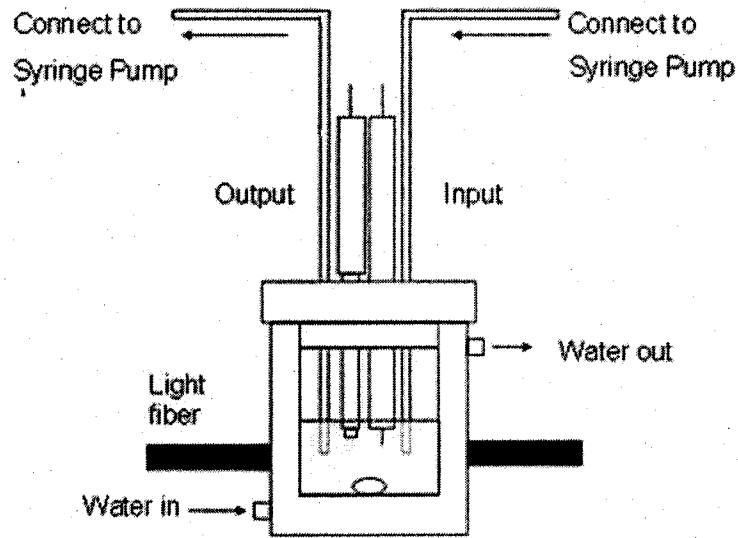
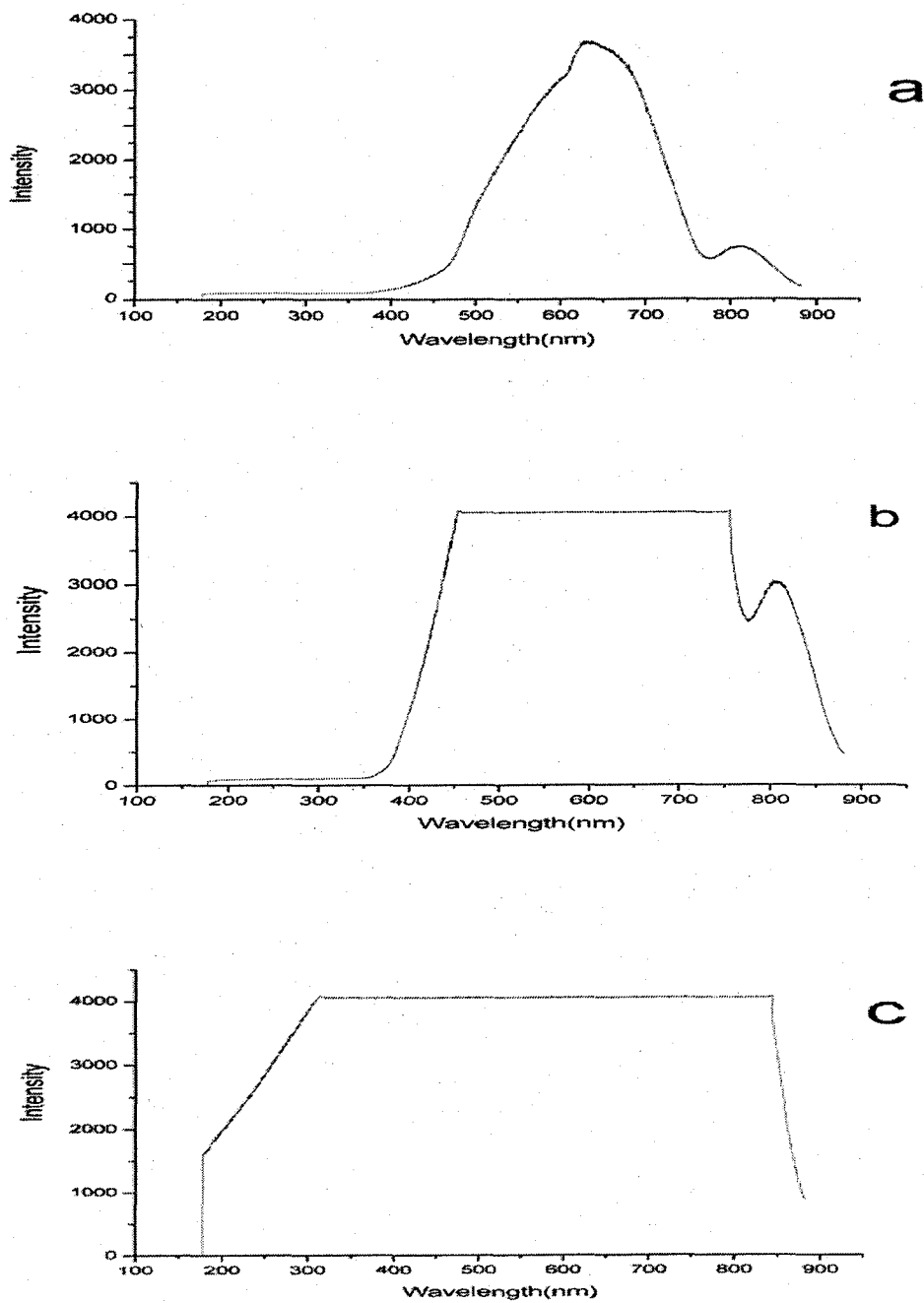


Figure 3.3 Equipment set up for study with CSTR method.

The spectra of the light resource was characterized by UV-Visible spectrometer as shown in Figure 3.4, which indicated that at low light intensity, the wavelength of the light from this lamp ranges from about 400nm to about 850nm (see in Figure 3.4a). We also find that increasing the light intensity will result in the dramatic increase for the light intensity between the wavelength of 500 and 750nm (see in Figure 3.4b). The light intensity below 400nm is very negligible until it is increased to 60% of the maximum light intensity of the lamp(see in Figure 3.4c).

Figure 3.4 The spectra of the halogen light source measure by UV-Visible spectrophotometer. (a) When light intensity is $30\%I_0$, (b) When the light intensity is $45\%I_0$, (c) When the light intensity is $60\%I_0$. (See below)



The light intensity was tuned from the control panel of the lamp which could be adjusted continuously between 0 and 100 percent of the maximum light power, I_0 . (see in Figure 3.5c) in the experiments. It would be much easier to describe the light intensity in the experimental procedure in terms of the percentage of the maximum light intensity I_0 . There are basically three protocols are used in this project: Protocol A, is the most commonly used as described above, using double fibers to illuminate the glass beaker from opposite sides; Protocol B, was applied to a few experiments for the study with CSTR, using the lamp bulb to illuminate directly at 3cm away from the double-layer glass reactor on one side, where the purpose is to get a higher light intensity; Protocol C is applied for a few experiments monitoring with UV-Visible spectrometer in a cuvette, in which illumination is implemented with a single light fiber directly from the top of the cuvette.

The correspondence of the light intensity measured and the percentage demonstrated from the control panel was summarized in Table 3.1, respectively for Protocol A and Protocol B. The plots in Figure 3.5 a and b demonstrate that over most of the range(20% to 80%), the percentage shown on the panel linearly correlated with the measured light intensity. However, for the range above 80%(from Figure 3.5a 80%-100%, from Figure 3.5b 90%-100%), the slop becomes slow,

Table 3.1 The light intensity correspondence between the control panel of the lamp and intensity measured by the optical photometer

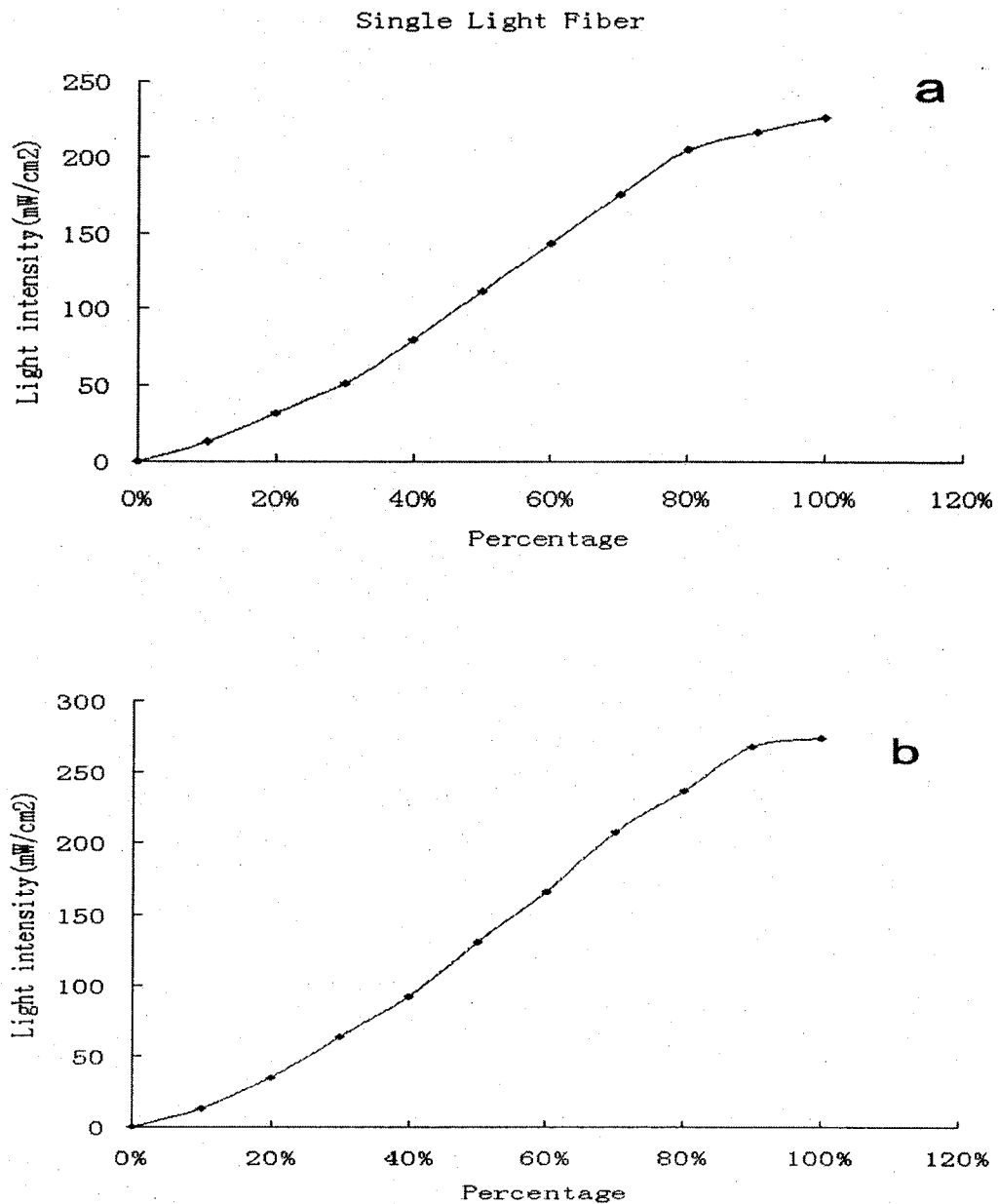
Protocol A: Light intensity from Single fiber directly through the water circulating double layer glass

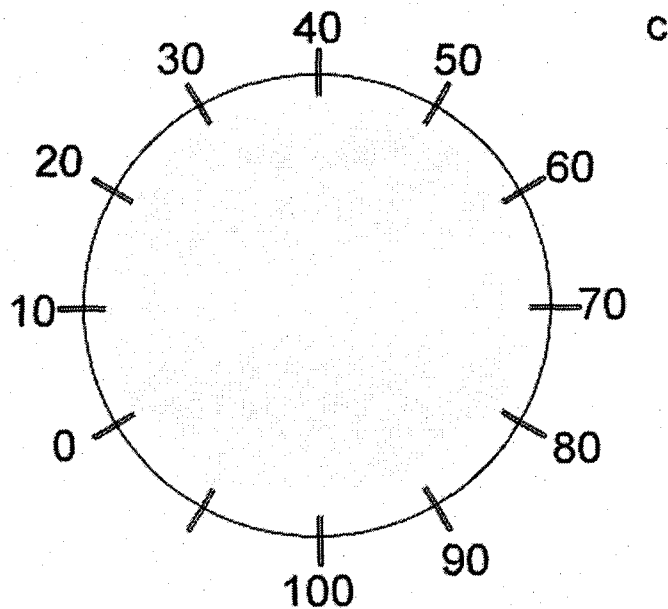
Protocol B: Light intensity from the bulb 3cm away and through the water circulating double layer glass

	Light Intensity for Protocol A (mW/cm ²)	Light intensity for Protocol B (mW/cm ²)
100%I ₀	226.1146	273.8854
90% I ₀	216.5605	267.5159
80% I ₀	205.0955	235.6688
70% I ₀	175.1592	207.0064
60% I ₀	143.3121	165.6051
50% I ₀	111.465	130.5732
40% I ₀	79.61783	92.35669
30% I ₀	50.95541	63.69427
20% I ₀	31.84713	35.03185
10% I ₀	12.73885	12.73885
0% I ₀	0	0

The diameter of the photometer is 2.0cm, and the area of the sensor part is 3.14cm²

Figure 3.5 The relationship of the percentage tuner and the light intensity. (a) from a single fiber through double layer glass filled with water, (b) from the light bulb 3cm away through double layer water circulating glass. (c) The scheme of the control panel of the halogen lamp. (see below)





3.3 Experimental Results in a closed system

3.3.1 Behavior at Different Compositions

In a batch reactor, a series of experiments are performed to study the dependence of reaction behavior on the light intensity, the concentration of each species, temperature, volume, stirring rate, and the flow rate of the protection gas. The color of the solution under the illumination changes from yellow at the beginning into colorless at the time when oscillations begin. In contrast, the mixed solution without illumination remains at the yellow color for at least one day. This observation indicates that light illumination is a critical factor for the reaction to take place.

Figure 3.6 presents the reaction behavior under different light intensities. This light series clearly demonstrates that illumination is a critical parameter of the oscillation.

When there is no light illumination, the potential first goes up slowly then reaches to a flat level and stays there(see in Figure 3.6e). While with illumination, at the beginning of the reaction, there is a very fast reaction step which is so short that it could not be reflected on this graph (Figure 3.6). As shown in Figure 3.7, the potential went down first and jumped back to a high potential and then became nearly stable. This behavior indicates that benzoquinone may have reacted with bromate.

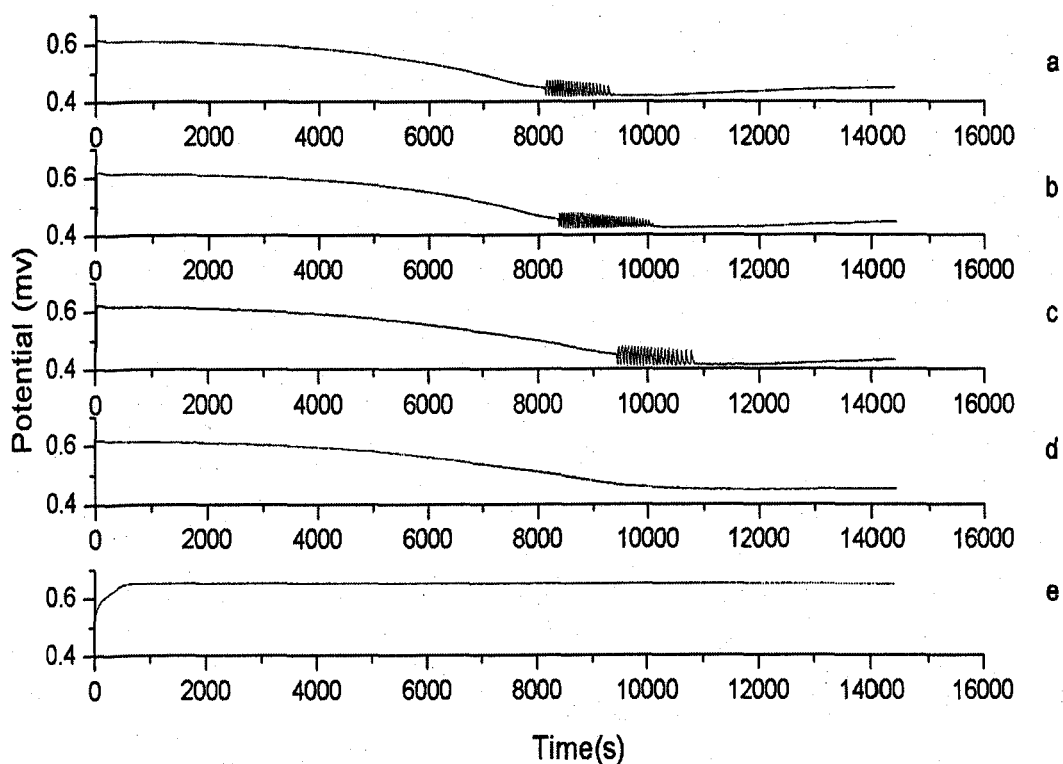


Figure 3.6 Reaction behavior at different illumination intensity, (a) 100% I_0 , (b) 90% I_0 , (c) 80% I_0 , (d) 75% I_0 and (e) 0% I_0 . The other conditions are: $[Q] = 0.02M$, $[H_2SO_4] = 1.8M$, $[NaBrO_3] = 0.05M$, total volume of the reaction is 30ml, stirring rate 700 RPM, N_2 protection and $T = 25^\circ C$.

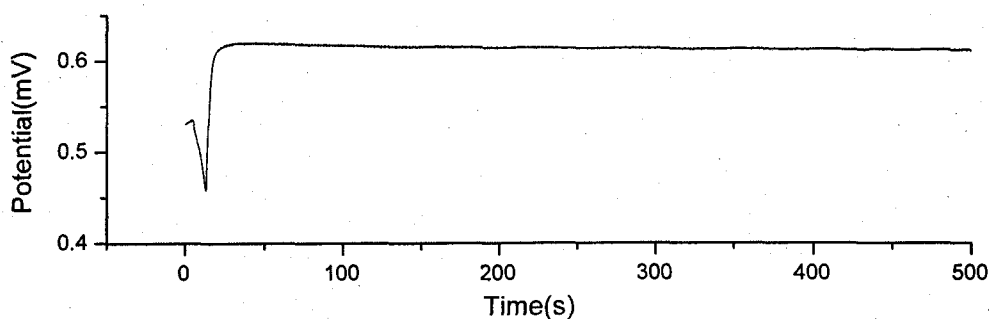


Figure 3.7 The potential curve at the beginning of the reaction in a batch reactor under the condition of $[Q] = 0.02\text{M}$, $[\text{H}_2\text{SO}_4] = 1.8\text{M}$, $[\text{NaBrO}_3] = 0.05\text{M}$, total volume of the reaction is 30ml, stirring rate 700 RPM, N_2 protection, $T = 25^\circ\text{C}$, light intensity $100\% I_0$.

From Figure 3.6, we could also observe that the induction time and oscillation behavior are strongly affected by the light intensity. The induction time has the inverse relationship with the light intensity, that is, when light intensity increases, the induction time keeps on decreasing. However, for the length of oscillation window, it seems there is an optimized light intensity to favor the oscillation behavior. More specifically, the $90\%I_0$ light could sustain the longest oscillatory behavior, even though the amplitude of the oscillation is slightly smaller than that of the $100\%I_0$ ones. When light intensity is decreased to $75\%I_0$, it becomes too low to induce any oscillation. When the light intensity is too high, on the other hand it may cause some reaction steps become too fast to support oscillation. Therefore, the longest oscillation happens only when the light intensity is moderate.

Experiments conducted at 15°C also show that the $90\%I_0$ light could produce longer

oscillation behavior than that of 100% I_0 . The results are presented in Figure 3.8.

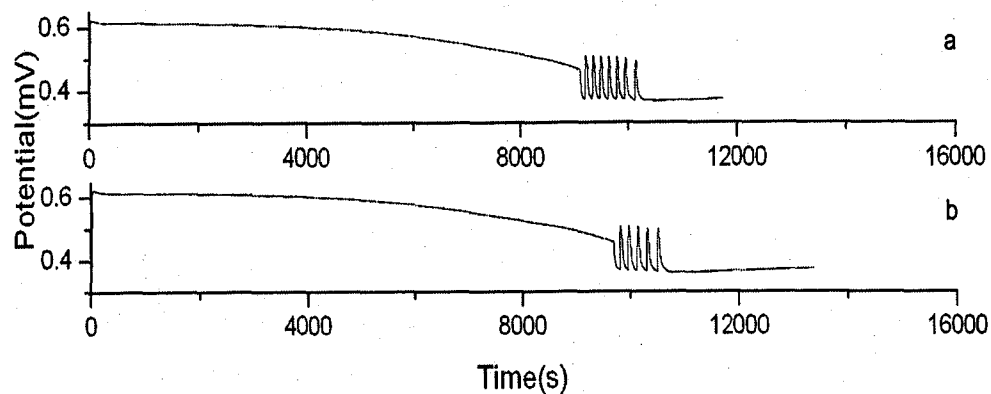


Figure 3.8 Comparison of oscillations at different light intensities. (a) 90% I_0 , (b) 100% I_0 .

The other reaction conditions are $[Q] = 0.02\text{M}$, $[\text{H}_2\text{SO}_4] = 1.8\text{M}$, $[\text{NaBrO}_3] = 0.05\text{M}$, total volume 30ml, stirring rate 700 RPM, N_2 protection and $T = 15^\circ\text{C}$.

Figure 3.9 shows that when the concentration of NaBrO_3 was decreased from 0.05M to 0.03M, 50% I_0 could still produce oscillation, and the number of peaks is more than that of 75% I_0 light. Note that under the condition of $[\text{NaBrO}_3] = 0.05\text{M}$, even 75% I_0 light could not initiate any oscillation. It demonstrates that influences of light intensity on the reaction behavior depend on the composition of the solution.

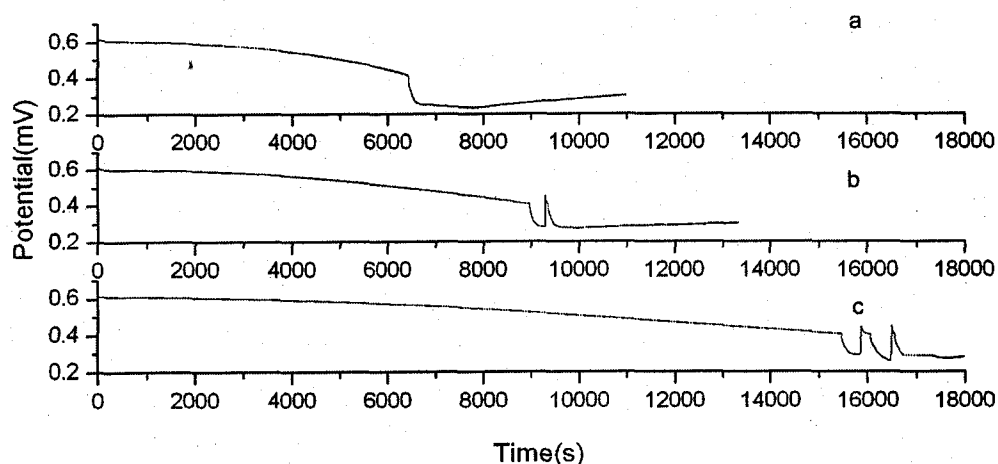


Figure 3.9 Time series obtained at different light intensity. (a) $100\%I_0$, (b) $75\%I_0$, (c) $50\%I_0$, Reaction conditions are $[Q] = 0.02M$, $[H_2SO_4] = 1.8M$, $[NaBrO_3] = 0.03M$, total volume 30ml, stirring rate 700 RPM, N_2 protection and $T = 25^\circ C$.

Influences of H_2SO_4 concentrations on oscillations in the photo-mediated bromate-Q reaction are presented in Figure 3.10, in which $[H_2SO_4] =$ (a) 1.0M, (b) 1.4M, (c) 1.8M and (d) 1.9M. As is shown in the figure, increasing H_2SO_4 concentration enhances the frequency of oscillation. The optimum H_2SO_4 concentration appears to be around 1.8M, in which more oscillation peaks are obtained. Oscillations become barely visible at $[H_2SO_4] = 1.9$ and disappears completely as H_2SO_4 concentration is increased further. On the other end, only one peak is observed at $[H_2SO_4] = 1.0M$. Also shown here is that the induction time is slightly reduced by increasing H_2SO_4 concentration.

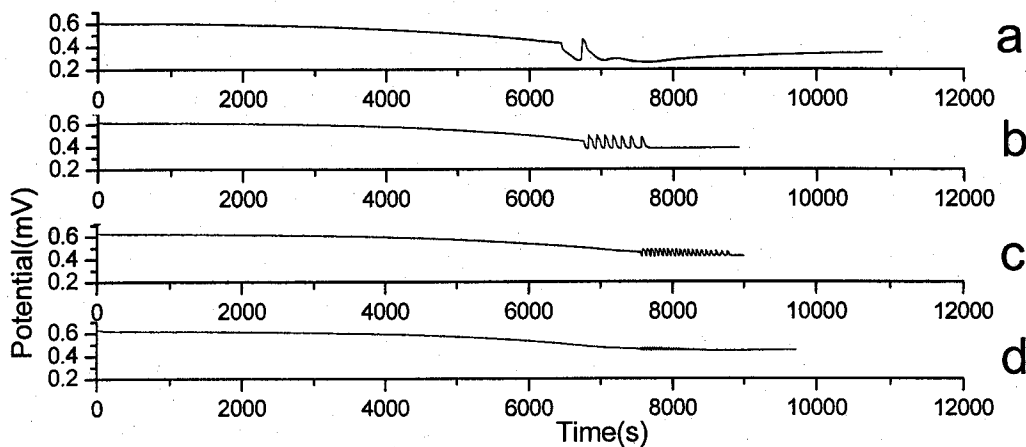


Figure 3.10 Changes of the oscillation behavior with respect to varying the concentration of H_2SO_4 : (a) 1.0M, (b) 1.4M, (c) 1.8M, (d) 1.9M. The other conditions are $[\text{Q}] = 0.02\text{M}$, $[\text{NaBrO}_3] = 0.05\text{M}$, total volume 30ml, stirring rate 700 RPM, N_2 protection and $T = 25^\circ\text{C}$

Figure 3.11 presents the effect of Q concentration on the oscillatory behavior, in which $[\text{Q}] =$ (a) 0.015M, (b) 0.02M, (c) 0.025M, and (d) 0.03M. No oscillations could be achieved if concentrations of the photosensitive reagent 1,4-benzoquinone are lower than 0.015M. As 1,4-benzoquinone concentration is increased, amplitudes of these transient oscillations increase, but the total number of peaks decreases. For example, only five peaks are observed when the initial concentration of 1,4-benzoquinone is 0.03M. When $[\text{Q}] = 0.04\text{M}$, precipitations appear in the system, which hinders us to investigate the nonlinear behavior at higher Q concentrations. There is also a slight decrease in the induction time when the concentration of 1,4-benzoquinone is increased from 0.015M to 0.03M.

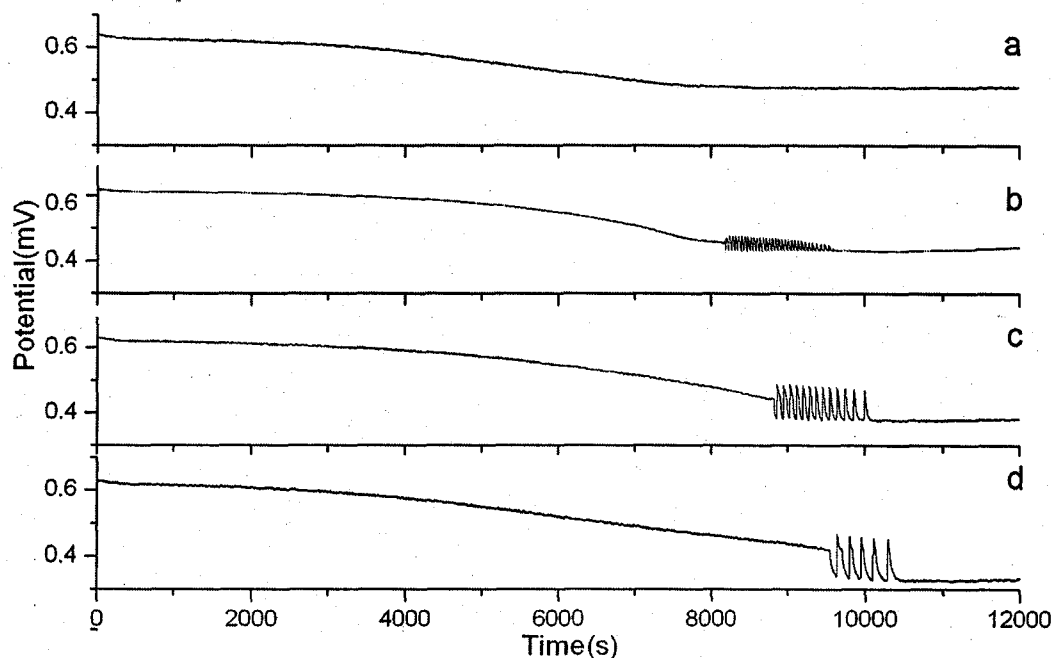


Figure 3.11 Oscillatory behavior under different concentrations of Q: (a) 0.015M, (b) 0.02M, (c) 0.025M, (d) 0.03M. The other reaction conditions are $[\text{H}_2\text{SO}_4] = 1.8\text{M}$, $[\text{NaBrO}_3] = 0.05\text{M}$, total volume 30ml, stirring rate 700 RPM, N_2 protection and $T = 25^\circ\text{C}$.

Figure 3.12 presents the dependence of the nonlinear dynamics on the initial concentrations of bromate: (a) 0.03M, (b) 0.04M, (c) 0.05M, and (d) 0.06M. In Figure 3.12a, a sudden drop in the Pt potential occurred after a long induction time, but no oscillations were observed there. Increasing bromate concentration to 0.04M in Figure 3.12b allows the oscillatory behavior to take place. The total number of peaks as well as the frequency of oscillation is increased as a result of further increasing bromate

concentration. Still increase of bromate concentration leads to the disappearance of oscillations (see Figure 3.12d). This result indicates that, same as observed in other bromate-based chemical oscillators, the concentration of bromate shall be within a proper range in order to see oscillations in the photo-driven chemical oscillator. Notably, the transition from oscillatory to non-oscillatory state at the low bromate condition is different from that at the high bromate concentration end. Reducing bromate concentration from 0.06M appears to result in a supercritical Hopf-bifurcation.

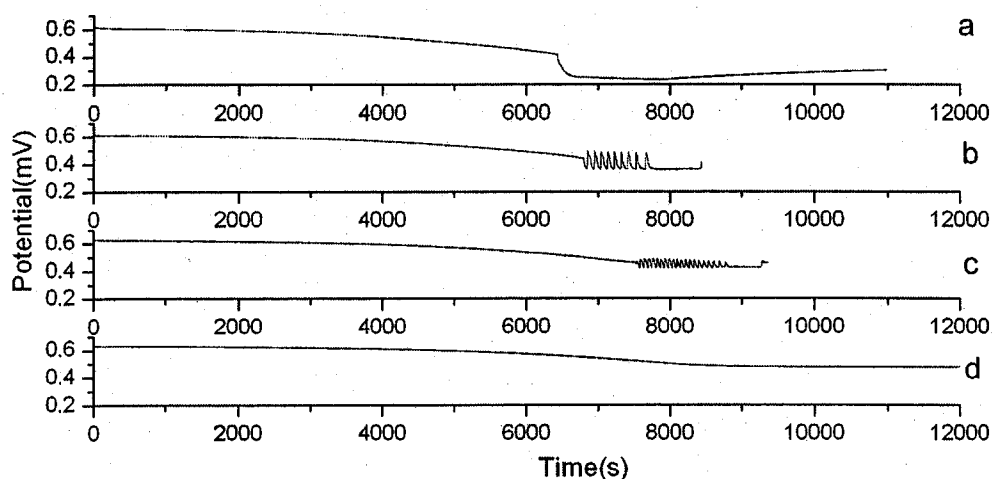


Figure 3.12 Changes of oscillation behavior with respect to varying the concentration of $[\text{NaBrO}_3]$: (a) 0.03M, (b) 0.04M, (c) 0.05M, (d) 0.06M, Other reaction conditions are $[Q] = 0.02\text{M}$, $[\text{H}_2\text{SO}_4] = 1.8\text{M}$, $100\%I_0$ total volume 30ml, stirring rate 700 RPM, N_2 protection and $T = 25^\circ\text{C}$.

Figure 3.13 illustrates temperature-dependence of the reaction behavior in the bromate-Q system. Oscillations have been achieved for the temperature as low as 10.0°C. As is shown in the figure, in general increasing reaction temperature will reduce the induction time and increases the frequency of oscillation. Meanwhile, the amplitude of oscillation appears to decrease with reaction temperature. When temperature is higher than 27.0°C, no oscillatory behavior could be achieved. Therefore, 20°C to 25°C are considered to be the suitable temperature range for this new photo chemical oscillator.

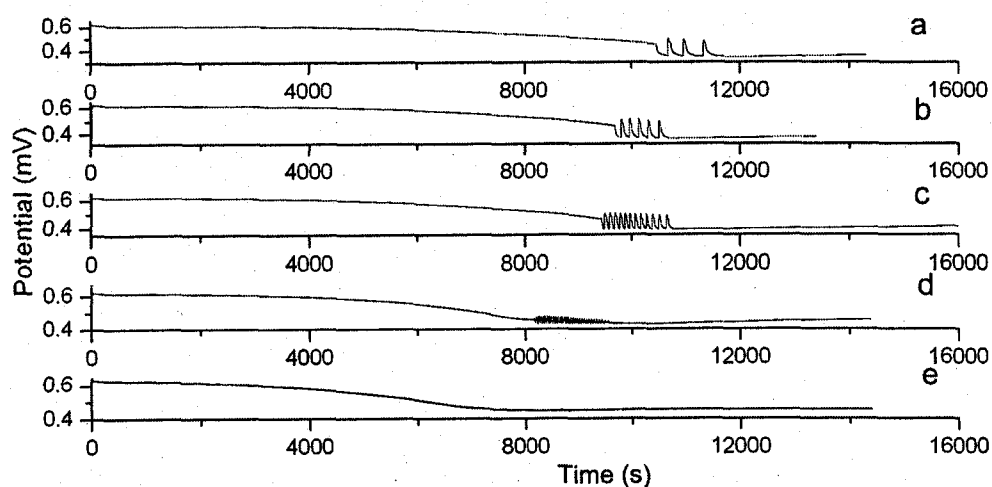


Figure 3.13 Changes of Oscillation behavior with respect to varying the temperature. (a) 10°C, (b) 15°C, (c) 20°C, (d) 25°C, (e) 30°C. Other conditions are $[Q] = 0.02M$, $[H_2SO_4] = 1.8M$, $[NaBrO_3] = 0.05M$, 100% I_0 total volume 30ml, stirring rate 700 RPM, N_2 protection.

An alternative approach of characterizing the dependence on illumination intensity is through changing the volume of the reaction mixture while keeping the light intensity

constant. Experiments conducted with different solution volumes were presented in Figure 3.14, in which the solution volume was (a) 44.0ml, (b) 30.0ml, (c) 20.0ml, and (d) 10.0ml. Other reaction conditions are $[\text{BrO}_3^-] = 0.05\text{M}$, $[\text{H}_2\text{SO}_4] = 1.8\text{M}$, $[\text{Q}] = 0.02\text{M}$ and $100\%I_0$. Figure 3.14 illustrates that decreasing the volume of reaction solution shortens the induction time. When the volume becomes too small, the total number of oscillation peaks decreases. As expected, such a scenario is exactly opposite to influences of light intensity on the reaction dynamics. It is simply because decreasing the volume of reaction solution corresponds to an increase of the applied light intensity. Notably, a small peak appears at the end of the oscillatory window, followed by another large peak. Such a result implicates that the system has the potential to even exhibit complex oscillations.

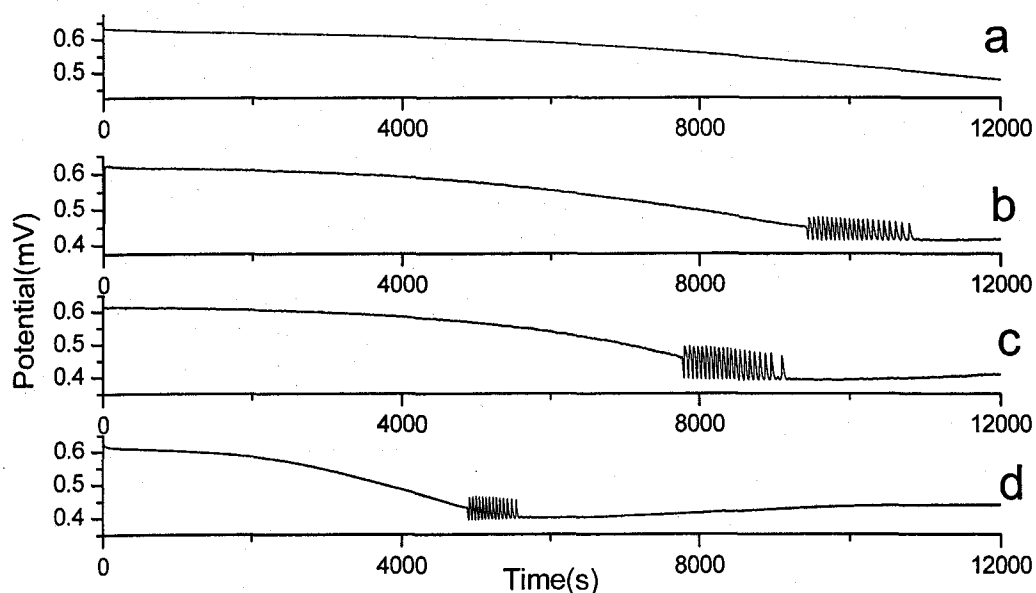


Figure 3.14 Oscillations at different volume of solution. (a) 44ml, (b) 30ml, (c) 20ml, (d) 10ml. Other reaction conditions are $[\text{Q}] = 0.02\text{M}$, $[\text{H}_2\text{SO}_4] = 1.8\text{M}$, $[\text{NaBrO}_3] = 0.05\text{M}$,

100%I₀, stirring rate 700 RPM, N₂ protection and T = 25°C.

The influence of oxygen on the reaction system is investigated by purging N₂ or Air at a certain speed above the solution or bubble the air into the solution. In Figure 3.15, the major difference appears at the induction time. Generally, the induction time is slightly shorter in the presence of air. It may be because that the oxygen in the air reacts with some species in the solution, which then accelerate the reaction. From this assumption, we can expect that the more air we give, the shorter the induction time is, or the more N₂ we give, the longer induction time is. Interestingly, the experimental observation is different from the assumption, implying that more than one factor may be responsible here. The volatile species like Br₂ in the solution could be affected by the flow rate of the gas. Increasing the flow rate of N₂ reduces the induction time, it may be because the volatile Br₂ is brought up into the air and lost from the solution so that some process is slow down. For the air, it exhibits different trend, it may be due to the competition of the factors of O₂ and Br₂.

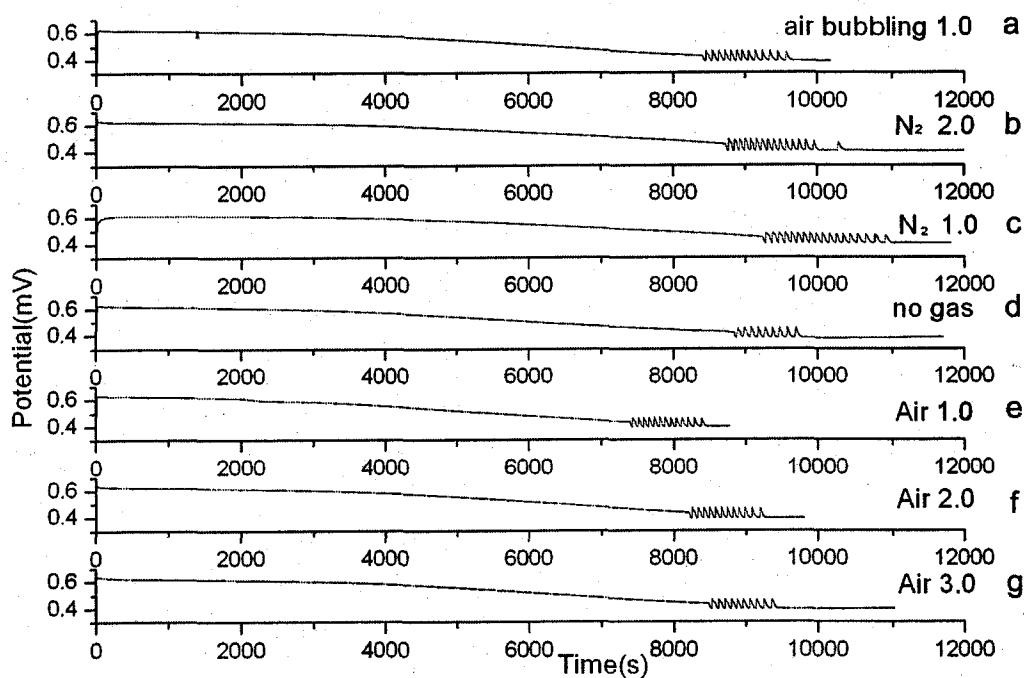


Figure 3.15 The influence of N_2 /Air purging on the reaction behavior. (a) air bubbling 1.0 Reaction conditions are $[Q] = 0.02M$, $[H_2SO_4] = 1.8M$, $[NaBrO_3] = 0.05M$, $100\%I_0$, total volume 30ml, stirring rate 700 RPM, N_2 or Air, $20^\circ C$.

Another mechanical factor, stirring rate, is also studied here and the result is shown in Figure 3.16. With increasing the stirring rate, the amplitude of oscillation is significantly increased. The induction time of the one with the stirring rate of 700RPM is obviously shorter than the ones at 500RPM and 300RPM. These phenomena indicate that mechanical stirring has important influence on the reaction behavior. Such influences may occur in the same way as discussed in Chapter 2.

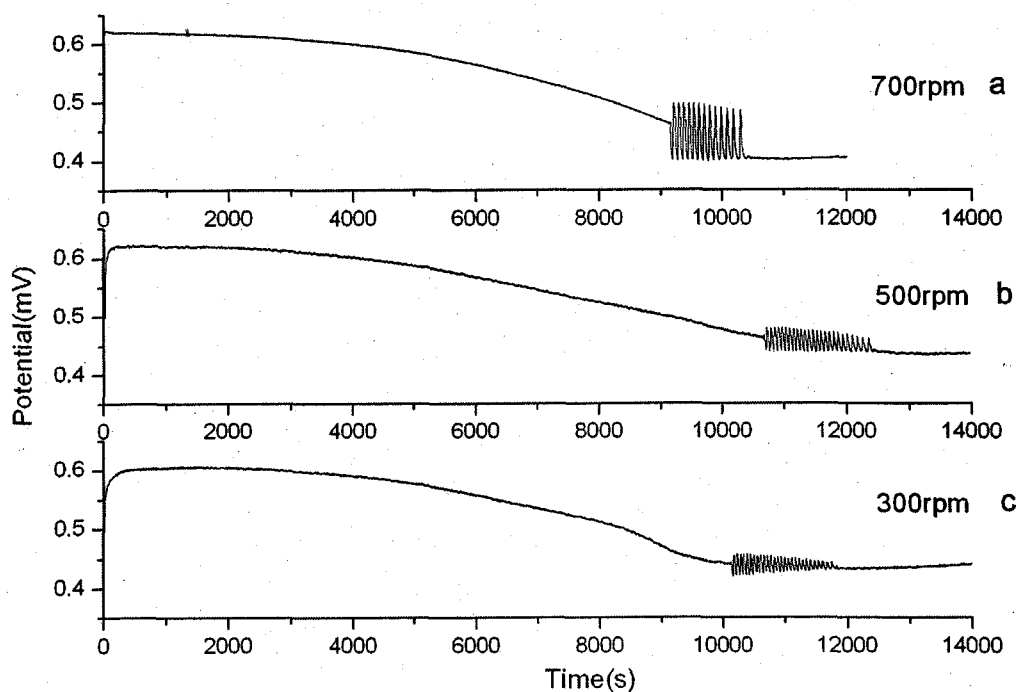


Figure 3.16 The influence of stirring on the oscillations. (a) 700RPM, (b) 500RPM and (c) 300RPM. Reaction conditions are $[Q] = 0.02\text{M}$, $[\text{H}_2\text{SO}_4] = 1.8\text{M}$, $[\text{NaBrO}_3] = 0.05\text{M}$, $100\%I_0$, total volume 30ml, stirring rate 700 RPM, N_2 protection and $T = 25^\circ\text{C}$.

3.3.2 The influence of $[\text{Br}^-]$

To gain insights into the underlying reaction mechanism, Br^- selective electrode is also employed. Oscillations of Br^- species are observed as shown in Figure 3.17 b. Figure 3.17 illustrates that the oscillation time, frequency and peak numbers in the Pt potential and Br^- concentration are coincident with each other, yet there is a phase difference between the two oscillations. The amplitude of the oscillation in Figure 3.17b is much smaller than the one monitored with Pt electrode. Measurements with the bromide

selective electrode also show that Br^- concentration increases steadily during the induction period and starts oscillating toward higher concentrations (i.e. lower potential value) after it reaches a threshold value. A possible explanation for the above observation is that during the induction period the production of Br^- , an inhibitor of the autocatalytic reaction between Q and bromate, is not faster enough to quench the autocatalytic process. As more and more Br^- precursor is produced through Q and bromate reaction, the Br^- production eventually reaches a level where it can compete with the autocatalysis.

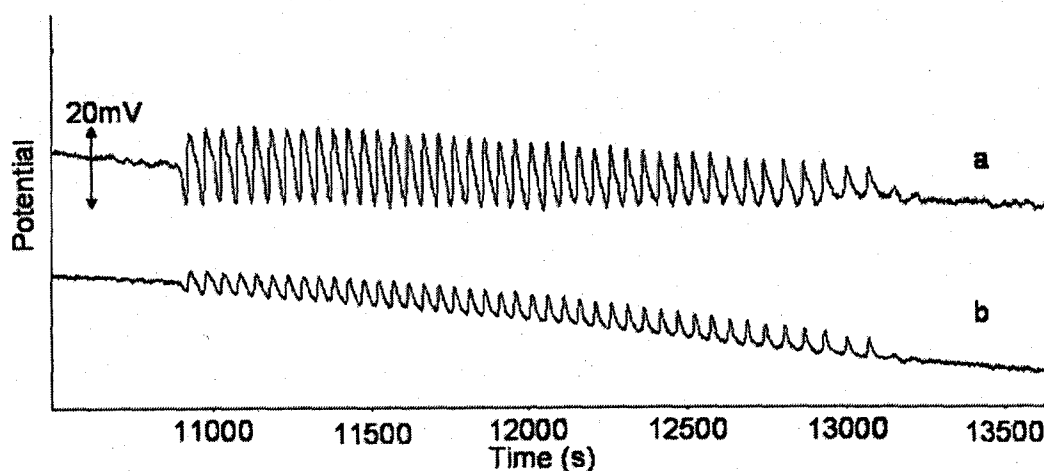


Figure 3.17 Oscillations monitored simultaneously by Pt electrode (a) and by Br^- -selective electrode (b). Reaction conditions are $[\text{Q}] = 0.02\text{M}$, $[\text{H}_2\text{SO}_4] = 1.8\text{M}$, $[\text{NaBrO}_3] = 0.05\text{M}$, $100\%I_0$, stirring rate 700 RPM, N_2 protection and $T = 25^\circ\text{C}$.

The observation of Br^- oscillations leads us to speculate that this new photochemical oscillator may also be Br^- -controlled, similar to other bromate based oscillations. In order to study the influence of Br^- precursor in the system, some effort is

taken by adding different concentrations of Br_2 initially into the solution which is conducted by mixing certain amount of NaBr . The solution turns to orange color after the addition of Br^- , indicating that Br_2 is formed due to the reaction behavior between Br^- and BrO_3^- . Figure 3.18 presents the differences of the oscillation with different concentration of Br_2 . First of all, the induction time of the oscillation increases from 11266s to 20205s when Br_2 concentration is increased from 0.001M to 0.01M. The amplitude of the oscillation is also reduced significantly. Moreover, potential changes at the beginning of the reaction are very different from the one without the presence of Br_2 initially (see in Figure 3.7). These phenomena indicate that Br_2 do play a significantly role in the oscillation system, confirming that the accumulation of QBr may be responsible for the long induction time in the bromate-Q oscillator. Considering that adding Br_2 at the beginning may consume Q to form QBr or QBr_2 , which consequently alternates the reaction condition, Br_2 and Q were added together at the ratio of 1:2, which is equivalent to add QBr initially. Comparing Figure 3.18a and 3.18d, Figure 3.18b and 3.18e, we can see that the extra amounts of Q help to reduce the induction time in comparison to the one with the addition of only Br_2 .

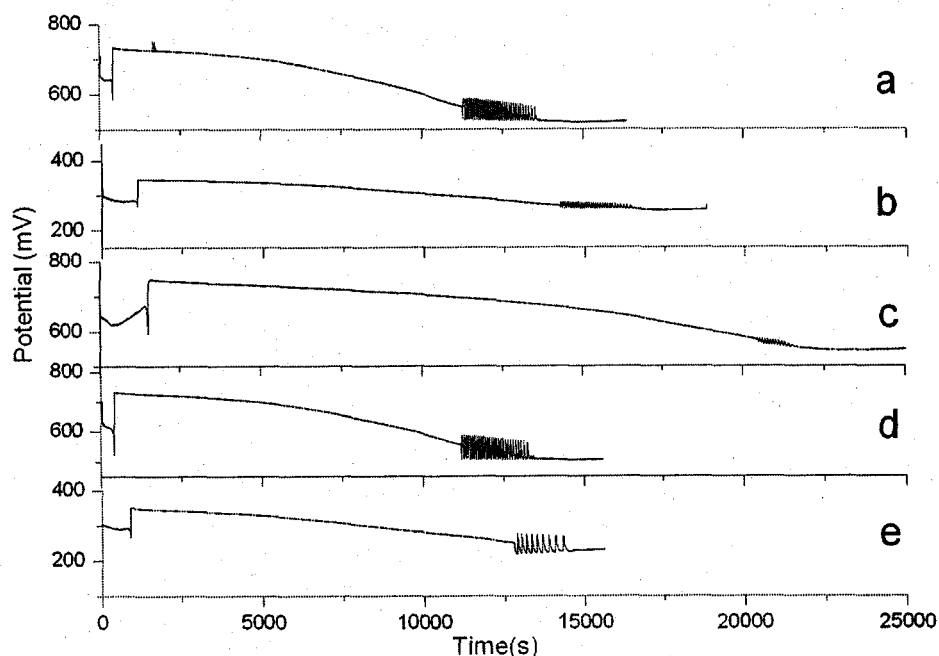


Figure 3.18 Reaction behaviors in the presence of different concentrations of Br_2 initially. (a) $[\text{Br}_2] = 0.001\text{M}$, induction time 11266s, (b) $[\text{Br}_2] = 0.005\text{M}$, induction time 14217s, (c) $[\text{Br}_2] = 0.01\text{M}$, induction time 20334s, (d) $[\text{Br}_2] = 0.001\text{M}$, extra $[\text{Q}] = 0.002\text{M}$, induction time 11197s, (e) $[\text{Br}_2] = 0.005\text{M}$, extra $[\text{Q}] = 0.01\text{M}$, induction time 12763s. Other reaction conditions are $[\text{Q}] = 0.02\text{M}$, $[\text{H}_2\text{SO}_4] = 1.8\text{M}$, $[\text{NaBrO}_3] = 0.05\text{M}$, 100% I_0 , stirring rate 700 RPM, N_2 protection and $T = 25^\circ\text{C}$.

MA is introduced to the above reaction system to affect the accumulation of QBr. It is well known that bromine can react with malonic acid to produce bromomalonic acid. Our separate measurements indicate that bromine reacts faster with MA than with H_2Q . In this way, the competition of forming QBr and BrMA is introduced, which may

consequently result in different reaction behavior. The experimental results are shown in Figure 3.19. The oscillation duration and oscillation amplitude was decreased with the increasing amount of MA added. On the other hand the induction time increases with more addition of MA.

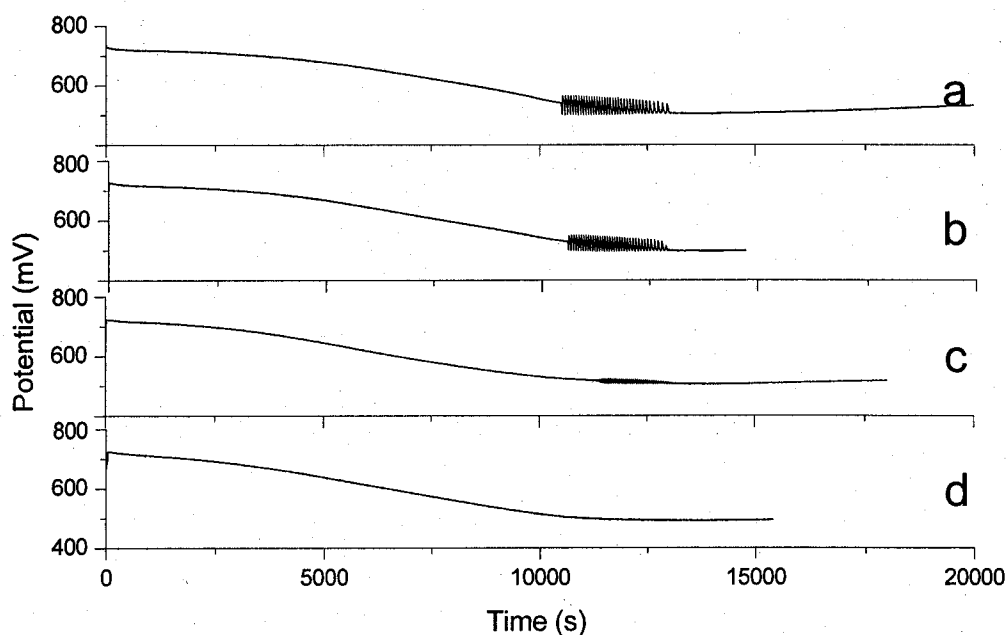


Figure 3.19 The study of influence of adding malonic acid (a) $[MA] = 0.01M$, (b) $[MA] = 0.02M$, (c) $[MA] = 0.05M$, (d) $[MA] = 0.06M$. Other reaction conditions are $[Q] = 0.02M$, $[H_2SO_4] = 1.8M$, $[NaBrO_3] = 0.05M$, $100\%I_0$, stirring rate 700 RPM, N_2 protection and $T = 25^\circ C$.

The role of Br^- ion in the system was further investigated with the quenching method. Figure 3.20 presents responses of the bromate-Q oscillator to Br^- perturbation, in which both the Pt potential and the potential of Br^- selective electrode are presented. The sudden

increase of Br^- concentration, which is reflected as an abrupt decrease in the Br^- potential, temporarily stops the oscillatory behavior. After the perturbation, the concentration of Br^- decreases slowly and oscillations resume after $[\text{Br}^-]$ becomes smaller enough. As is indicated in Figure 3.20b, it does not require Br^- concentration to recover to the level before the perturbation takes place in order to get the oscillations back. It is interesting to point out that after a large Br^- perturbation being applied, oscillations resume with a large peak and then the amplitude of oscillation decreases gradually. This is opposite to the response of the system to a small Br^- perturbation (see the last two perturbations in the figure), where amplitude of the resumed oscillation increases gradually. Notably, toward the end of the oscillatory window, where dynamics of the oscillator is close to a bifurcation point, a small peak is observed after Br^- perturbation. Such a scenario is similar to the quenching experiments conducted near a supercritical Hopf-bifurcation point in a CSTR. Results shown in this figure confirms that, similar to other bromate-based oscillators, oscillations in this photo-mediated bromate-Q reaction is also Br^- controlled.

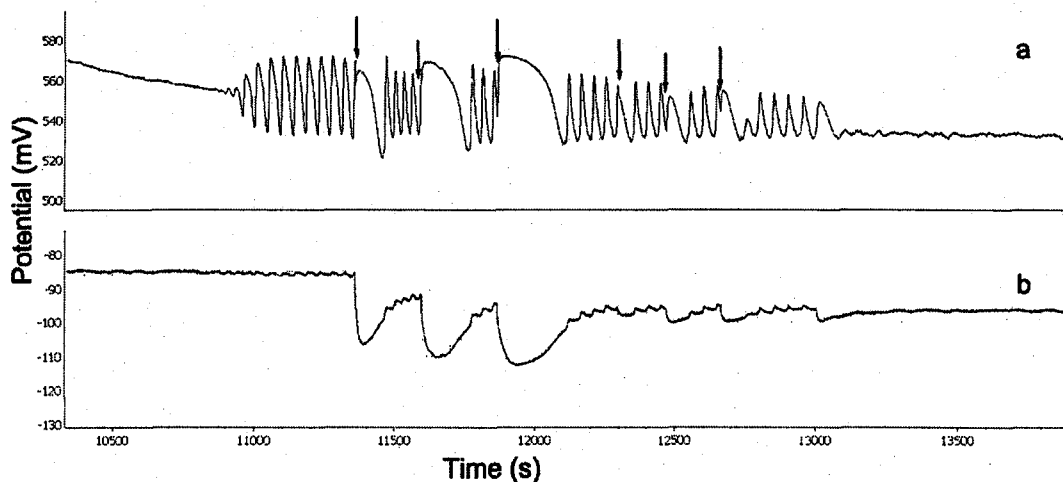


Figure 3.20 Perturbation study by adding Br^- at different phase angles using a syringe (Hamilton 25 μL); the first three perturbations are the addition of 2 μL 0.01M NaBr each time; the last three perturbations are 4 μL 0.001M NaBr each time, (a) monitored by Pt electrode, (b) monitored by Br^- selective electrode. The reaction conditions are $[\text{Q}] = 0.02\text{M}$, $[\text{H}_2\text{SO}_4] = 1.8\text{M}$, $[\text{NaBrO}_3] = 0.05\text{M}$, 100% I_0 , stirring rate 700 RPM, and $T = 25^\circ\text{C}$.

Figure 3.21 demonstrates the response of the system to the addition of different amounts of NaBr. With the addition of a moderate amount of NaBr, 10 μL 0.01M, the oscillation revived, but experienced a longer quiescent time than the one with 2 μL addition of NaBr (see in Figure 3.20). After the second addition of NaBr in Figure 3.21 a, the oscillation doesn't come back immediately after the potential falls down to the flat bottom, some small oscillations appear first, followed by larger oscillations. When the addition of 0.01M NaBr is increased to 25 μL , similar potential changes happen, but the

oscillation never recovers, which indicates that the perturbation of Br^- is excessive.

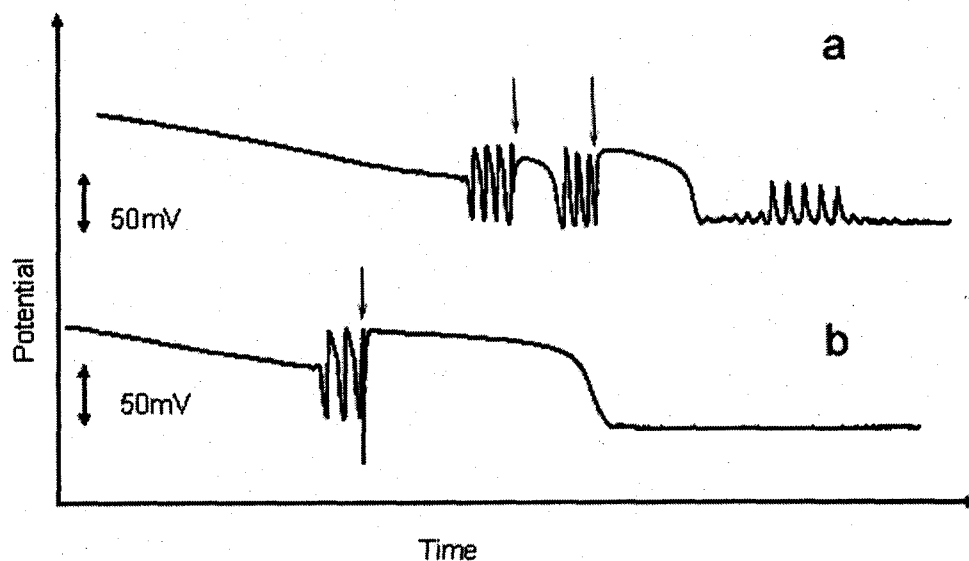


Figure 3.21 Perturbation study by adding (a) 10 μL and (b) 25 μL 0.01M NaBr at different phase angles at the condition of $[\text{Q}] = 0.02\text{M}$, $[\text{H}_2\text{SO}_4] = 1.8\text{M}$, $[\text{NaBrO}_3] = 0.05\text{M}$, $100\%I_0$, stirring rate 700 RPM, and $T = 25^\circ\text{C}$.

3.3.3 The study of a pulse-light perturbation

Since this oscillator is greatly affected by light, a series of investigation was conducted to examine the response of the system to the temporal changes of light illumination during a reaction process. Figure 3.22 presents the revival of oscillation by reducing the light intensity. $100\%I_0$ illumination is employed from the beginning of the experiment. After the oscillation disappears, light intensity is reduced to $90\%I_0$, but the oscillation doesn't come back. Reducing the intensity further to $80\%I_0$, the potential jumps up immediately and two peaks appear. Keep on reducing to $70\%I_0$, the potential

rises to a higher level with one small peak.

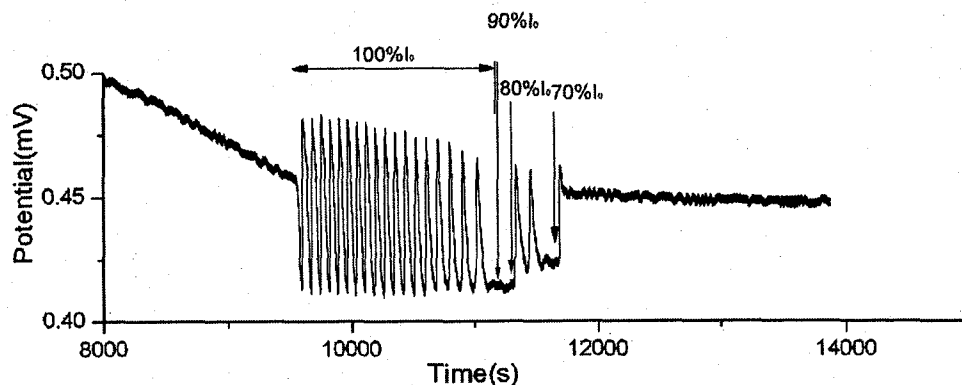


Figure 3.22 Oscillation is revived by reducing light intensity at the end of the oscillation window. Reaction conditions are $[Q] = 0.02\text{M}$, $[\text{H}_2\text{SO}_4] = 1.8\text{M}$, $[\text{NaBrO}_3] = 0.05\text{M}$, $100\%I_0$, total volume 30ml, stirring rate 700 RPM, and $T = 25^\circ\text{C}$.

In order to better understand the chemical influence of light and overcome the limitation of the light intensity of one halogen lamp, two sets of halogen lamps with four light fibers are introduced to change the total light intensity (see in Figure 3.23). Initially, one set of halogen lamp with two light fibers are used at $100\%I_0$ to produce the oscillation. After three peaks of oscillation, one more light fiber at $100\%I_0$ from another halogen lamp is introduced to illuminate the solution. A significant increase in amplitude is observed. Adding another light fiber at $100\%I_0$ further increases the oscillation amplitude of oscillation. Removing one light fiber, the amplitude of the oscillation is reduced accordingly, which indicates that stronger light intensity could enhance the

amplitude of oscillation. With three light fibers, the oscillation only lasts for another two peaks and then disappears. Afterwards removing one light fiber revived the oscillatory behavior.

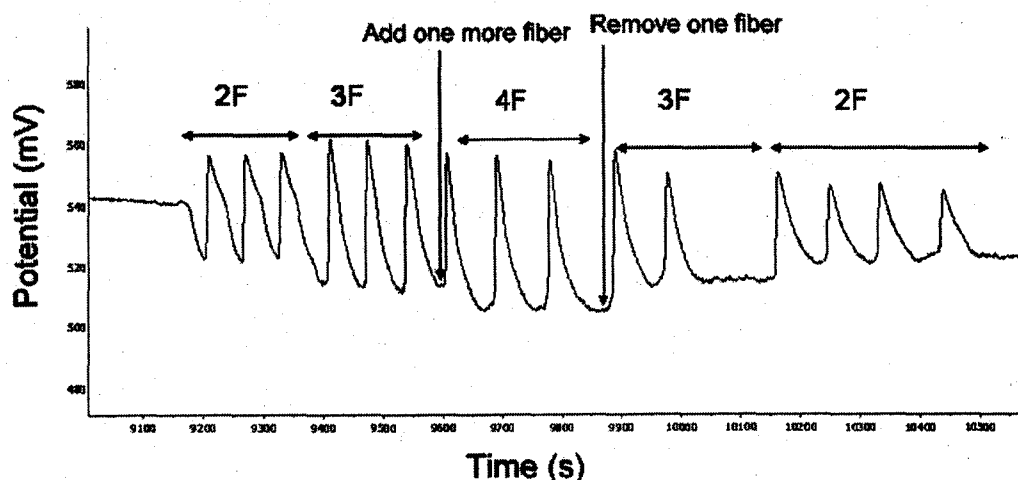


Figure 3.23 Oscillations under different light intensities. Other reaction conditions are $[Q] = 0.02\text{M}$, $[\text{H}_2\text{SO}_4] = 1.8\text{M}$, $[\text{NaBrO}_3] = 0.05\text{M}$, $100\%I_0$, total volume 30ml, stirring rate 700 RPM, and $T = 25^\circ\text{C}$.

In the system studied here, we assumed that the light-induced production of H_2Q , i.e. reaction $Q + 2\text{H}^+ \xrightarrow{h\nu} \text{H}_2\text{Q}$, is responsible for the reactivity. To shed light on the above reaction process, some preliminary exploration of light wavelength dependence is conducted here with narrow band filters (Melles Griot Filters). One set of halogen lamp with two light fibers are used to produce the oscillation as usual. Two more light fibers from another halogen lamp are placed against the optical filter so that the filtered light could illuminate the system as an addition. The influence of additional illumination at different wavelength is shown in Figure 3.24 and summarized in Figure 3.25 and Table

3.2, in which the amplitude and the number of oscillation are summarized in Table 3.2.

The relationship of wavelength vs amplitude, wavelength vs peak numbers and amplitude vs peak numbers are plotted in Figure 3.25 b, c and d.

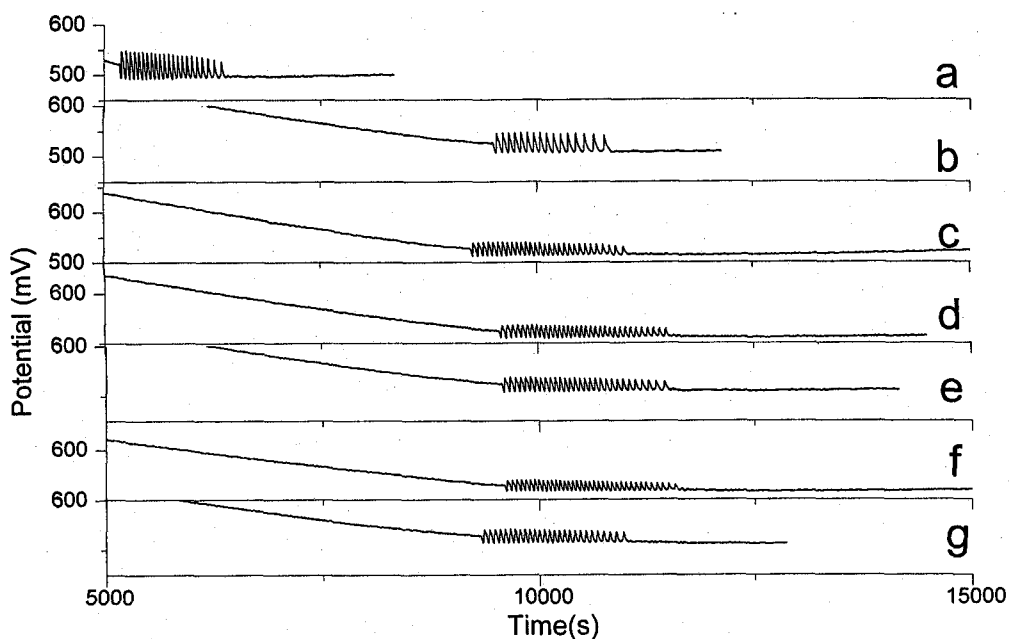
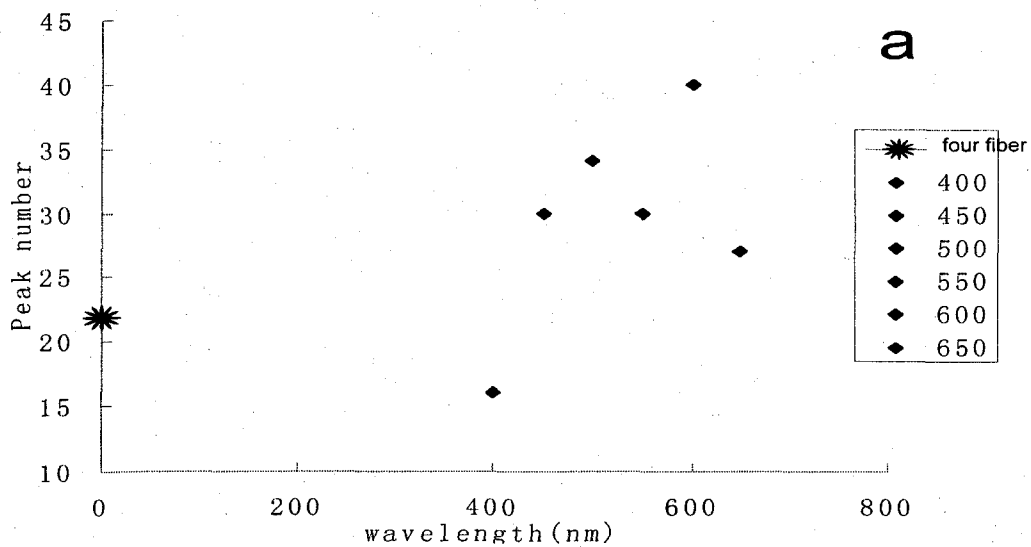


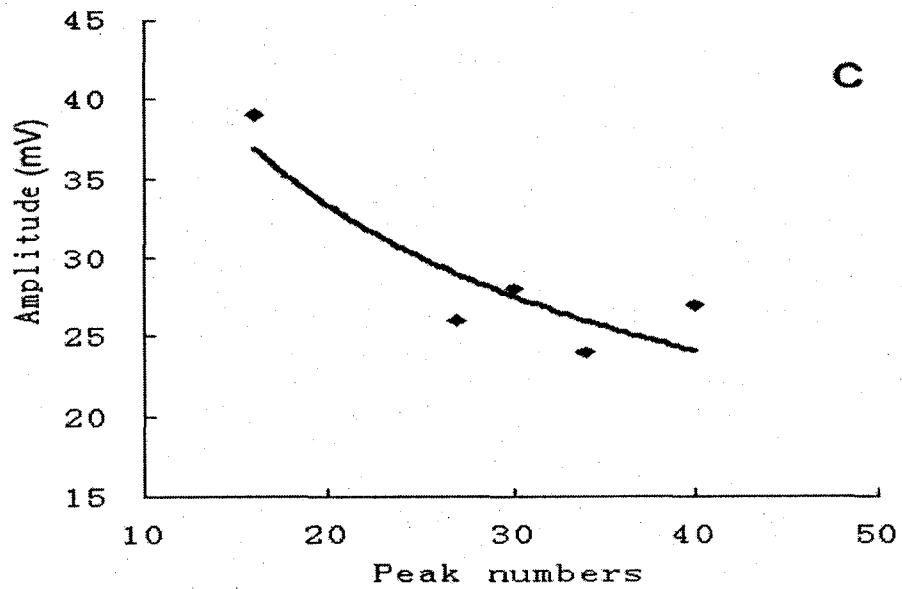
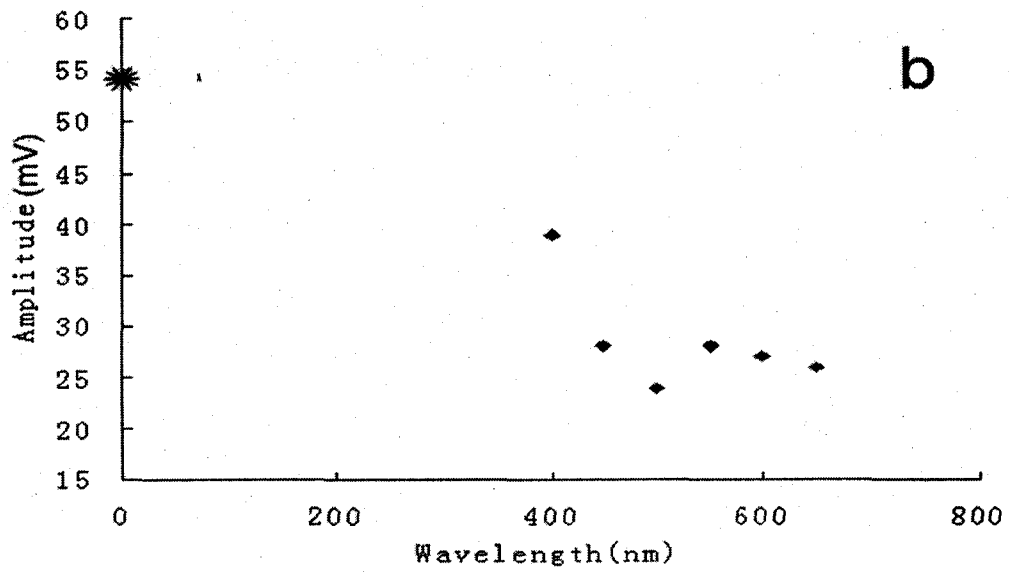
Figure 3.24 Oscillation with additional illumination at different wavelength range (a) using four light fibers to illuminate. The illumination for others are using two light fibers illuminate directly and another two fiber filtered with a narrow band filter which allows the light to pass through at the wavelength of: (b) 400nm, (c) 450nm, (d) 500nm, (e) 550nm, (f) 600nm, (g) 650nm. Other reaction conditions are $[Q] = 0.02M$, $[H_2SO_4] = 1.8M$, $[NaBrO_3] = 0.05M$, $100\%I_0$, total volume 30ml, stirring rate 700 rpm, and $T = 25^\circ C$.

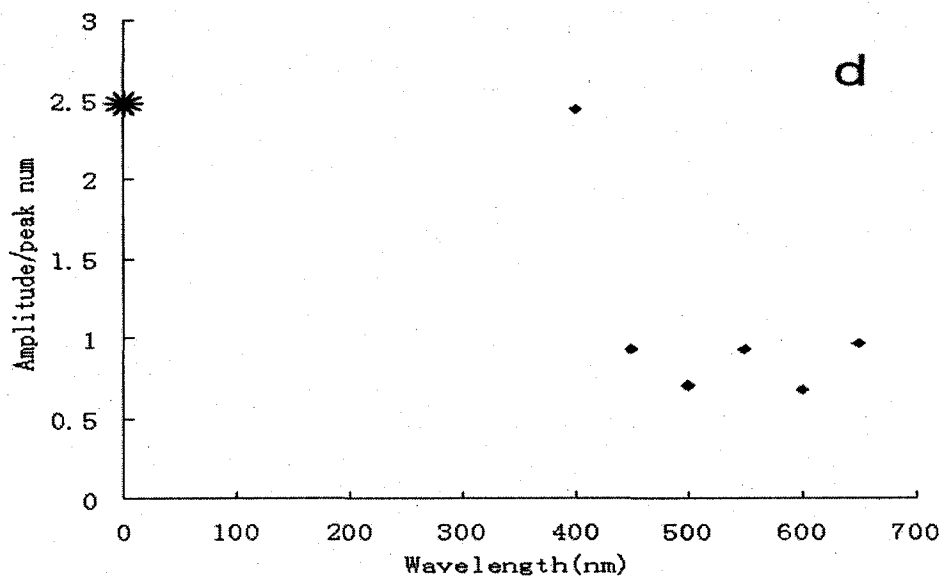
Table 3.2 The peak number and amplitude of oscillation at different wavelengths.

Wavelength(nm)	Peak numbers	amplitude(mV)max
0(four light fibers without using light filter)	22	54
400 (10nm)	16	39
450 (10nm)	30	28
500 (40nm)	34	24
550 (40nm)	30	28
600 (40nm)	40	27
650 (10nm)	27	26

Figure 3.25 Results analysis for Figure 3.24. (a) The relation of the number of peak vs the central wavelength of the band filters. (b) The relation of the amplitude vs the central wavelength of the narrow band filters. (c) The relation of the amplitude vs the peak number. (d) The relation of amplitude/ peak number vs the wavelength of the narrow band filters. (see below)







Figures 3.25a, b and d show that the oscillation amplitude and the number of oscillation peaks at the wavelength of 400nm of the additional illumination are very different from the ones at other wavelengths. The oscillation with additional illumination at 400nm has the least numbers of peak (only 16), but the highest amplitude of oscillation. It indicates that the additional illumination at 400nm is more effective than illuminations from other wavelengths to affect this reaction system. As is illustrated in Figure 3.34, Q has an absorption peak at around 400nm. Therefore the above study supports the light-induced production of H₂Q from Q.

3.3.4 Perturbations with radical scavenger

Perturbations by ethanol, a radical scavenger, are presented in Figure 3.26, in which the presence of ethanol reduces the amplitude of oscillation. After adding 5uL and 10uL

1%(V/V) ethanol solution, the amplitude of the oscillation decreased obviously. When adding 25 μL 1%(V/V) ethanol, the oscillation immediately stops. As is shown in the figure, the influence of adding ethanol is irreversible. This is an essential difference from perturbations of Br^- . Our experiments show that effects of ethanol do not depend on the oscillation phase when the perturbation is applied. The above results suggest that radical reactions play an important role in the bromate-Q oscillator. This observation is consistent with the mechanism proposed for the 1,4-cyclohexanedione-bromate reaction, in which H_2Q reacts with bromine dioxide to form H_2Q radicals which undergo subsequent reaction with bromine dioxide radicals to complete an autocatalytic cycle. In addition to the potential effect on bromine dioxide radicals, the presence of ethanol may hinder the overall autocatalytic cycles by removing H_2Q radicals, which consequently reduces the amplitude of oscillation.

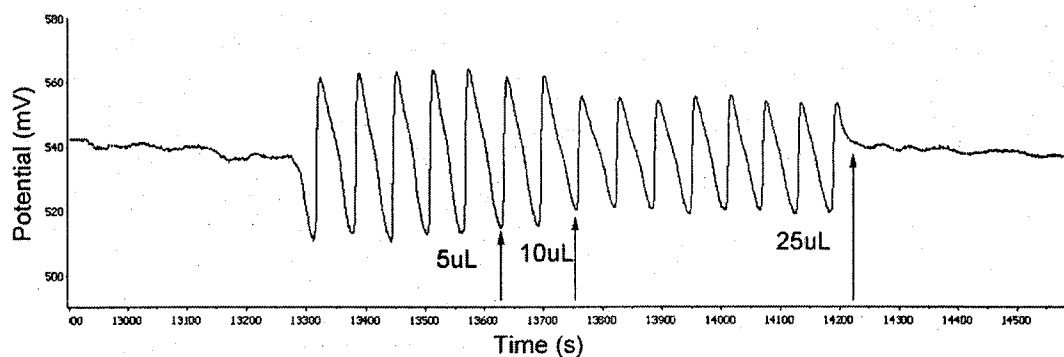


Figure 3.26 Response of the reaction behavior to the addition of 1%(V/V) ethanol. monitored by Pt electrode, Reaction conditions are $[\text{Q}] = 0.02\text{M}$, $[\text{H}_2\text{SO}_4] = 1.8\text{M}$, $[\text{NaBrO}_3] = 0.05\text{M}$, $100\%I_0$, total volume 30ml, stirring rate 700 RPM, and $T = 25^\circ\text{C}$.

If adding small amount of ethanol(1:100) initially (see in Figure 3.27), the starting potential behavior is very different from the one in Figure 3.26. However, there seems no big influence on the oscillation behavior for all of them. This may be due to that ethanol is volatile species which is very easy to lose from the system with mechanical stirring during the induction time.

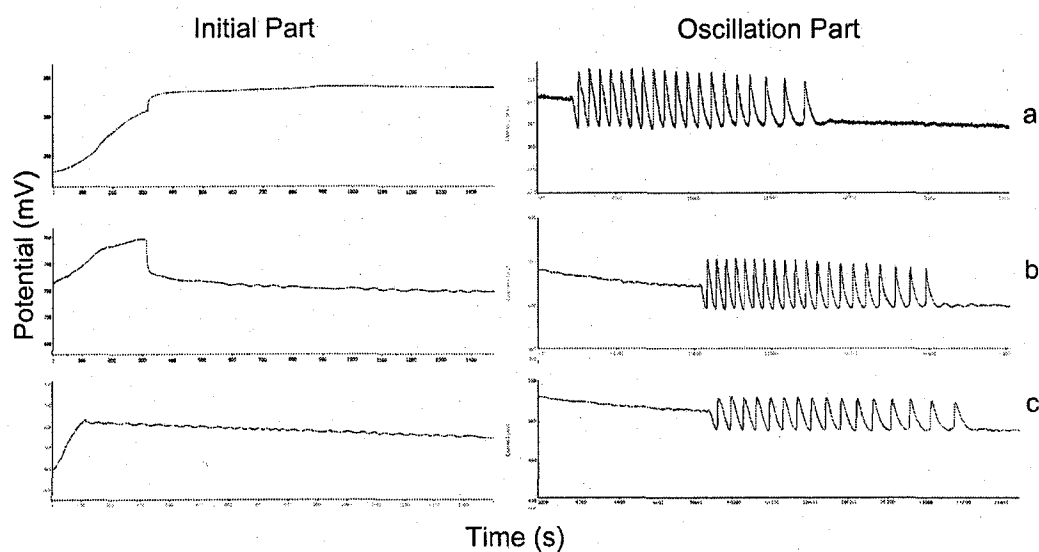


Figure 3.27 Different reaction behaviors with the different addition of 1%(V/V) ethanol at the beginning.(a) 10uL, (b) 25uL, (c) 75uL. Other reaction conditions are $[Q] = 0.02M$, $[H_2SO_4] = 1.8M$, $[NaBrO_3] = 0.05M$, 100% I_0 , total volume 30ml, stirring rate 700 RPM, and $T = 25^\circ C$.

3.3.5 Perturbations with Q

For this new photochemical oscillator, oscillations usually last for about 20min.

Figure 3.28 shows that with the additional of Q, the oscillation could keep on going for at

least 2 hours. During the oscillation, the addition of 20uL 0.02M Q could enhance the amplitude of the oscillation. In the above discussion we postulates that Q is partially converted to products such as 2-bromo-1,4-benzoquinone during the above photochemical process, thus the disappearance of oscillations presumably arises from the depletion of Q. The above hypothesis is supported by adding 0.2 ml or 0.4ml of 0.02M 1,4-benzoquinone to the reaction mixture after oscillations have stopped, which results in the immediate revival of oscillatory behavior (see Figure 3.28). Such a scenario can be repeated for several times. Notably, here there is no induction period, implicating that in addition to light-induced production of 1,4-hydroquinone, accumulations of other reagents are also essential in the occurrence of chemical oscillations. In addition, Figure 3.28 also indicates the great potential of studying this reaction in a CSTR system.

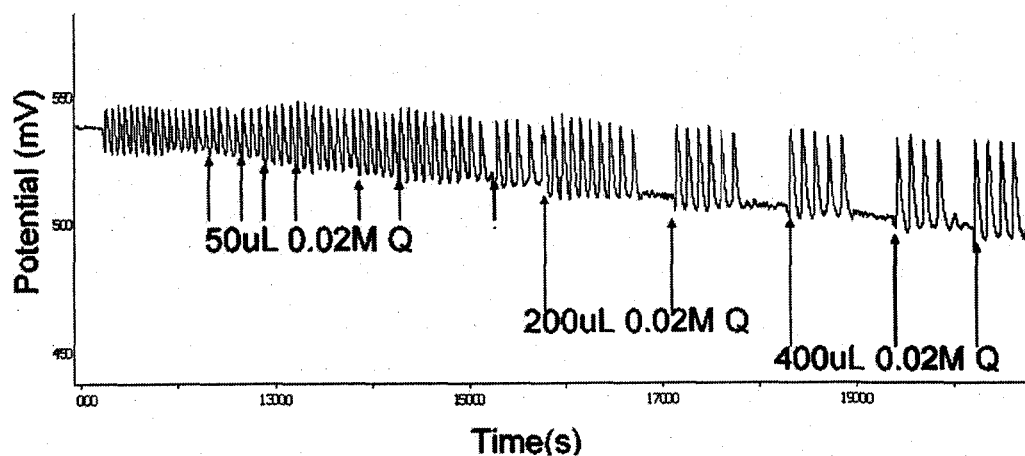


Figure 3.28 The response of the oscillatory system to the addition of Q. The reaction conditions are $[Q] = 0.02M$, $[H_2SO_4] = 1.8M$, $[NaBrO_3] = 0.05M$, 100% I_0 , total volume

30ml, stirring rate 700 RPM, and $T = 25^{\circ}\text{C}$.

3.4 The study in an open system.

Following the above assumption, CSTR experiments are conducted using illumination protocol B, which used the lamp bulb to supply the illumination directly to obtain higher light intensity. The experimental procedure is described in part 2. The reduced volume of 20ml solution is used in order to reduce the induction time. The results are shown in Figure 3.29, in which long period stable oscillation could be obtained. Both the inflow rate and the outflow rate are controlled at 30uL/min to keep the solution volume constant. In principle the oscillation can last as long as fresh chemicals are supplied are supported continuously. Therefore, this provides a good platform for further investigation of this oscillator.

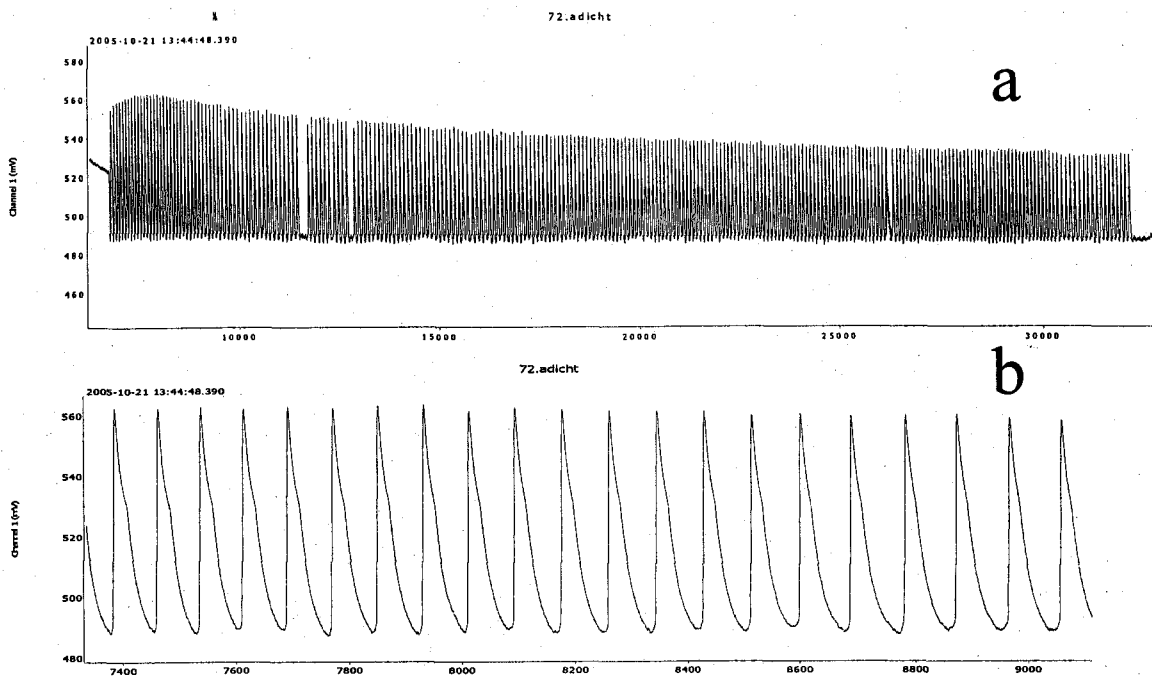


Figure 3.29 CSTR study of 1,4-benzoquinone-bromate-acid photo chemical oscillatory system at the condition of $[Q] = 0.02\text{M}$, $[\text{H}_2\text{SO}_4] = 1.8\text{M}$, $[\text{NaBrO}_3] = 0.05\text{M}$, $100\%I_0$, stirring rate 700RPM, $T = 25^\circ\text{C}$, flow rate 30uL/min. (a) Time series plotted over extended time period.(b) Time series within a short time frame.

As is well known in existing studies, the flow rate demonstrates significant influence on the research dynamics. As are shown in Figure 3.30a to Figure 3.30c, when the flow rate drops from 30uL/min (Figure 3.29a) to 20uL/min (Figure 3.30a), the oscillation behavior changes from regular oscillation into complex oscillations. When it is further decreased to 16uL/min, frequency of oscillation is reduced slightly as shown in Figure 3.30b. Figure 3.30 c indicates that when the flow rate is reduced to 14uL/min, the

oscillation completely disappears. When increasing the flow rate back to 20uL/min, the oscillation recovers again. Also it is observed that the amplitude of the oscillation reduces with the decrease of the flow rate. When the flow rate 30uL/min (see in Figure 3.29a), the amplitude is around 45-75mV. While the flow rate is reduced to 20uL/min and 16 uL/min, the approximate average amplitude changes into 35mV and 30mV respectively.

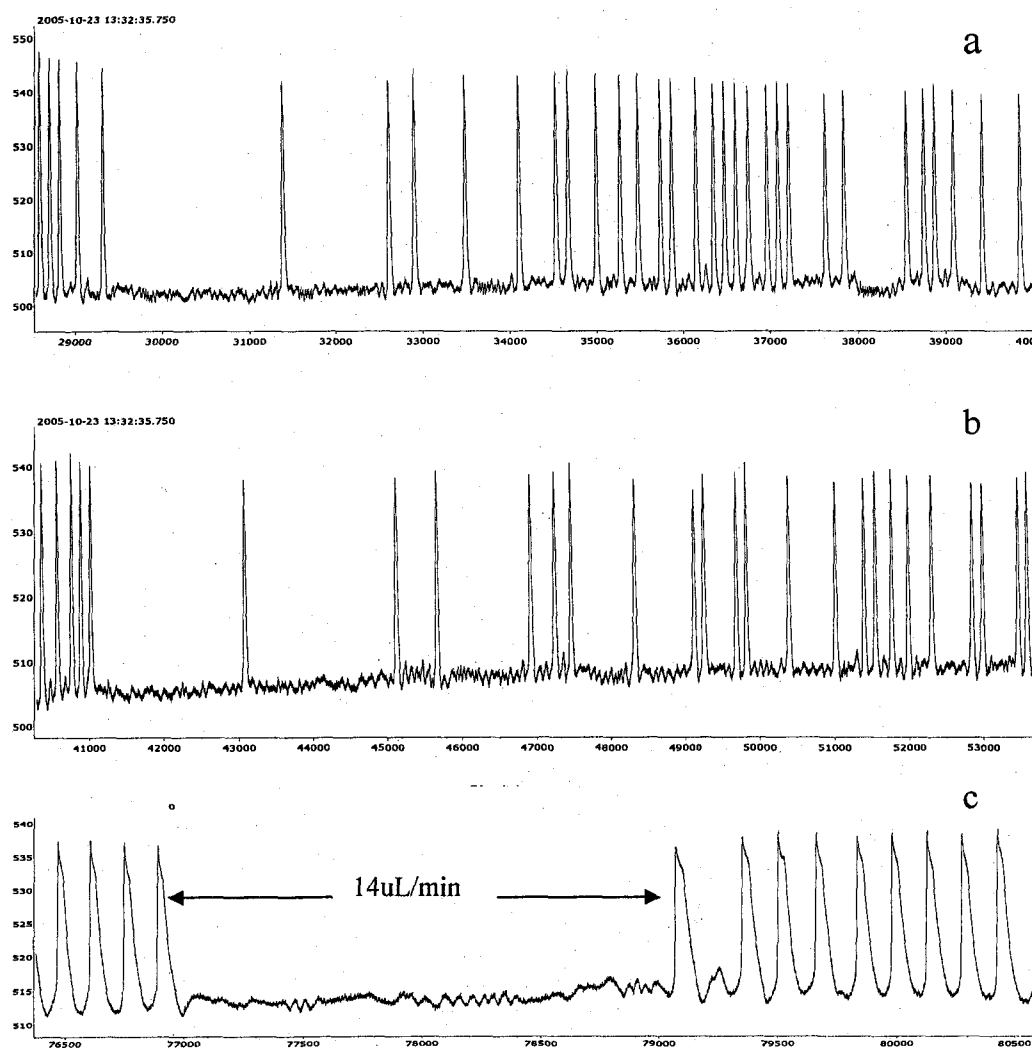


Figure 3.30 CSTR study of 1,4-Benzoquinone-bromate-acid photo chemical Oscillatory System at different flow rates. (a) 20uL/min, the average amplitude is 35mV, (b)

16uL/min, the average amplitude is 30mV, (c) 14uL/min. Other reaction conditions are $[Q] = 0.02\text{M}$, $[\text{H}_2\text{SO}_4] = 1.8\text{M}$, $[\text{NaBrO}_3] = 0.05\text{M}$, $100\%I_0$, stirring rate 700RPM, $T = 25^\circ\text{C}$.

The light perturbation and Br^- perturbation are also conducted in this CSTR system. Figure 3.31 presents the amplitude reduction due to the decrease of light intensity and oscillation revival with the increase of light intensity, which again confirms the light dependence of the reaction behavior. Figure 3.32 shows perturbations with Br^- at different phase angles, which demonstrates similar responses as seen in a closed batch reactor. To obtain successful quenching like reported in the BZ reaction, the reaction conditions need to be further refined to stay close to a bifurcation point. Nevertheless, it shows that this CSTR system is very suitable for the study of control in nonlinear chemistry.

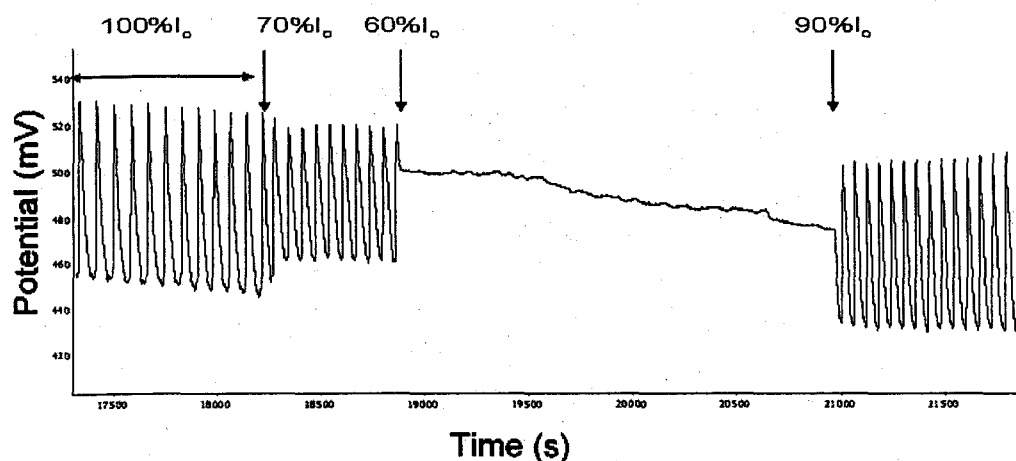


Figure 3.31 Light perturbation in a CSTR at the condition of $[Q] = 0.02\text{M}$, $[\text{H}_2\text{SO}_4] = 1.8\text{M}$, $[\text{NaBrO}_3] = 0.05\text{M}$, $100\%I_0$, stirring rate 700RPM, $T = 25^\circ\text{C}$, and flow rate

30uL/min.

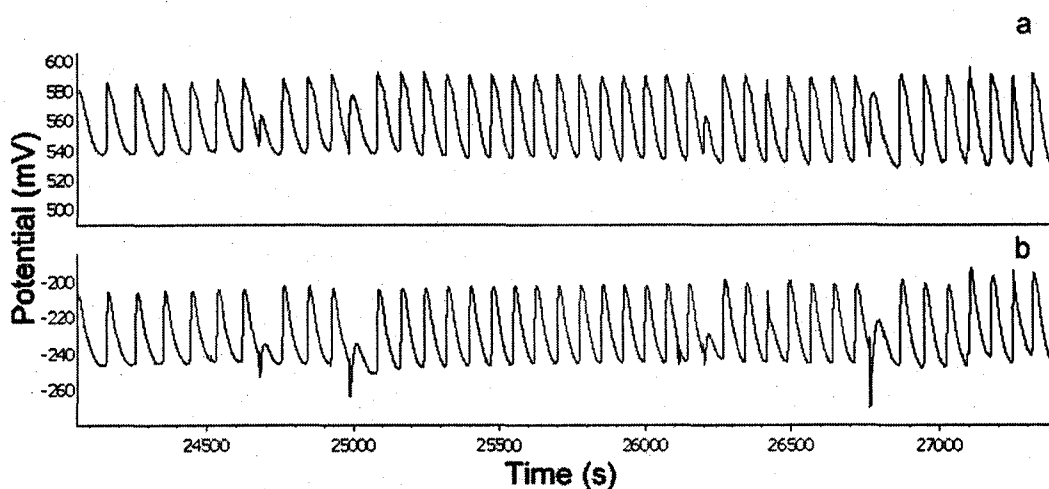


Figure 3.32 Br^- perturbation in a CSTR at the condition of $[\text{Q}] = 0.02\text{M}$, $[\text{H}_2\text{SO}_4] = 1.8\text{M}$, $[\text{NaBrO}_3] = 0.05\text{M}$, $100\%I_0$, stirring rate 700RPM, $T = 25^\circ\text{C}$, flow rate 30uL/min. (a) monitored by Pt electrode, (b) monitored by Br^- selective electrode simultaneously.

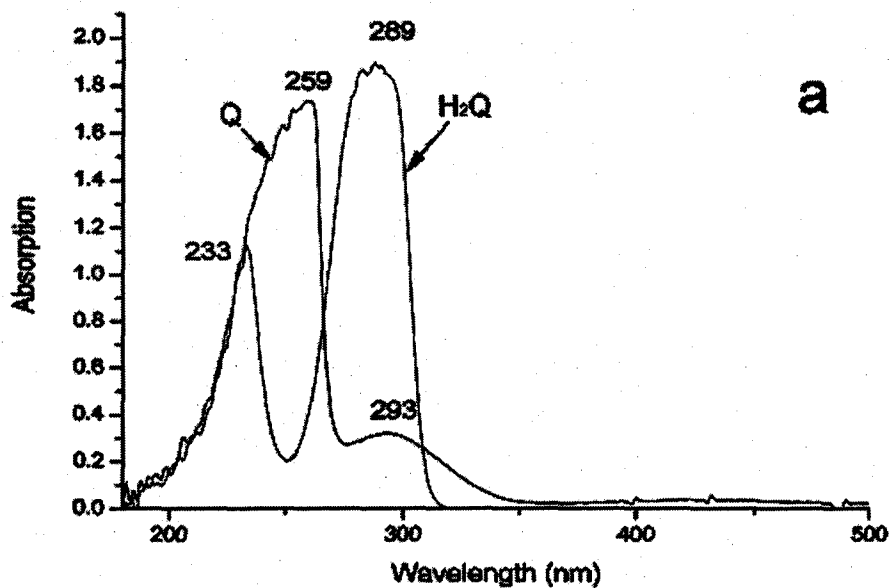
3.5 UV/Visible spectrophotometric measurements

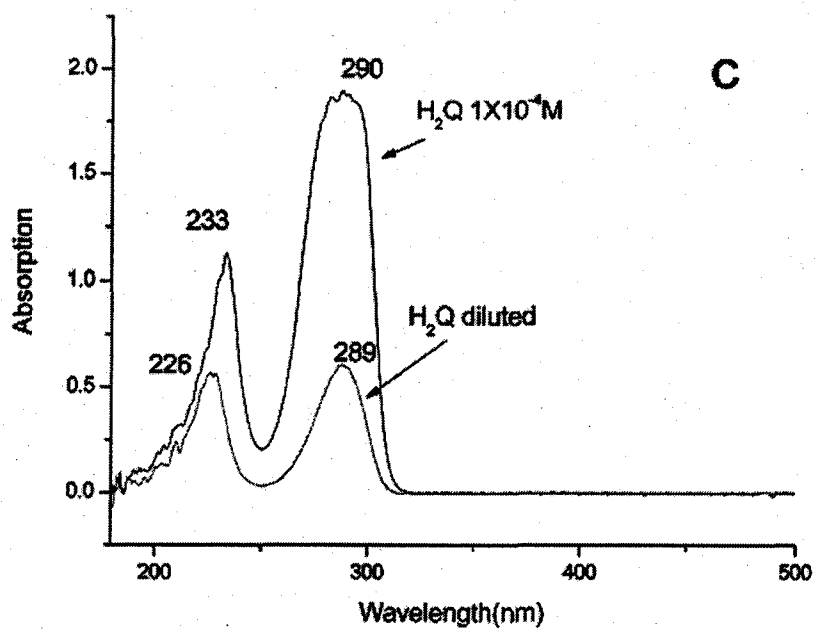
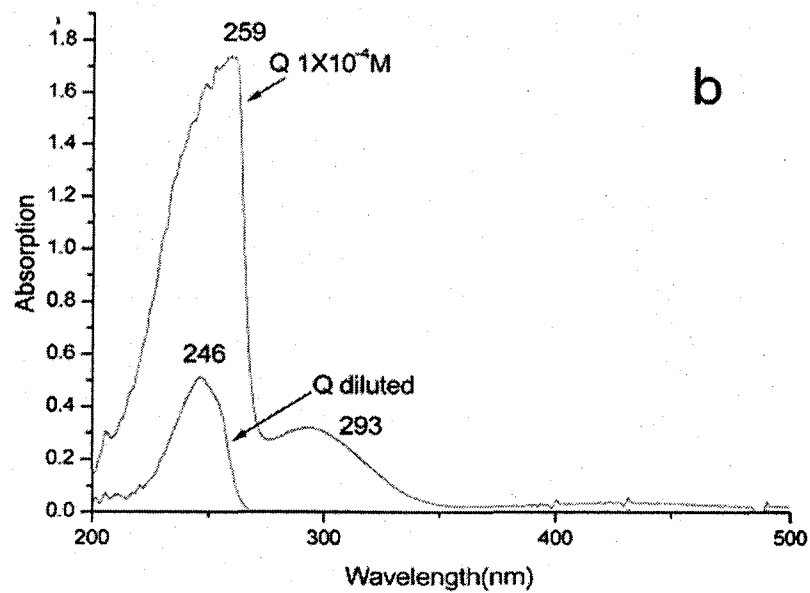
UV/Visible spectrophotometer is used to investigate the mechanism of the bromate-Q. The experimental procedure and equipment set have been described in earlier section.

Figure 3.4 illustrates that the power of the halogen light concentrates within the visible light region. Indeed, in order to raise the light intensity within the UV region, the overall light intensity needs to be increased above $50\%I_0$. On the other hand, the maximum absorption peaks of Q and H_2Q falls in the range of 200nm~300nm(see in Figure 3.33). The mismatch between the maximum absorptions of Q and H_2Q and the

light distribution of halogen bulb could be responsible for the strong light illumination required in this study.

Figure 3.33 UV-visible Spectrum of diluted solution of Q and H₂Q. (a) UV-visible of spectra of Q and H₂Q at 1×10^{-4} M, (b) The comparison of the spectra plot of Q at the concentration of 1×10^{-4} M and approximately 2×10^{-5} M, (c) The comparison of the spectra plot of H₂Q at the concentration of 1×10^{-4} M and approximately 2×10^{-5} M. (see below)





The spectra of Q and H_2Q under different concentrations were obtained in order to characterize the UV/Visible spectra of the oscillatory system. Figure 3.33a illustrates

the absorption of Q and H₂Q at 1×10^{-4} M. There is one strong absorption peak for Q at 259nm and a weak one at 293nm. H₂Q has one strong absorption peak at 289nm and a smaller one at 233nm. A overlap exists around 290nm for Q and H₂Q. We also found that the absorption peaks shift slightly after the Q or H₂Q solution was diluted. In Figure 3.33b, the maximum absorption peak at 259nm was significantly reduced and shifted to 246nm, while the weak absorption at 293nm disappeared from the graph. The same thing happened to the absorption of H₂Q after the solution was diluted to 2×10^{-5} M. In Figure 3.33c, the absorption peak at 233nm shifted to 226nm and the absorption peak at 289nm was significantly reduced. The absorption spectra of Q and H₂Q at the experimental concentrations are demonstrated in Figure 3.34. H₂Q at 0.02M mixed with 1.8M H₂SO₄ has a broad absorption from 230nm to 320nm. Notably, the absorption plot dramatically drops at 312nm. While for Q, the first absorption band is obviously broader than the one of H₂Q and there is a weak absorption peak centered at about 428nm.

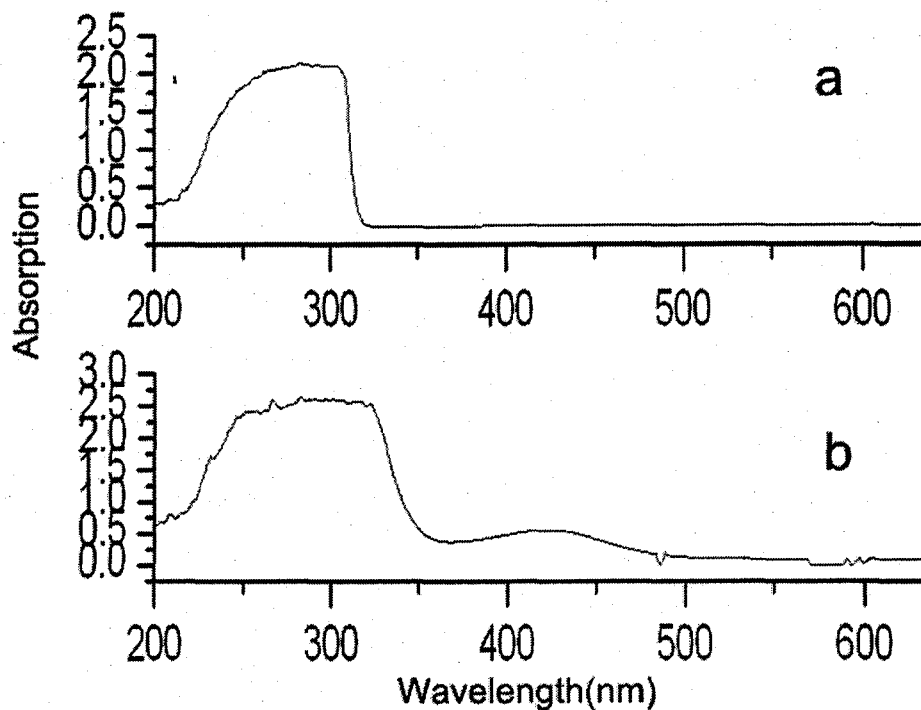
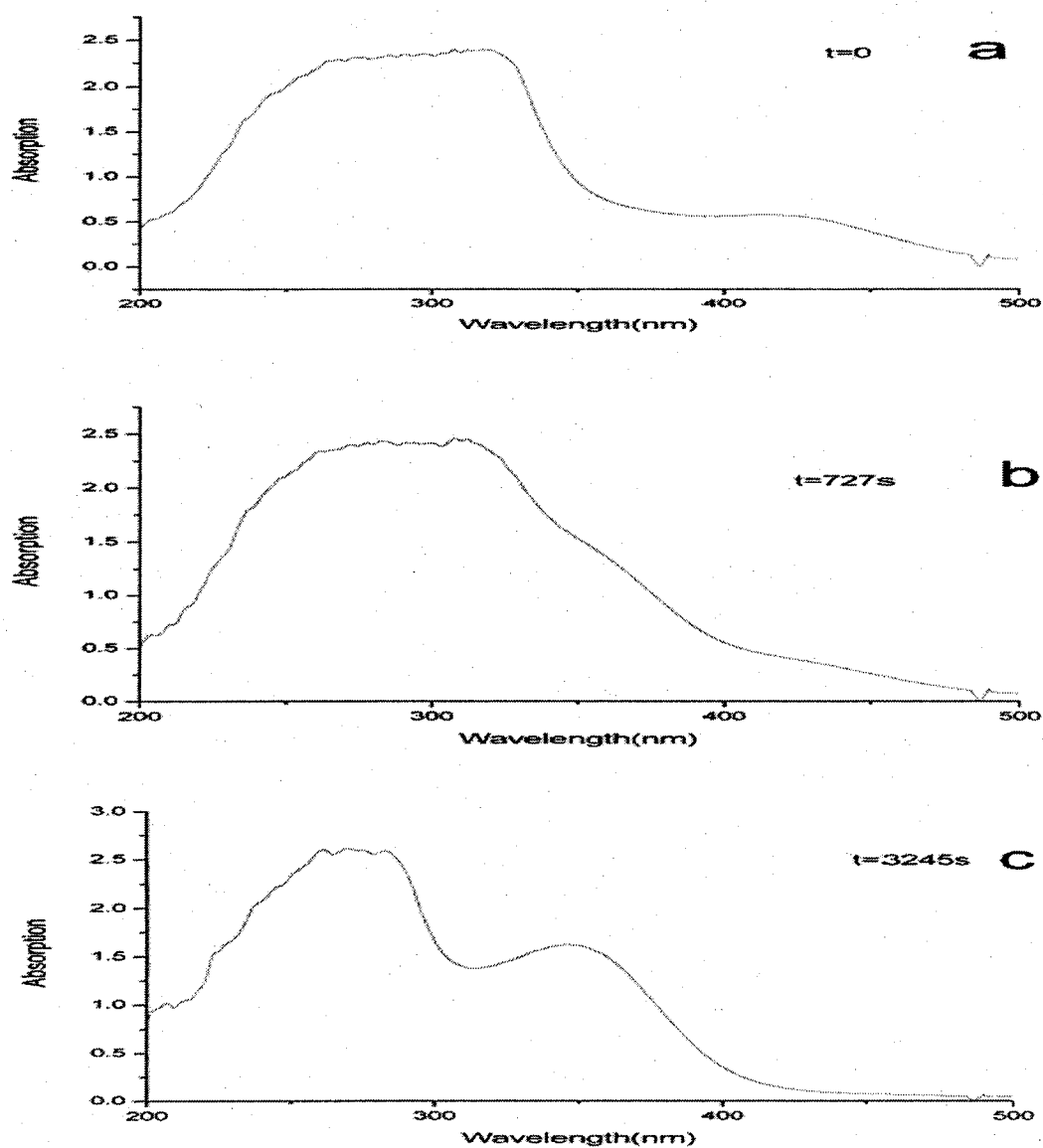


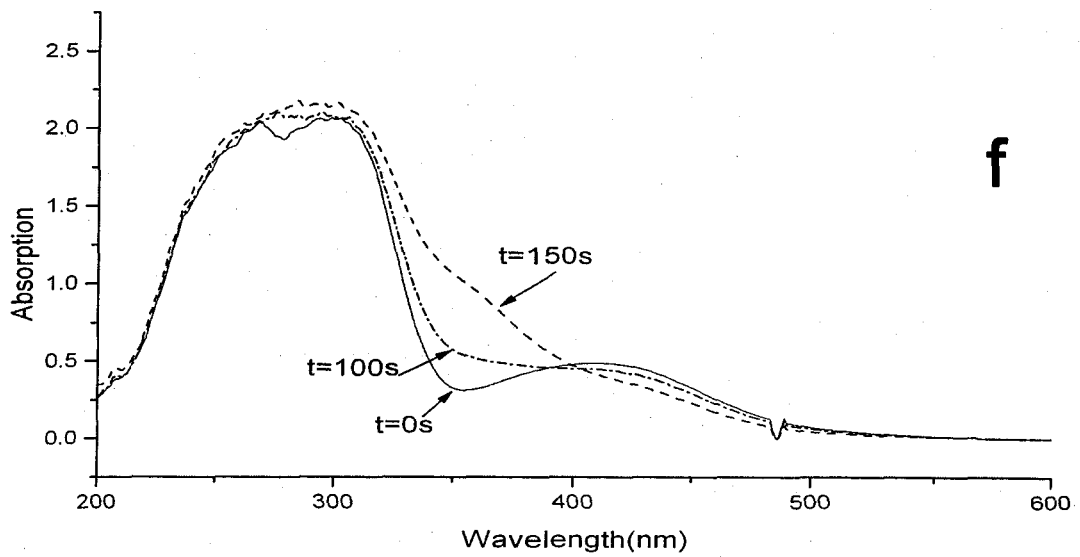
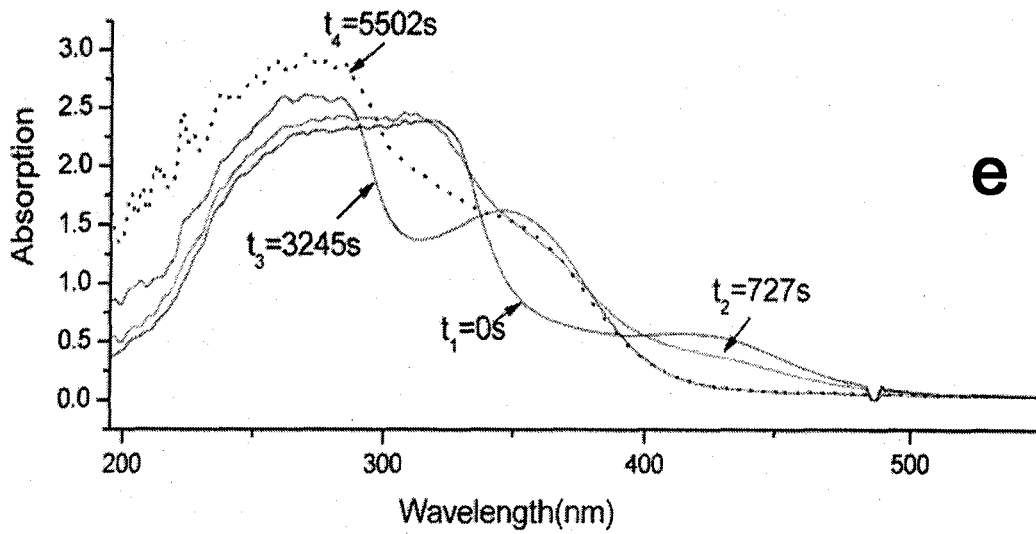
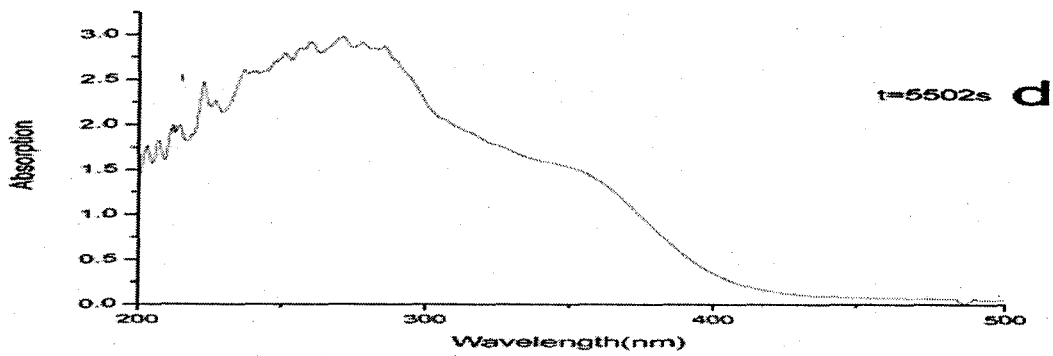
Figure 3.34 UV-visible Spectra of (a) mixed solution of 0.02M H₂Q and 1.8M H₂SO₄, (b) mixed solution of 0.02M Q and 1.8M H₂SO₄.

The absorption spectra collected at the different reaction times were shown in Figure 3.35. The reference experiment was conducted with out illumination, which produced an unchanged absorption spectra for at least 6 hours. It indicates light illumination is an indispensable factor to mediate the reaction in this system. After the single fiber was applied to the solution, the reaction immediately started. There is a dramatic change in the absorption spectra within the first 150s as shown in Figure 3.35f. The absorption at 428 nm quickly reduced and the absorption at around 360nm rapidly increased. It indicated a fast photo-dependent reaction step happened, which could be critical to

produce important species for the oscillation. At $t = 727\text{s}$ (see in Figure 3.35b), the absorption at 428nm has completely disappeared and the absorption at 360nm grew up obviously. When it's close to the oscillation time around 3300s, there are evidently two absorption peaks centered at 273nm and 360nm in Figure 3.35c. After the oscillation disappeared, the absorption at 360nm began to drop slowly and the absorption at 310nm started to grow. Comparisons of the above spectra are summarized in Figure 3.35e. It's obvious to see that the compositions of the reaction system keep on changing from beginning to the end. Another evidence is that the color of the solution keeps on reducing from dark yellow to colorless in time. The initial species Q (yellow) is changed into other colorless species. The other absorption band in Figure 3.35d could be due to the side product of the reaction.

Figure 3.35 UV-visible spectra collected at different reaction time. (a) $t = 0$ s, (b) $t = 727$ s, (c) $t = 3245$ s, (d) $t = 5502$ s, (e) the comparison of above spectras. (f) The fast reaction at the beginning. The reaction conditions are $[Q] = 0.02\text{M}$, $[\text{H}_2\text{SO}_4] = 1.8\text{M}$, $[\text{NaBrO}_3] = 0.05\text{M}$, illumination method using Protocol C, $100\%I_0$, stirring rate 700RPM, $T = 23^\circ\text{C}$. (see below)





A few important wavelengths were selected to obtain the time series of the oscillation with UV/Visible spectrophotometer. The results are shown in Figure 3.36. At the wavelengths of 312nm and 360nm oscillation were clearly observed in the time series. However, for other wavelengths such as 289nm and 428nm, oscillations were not as evident as the ones at 312nm and 360nm. It may be because absorption varies more distinctly around 312nm and 360nm. These oscillations observed from UV/Visible spectrophotometer firmly indicate that oscillations arise from the periodic formation of intermediate reaction species.

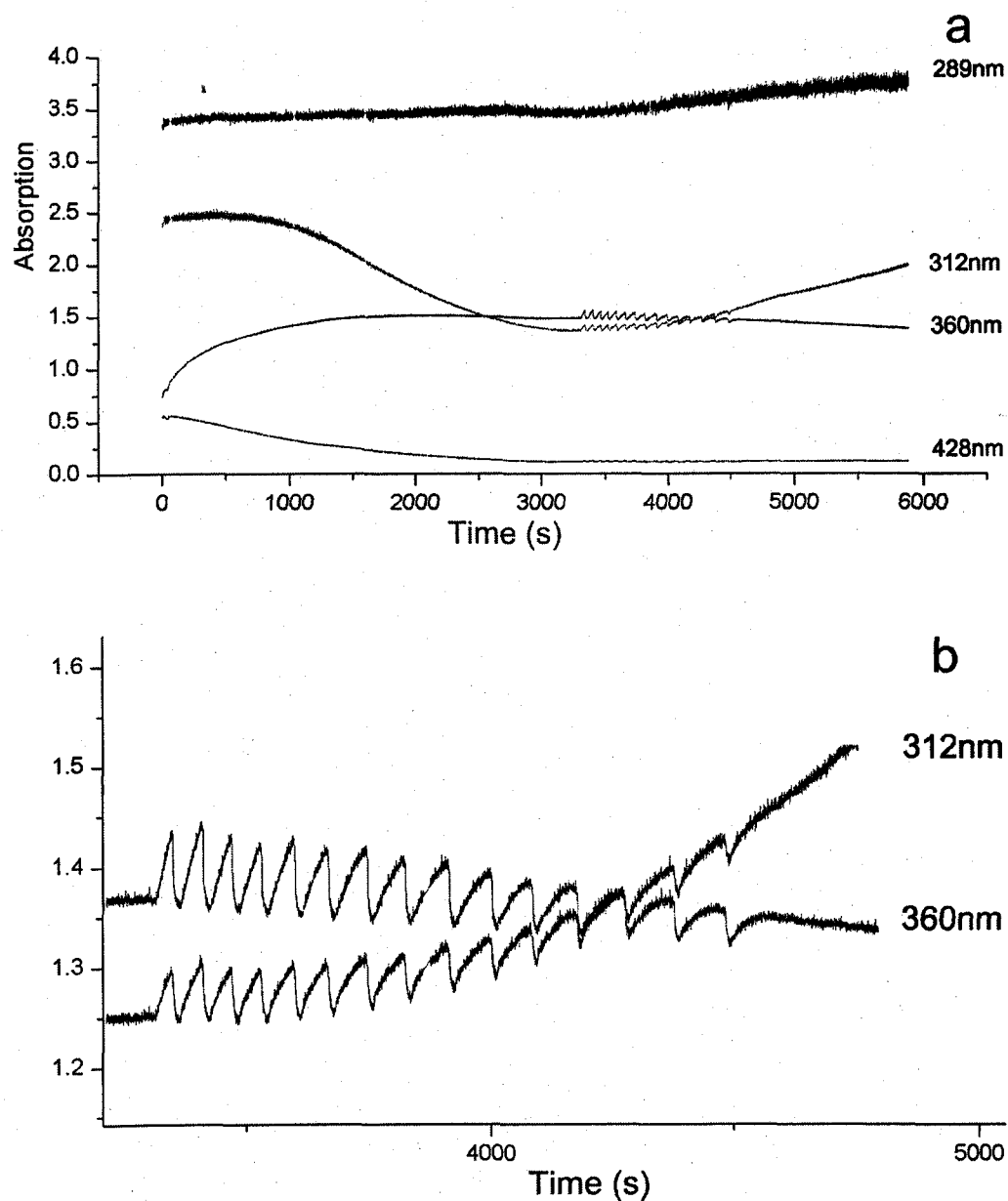


Figure 3.36 Time series of the Q-bromate oscillation monitored by UV-visible spectrophotometer at different wavelength. (a) Time series at the 289nm, 312nm, 360nm, 428nm, (b) The zoom-in window of the oscillation at 312nm and 360nm. The reaction conditions are $[Q] = 0.02\text{M}$, $[\text{H}_2\text{SO}_4] = 1.8\text{M}$, $[\text{NaBrO}_3] = 0.05\text{M}$, illumination method using Protocol C, $100\%I_0$, stirring rate 700RPM, $T = 23^\circ\text{C}$.

3.6 H₂Q and H₂Q-Q-Bromate Oscillation

In order to characterize the function of H₂Q, we use H₂Q to replace Q and observed similar oscillation as well (see in Figure 3.37). When the reaction solution was prepared, the color of the solution of mixed H₂Q and H₂SO₄ immediately changed from colorless to deep yellow after the addition of NaBrO₃. From this observation, we can postulate that H₂Q was oxidized into Q immediately by BrO₃⁻ at the beginning of the reaction, then the produced Q forms the oscillatory reaction with bromate. While the reaction is processing, H⁺ and BrO₃⁻ are consumed so that the oxidation ability was reduced. The autocatalytic reaction $BrO_2^* + 2H^+ \rightarrow 2HBrO_2$, is proportional to the square of [H⁺]. That may be the reason that the concentration of H⁺ is so critical to the reaction behavior of the Q-bromate system.

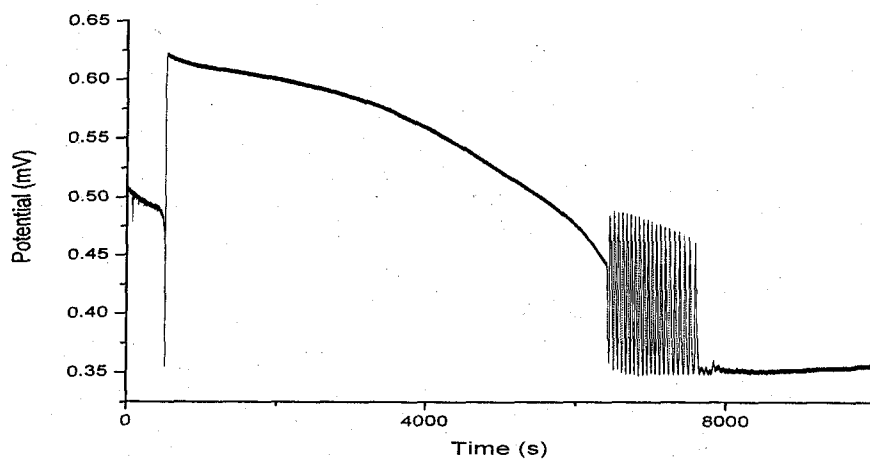


Figure 3.37 Time series H₂Q-bromate Oscillation. The reaction conditions are [H₂Q] = 0.02M, [NaBrO₃] = 0.05M, [H₂SO₄] = 1.8M, Light 100%I₀, stirring rate 700RPM, and T = 25°C.

To shed light on the above discussion about H^+ , H_2Q -bromate reactions were conducted under much lower concentrations of H^+ . We guess that under this condition, H_2Q wouldn't be completely oxidized into Q at the beginning and would further lead to different reaction behaviors. As we expected, at the condition of $[H_2Q] = 0.005M$ and $[NaBrO_3] = 0.06M$ and $100\%I_0$ illumination, while increasing the $[H_2SO_4]$ from $0.1M$ to $0.5M$, the reaction system behaves very differently from one to another (see in Figure 3.38). When $[H_2SO_4] = 0.1M$, there was only one peak appeared in Figure 3.38a after the reaction started 1200s. When $[H_2SO_4]$ was increased to $0.2M$, the first oscillation appears around 300s after the reaction started, and there are two more oscillations, one big and broad peak, followed by another weak later. At $[H_2SO_4] = 0.3M$, there are still three peaks, but the induction time of the first oscillation is only 150s and the time between the first oscillation and the second oscillation is significantly shorter than the one seen in Figure 3.38b with lower $[H^+]$. This trend is even more obvious in Figure 3.35d, where $[H_2SO_4] = 0.5M$. The decrease of induction time of the first oscillation with increasing $[H^+]$ indicates H^+ significantly speed up the reaction between H_2Q and bromate. The appearance of the last two oscillations when $[H_2SO_4]$ is above $0.2M$ indicates that some reaction steps could take place only when the concentration of H^+ is high enough.

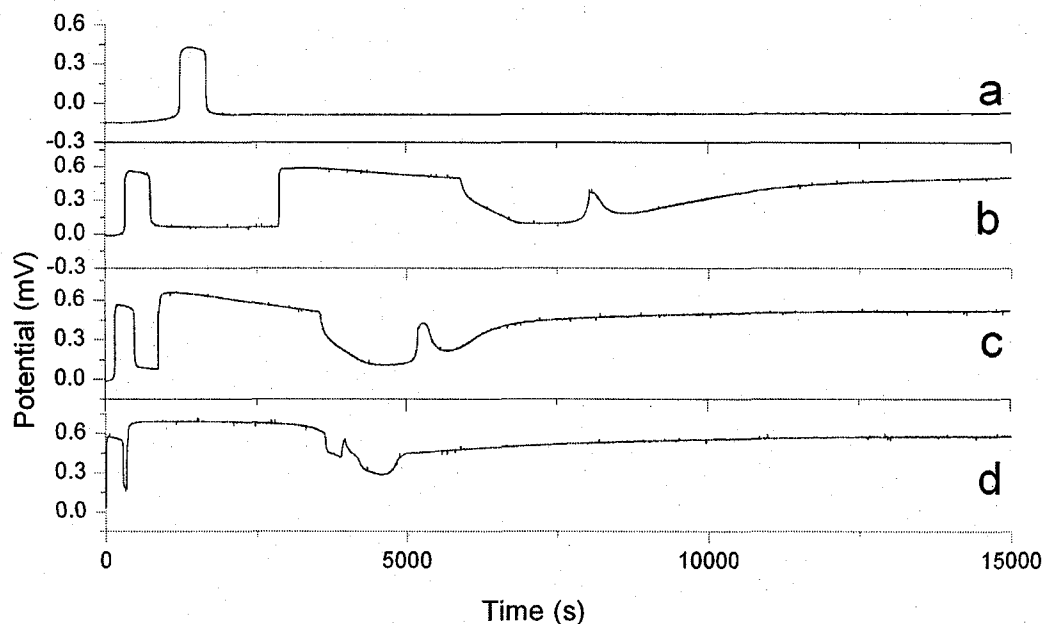


Figure 3.38 Time series of H_2Q -bromate system at different concentration of H_2SO_4 . (a) $[\text{H}_2\text{SO}_4] = 0.1\text{M}$, (b) $[\text{H}_2\text{SO}_4] = 0.2\text{M}$, (c) $[\text{H}_2\text{SO}_4] = 0.3\text{M}$, (d) $[\text{H}_2\text{SO}_4] = 0.5\text{M}$. Other reaction conditions are $[\text{H}_2\text{Q}] = 0.005\text{M}$, $[\text{NaBrO}_3] = 0.06\text{M}$, Light $100\%I_0$, stirring rate 700RPM , and $T = 25^\circ\text{C}$.

Since the reaction behavior in Figure 3.38a is so different from other three, where the H_2Q is expected to be only partially oxidized into Q , the interaction of H_2Q and Q at $[\text{H}_2\text{SO}_4] = 0.1\text{M}$ was studied in the Figure 3.39. Additional 0.01M Q was added into the system while condition are the same as used in Figure 3.38a. Very intriguing oscillatory behaviors were observed from this H_2Q and Q mixed system, which were also strongly influenced by the light illumination. When there is no illumination, Figure 3.39a only presents a broad oscillation. When $40\%I_0$ illumination was applied, two distinctive

oscillations appeared. The first oscillation was significantly sharp. The second oscillation peak also depends on the intensity of the illumination, since it was narrowed down obviously when the light intensity increased from $40\%I_0$ to $60\%I_0$ comparing Figure 3.39b and 3.39c. When the light intensity rises to $75\%I_0$, some very unique phenomena appear within the first 10000s there are a series small but regular oscillations appear. The time interval between these small oscillations increases gradually from 675s to 1056s as the reaction evolves. At 11534s, there is a sudden jump in the Pt potential, and a broad peak takes place. Compare Figure 3.39 d and c, a significant change is due to the increase of light intensity. Further increase the light intensity to $100\%I_0$ results in the decrease of the induction time and increase of the frequency of the small peaks. But the number of the oscillation peaks keeps constant. Moreover, the width of the broad oscillation is evidently reduced.

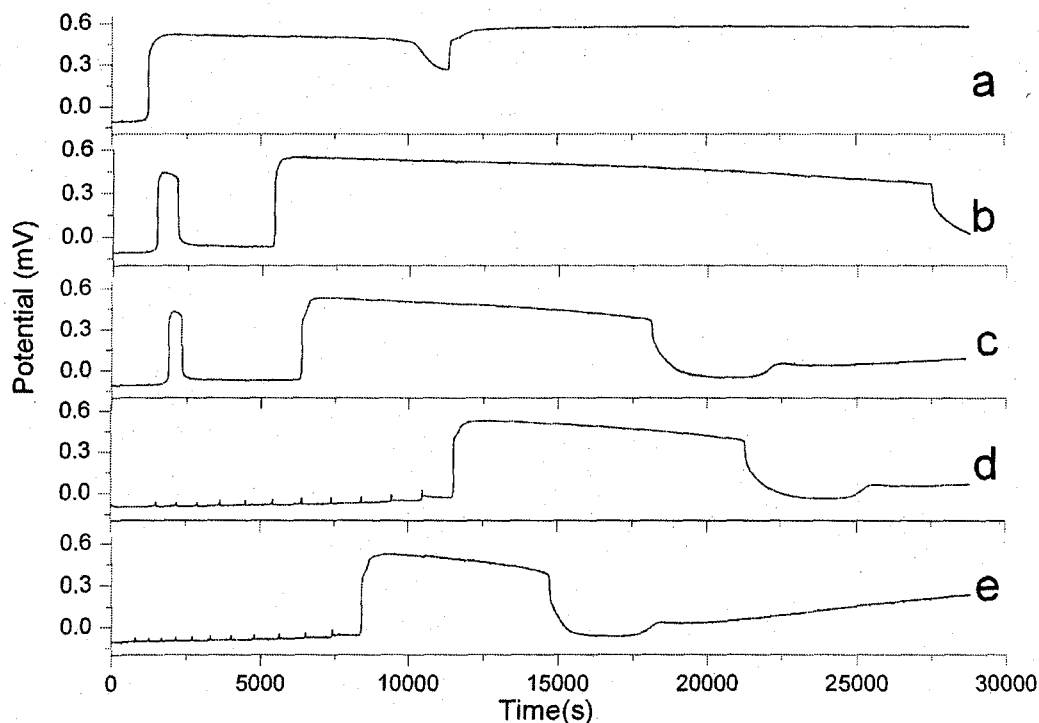


Figure 3.39 Time series of the H_2Q - Q -bromate system with different light illumination. (a) $0\%I_0$, (b) $40\%I_0$, (c) $60\%I_0$, (d) $75\%I_0$, (e) $100\%I_0$ Other reaction conditions are $[\text{H}_2\text{Q}] = 0.005\text{M}$, $[\text{Q}] = 0.01\text{M}$, $[\text{NaBrO}_3] = 0.06\text{M}$, $[\text{H}_2\text{SO}_4] = 0.1\text{M}$, Light $100\%I_0$, stirring rate 700RPM , and $T = 25^\circ\text{C}$.

To confirm that the phenomena in Figure 3.39d and e are due to the interaction of H_2Q and Q , H_2Q -bromate and Q -bromate photo reaction were conducted respectively at the low concentration of H_2SO_4 0.1M . The results are presented in Figure 3.40. The concentration of H_2Q and Q was chosen to be 0.015M here in order to be consistent with the conditions used in Figure 3.39, in which the summation of $[\text{H}_2\text{Q}]$ and $[\text{Q}]$ is 0.015M . There is only one single oscillation in Figure 3.40a, and one broad and a weak oscillation

in Figure 3.40b, which are very different from the phenomena in Figure 3.39. It supports that oscillations presented in Figure 3.39d is due to neither H_2Q or Q alone, instead, it is most probably caused by the interactions of the Q and H_2Q . However, this interaction is critically influenced by the condition of light intensity, pH and the ratio of $[H_2Q]$ and $[Q]$.

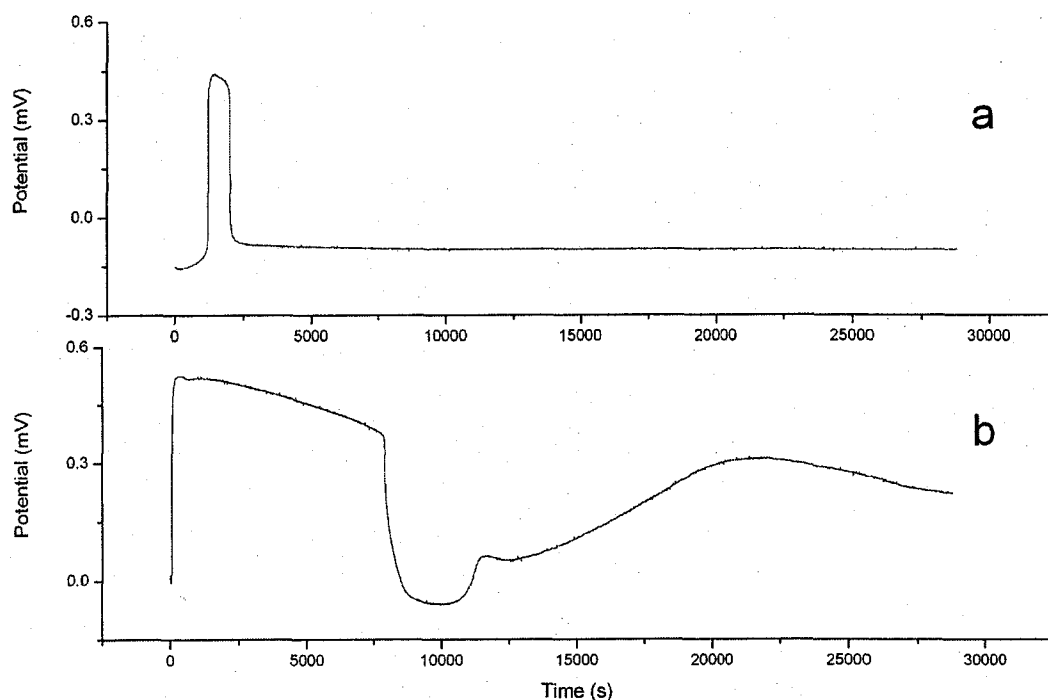


Figure 3.40 Time series of H_2Q -bromate and Q -bromate reaction system. (a) $[H_2Q] = 0.015M$, (b) $[Q] = 0.015M$. Other reaction conditions are $[H_2SO_4] = 0.1 M$, $[NaBrO_3] = 0.06M$, Light $75\%I_0$, stirring rate 700RPM, and $T = 25^\circ C$.

3.7 Simulations of the Q-Bromate Oscillations.

The mechanistic investigation has been performed for the Q -bromate oscillator. We referred some of the reaction steps and reaction constants from the reduced simulation model of 1,4-CHD-bromate model. We proposed a comparatively schematic mechanism

with 13 reaction steps shown in Table 3.3. The kinetic simulations were performed and plotted with the software Berkeley Madonna.

Table 3.3. Mechanism of 1,4-Benzoquinone- bromate- acid photo oscillator

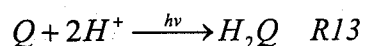
No.	Reaction steps	Rate constant
R1	$Br^- + HOBr + H^+ \leftrightarrow Br_2 + H_2O$	$k_1=8.0 \times 10^9 M^2 s^{-1}, k_{-1}=80 M^2 s^{-1}$
R2	$Br^- + HBrO_2 + H^+ \rightarrow 2HOBr$	$k_2 = 2.5 \times 10^6 M^2 s^{-1}$
R3	$Br^- + BrO_3^- + 2H^+ \leftrightarrow HOBr + HBrO_2$	$k_3 = 1.2 M^2 s^{-1}, k_{-3} = 3.2 M^2 s^{-1},$
R4	$2HBrO_2 \rightarrow HOBr + BrO_3^- + H^+$	$k_4 = 3400 M^2 s^{-1}$
R5	$HBrO_2 + BrO_3^- + H^+ \leftrightarrow 2BrO_2^* + H_2O$	$k_5 = 4.8 M^2 s^{-1}, k_{-5} = 6.4 \times 10^7 M^2 s^{-1}$
R6	$H_2Q + BrO_2^* \rightarrow HQ^* + HBrO_2$	$k_6 = 8.0 \times 10^5 M^2 s^{-1}$
R7	$HQ^* + BrO_2^* \rightarrow Q + HBrO_2$	$k_7 = 8.0 \times 10^9 M^2 s^{-1}$
R8	$2HQ^* \rightarrow H_2Q + Q$	$k_8 = 8.8 \times 10^8 M^2 s^{-1},$
R9	$H_2Q + Br_2 \rightarrow QBr + Br^- + 2H^+$	$k_9 = 3.0 \times 10^4 M^{-2} s^{-1}$
R10	$H_2Q + BrO_3^- + H^+ \rightarrow Q + HBrO_2 + H_2O$	$k_{10} = 2.0 \times 10^{-2} M^2 s^{-1},$
R11	$H_2Q + HOBr \rightarrow Q + Br^- + H^+ + H_2O$	$k_{11} = 6.0 \times 10^5 M^2 s^{-1}$
R12	$QBr \rightarrow Q + Br^-$	$k_{12} = 3.0 \times 10^{-6} M^1 s^{-1}$
R13	$Q + 2H^+ \xrightarrow{h\nu} H_2Q$	$k_{13} = 2.2 \times 10^{-4} M^1 s^{-1}$

Note: $[H_2O] = 55M$ are included in the rate constant.

Reactions 5, 6 and 7 build an autocatalytic cycle, which is a key condition in designing chemical oscillators. The autocatalytic reaction is inhibited by Br^- through

reaction 2.

The net outcome of reactions 1 to 12 is the production of Q and QBr. To account for the photo reproduction of H₂Q from Q, the following schematic step is included in our proposed mechanism.



Rate constant k_{13} is adjusted arbitrarily in this study to reflect variations of illumination intensity. Simulations are carried out by integrating the reaction rate laws derived from reactions 1 to 13. Since no H₂Q is presented initially in the system, no reactions take place in the absence of light, implemented by setting k_{13} to 0.0. Under small k_{13} values such as $1.0 \times 10^{-5} \text{ M}^{-1}\text{s}^{-1}$, i.e. illuminating the system with a low intensity light, no oscillation appears, only smooth decrease in Q concentration is observed (see in Figure 3.42a and b). Figure 3.41 presents the time series of QBr and Br⁻, in which k_{13} is increased to $k_{13} = 2.2 \times 10^{-4} \text{ M}^{-1}\text{s}^{-1}$. Similar to experimental observations, spontaneous oscillations are achieved here after a long induction time (>10,000 seconds).

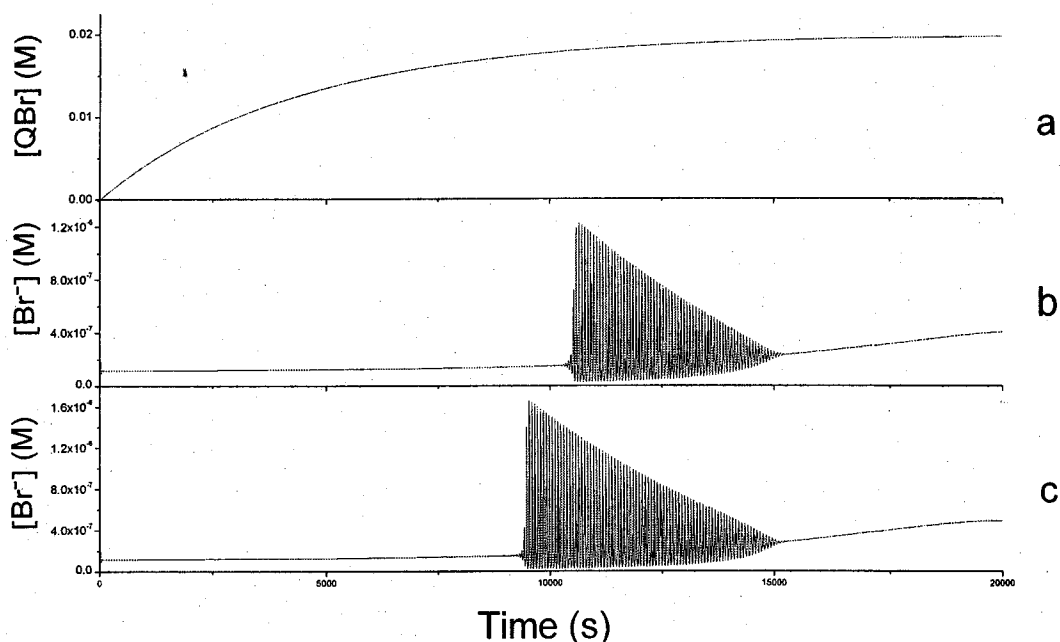


Figure 3.41 Simulations of Q-bromate photochemical oscillator in terms of (a) [QBr] (b) [Br⁻], and (c) [Br⁻] with additional 0.005M QBr. Other concentrations are [Q] = 0.02M, [H₂SO₄] = 1.8M, [NaBrO₃] = 0.05M. The rate constant $k_{13} = 2.2 \times 10^{-4} \text{ M}^{-1} \text{ s}^{-1}$.

In consistent with our experimental measurements, the concentration of Br⁻ increases slowly, but continuously, during the induction period and starts oscillating toward higher values after a threshold concentration is reached. Reactions 1 to 12 indicate that QBr is one of the Br⁻ precursors and, as is illustrated in Figure 3.41a, QBr concentration increases continuously in time. When small amounts of QBr are included initially in our modeling (see in Figure 3.41c), the induction time is decreased, implying that the accumulation of QBr may have been responsible for the long induction time seen in the experiments. Our simulation also illustrates that the inclusion of photo dissociation of molecular bromine $\text{Br}_2 \rightarrow 2\text{Br}^*$ does not affect the occurrence of chemical oscillations.

Figure 3.42 and Table 3.4 demonstrate the influences of light intensity by increasing k_{13} from low to high values. The figure shows that the induction time was shortened and the amplitude was enhanced with the increase of k_{13} , which is identical to the experimental results. In addition, this model also successfully simulates that the peak numbers of the oscillation and oscillation duration increase when k_{13} is going up at lower light intensity (from Figure 3.42c to d) but decrease at high light intensity. The good agreement of the simulation and the experimental results suggest that the assumption of the photochemical step and the selection of the rate constants are reasonable and reflect the understanding reaction mechanism.

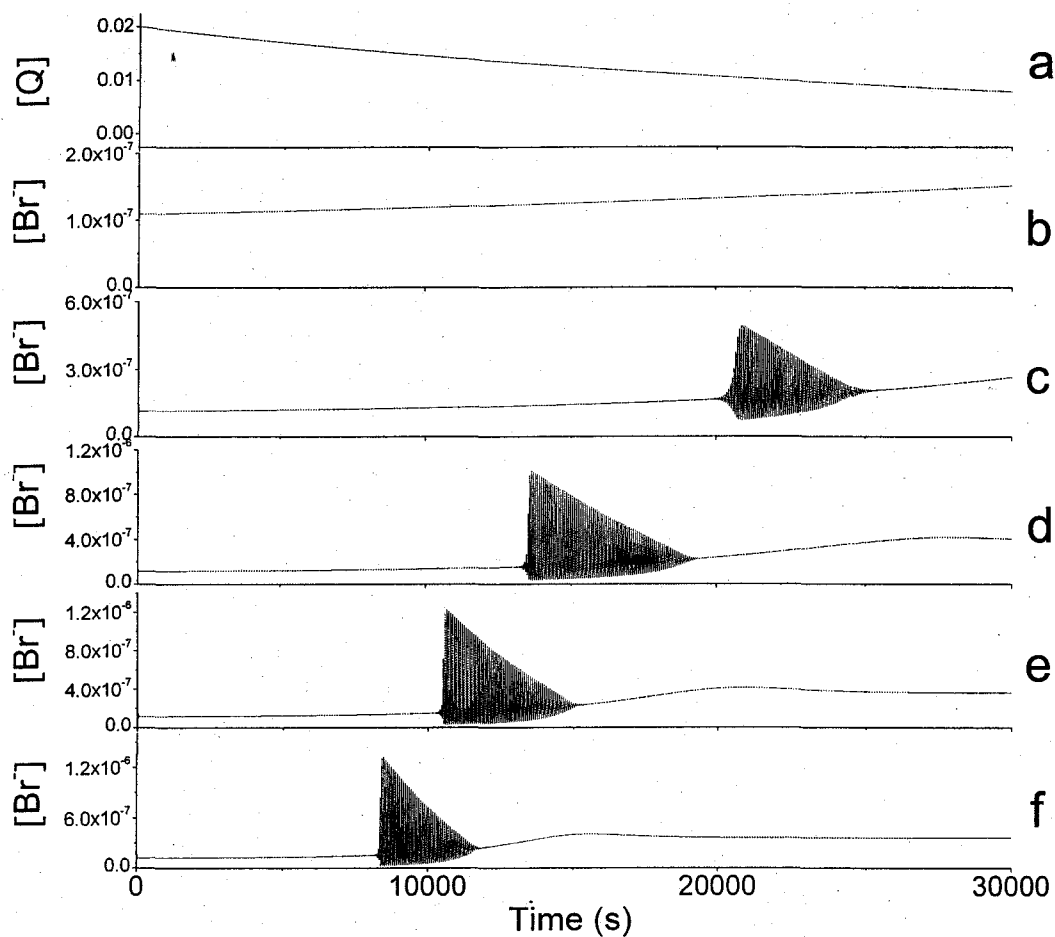


Figure 3.42 Simulation of Q-bromate oscillation under different light intensity. (a) [Q] at $k_{13} = 1.0 \times 10^{-5} \text{ M}^{-1}\text{s}^{-1}$, (b) [Br⁻] at $k_{13} = 1.0 \times 10^{-5} \text{ M}^{-1}\text{s}^{-1}$, (c) [Br⁻] at $k_{13} = 9.0 \times 10^{-5} \text{ M}^{-1}\text{s}^{-1}$, (d) [Br⁻] at $k_{13} = 1.5 \times 10^{-4} \text{ M}^{-1}\text{s}^{-1}$, (e) [Br⁻] at $k_{13} = 2.2 \times 10^{-4} \text{ M}^{-1}\text{s}^{-1}$, (f) [Br⁻] at $k_{13} = 3.2 \times 10^{-4} \text{ M}^{-1}\text{s}^{-1}$. The reaction conditions are [Q] = 0.02M, [H₂SO₄] = 1.8M, [NaBrO₃] = 0.05M.

Table 3.4 Results summary of Figure 3.42.

No.	Peak numbers	Induction time(s)	Oscillation duration(s)	k_{12} ($M^{-1}s^{-1}$)	k_{13} ($M^{-1}s^{-1}$)	[Br ⁻](M)
c	83	2.00×10^4	5.50×10^3		9.00×10^{-5}	4.205×10^{-7}
d	97	1.30×10^4	6.12×10^3		1.50×10^{-4}	9.757×10^{-7}
e	76	1.02×10^4	4.95×10^4		2.20×10^{-4}	1.197×10^{-6}
f	56	8.10×10^3	3.93×10^4	3.50×10^{-6}	3.20×10^{-4}	1.297×10^{-6}

Figure 3.43 successfully reproduces the perturbation of Br⁻. In Figure 3.43a, at t = 11540s, [Br⁻] was arbitrarily increased from 4.58×10^{-8} M to 3×10^{-4} M, the oscillation vanished and after a while it recovered. When [Br⁻] was increased to 5×10^{-4} M, i.e. a stronger perturbation is applied, the oscillation was completely quenched and never recovered. These phenomena are consistent with the experimental results shown in Figures 3.20 and 3.21. It indicated that this oscillator is a Br⁻ controlled oscillator.

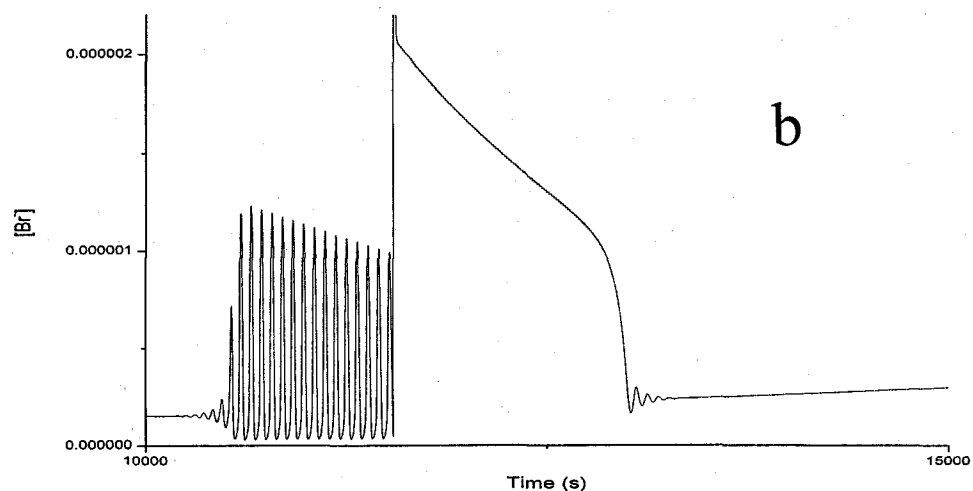
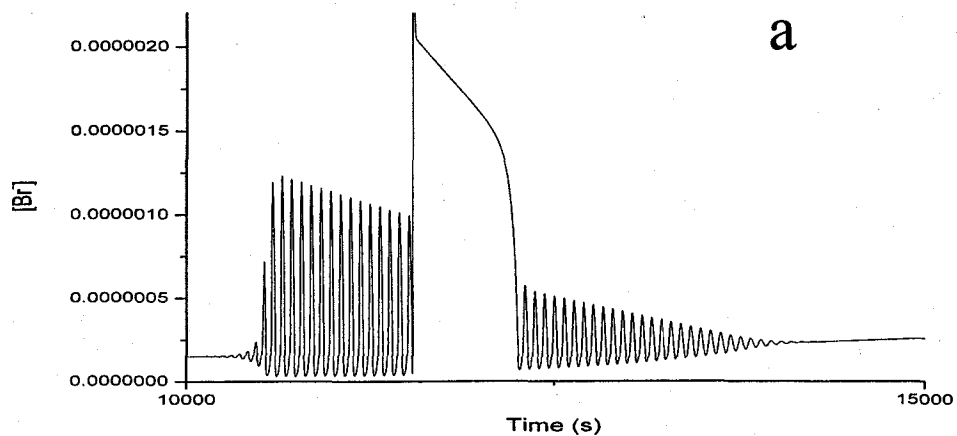


Figure 3.43 Simulation of Br^- perturbation in the Q-bromate oscillation. (a) $[\text{Br}^-] = 3 \times 10^{-4}\text{M}$, (b) $[\text{Br}^-] = 5 \times 10^{-4}\text{M}$. The reaction conditions are $[\text{Q}] = 0.02\text{M}$, $[\text{H}_2\text{SO}_4] = 1.8\text{M}$, $[\text{NaBrO}_3] = 0.05\text{M}$.

The simulation in Figure 3.44 demonstrated how the addition of Q at the end of the oscillation window could revive the oscillation, which is again in good agreement with the exceptional results in Figure 3.28. It confirms our earlier discussion which considers the depletion of Q is a major factor that causes the oscillation disappears.

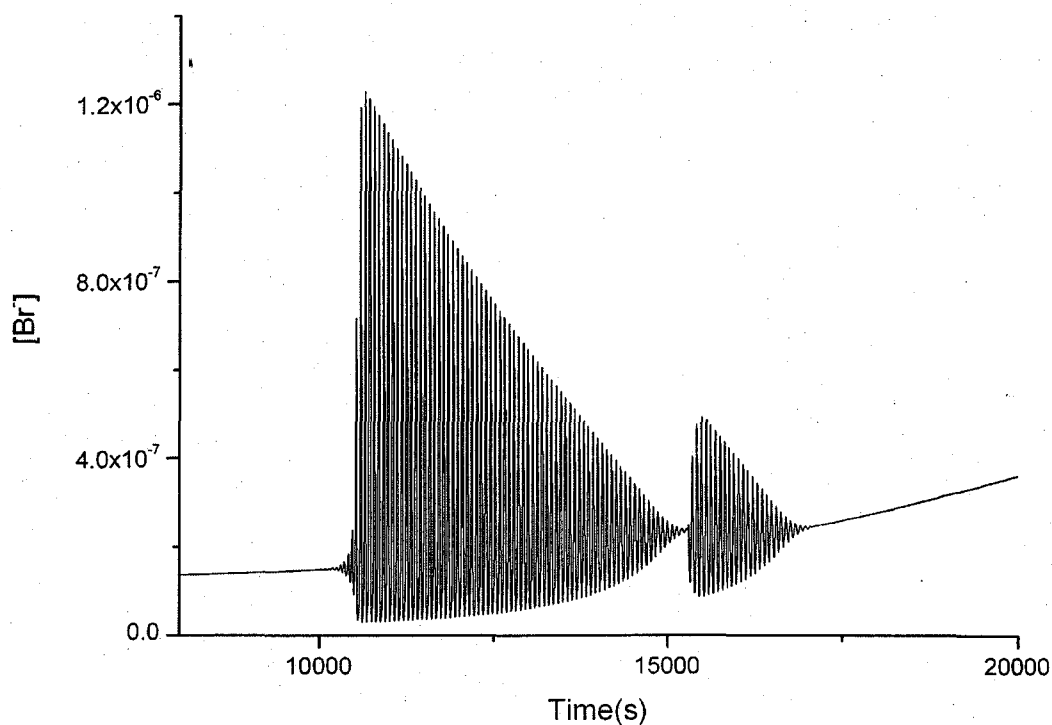
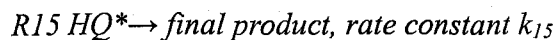
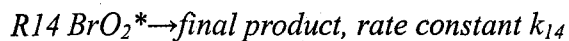


Figure 3.44 Simulation of the oscillation revival with the addition of Q at the end of the oscillation. The reaction conditions are $[Q] = 0.02\text{M}$, $[\text{H}_2\text{SO}_4] = 1.8\text{M}$, $[\text{NaBrO}_3] = 0.05\text{M}$.

Moreover, the experiment with the perturbation of radical scavenger ethanol is also simulated and is shown in Figure 3.45. The simulation is implemented by adding two reaction steps to the model in Table 3.3 as follows:



We suppose that ethanol will react with the radical BrO_2^* and HQ^* in the system and generate some final products which are not going to be involved into the oscillatory

system. This series simulation indicates that the quenching of radicals could cause the decrease of the oscillation amplitude and the irreversible vanishment of the oscillation.

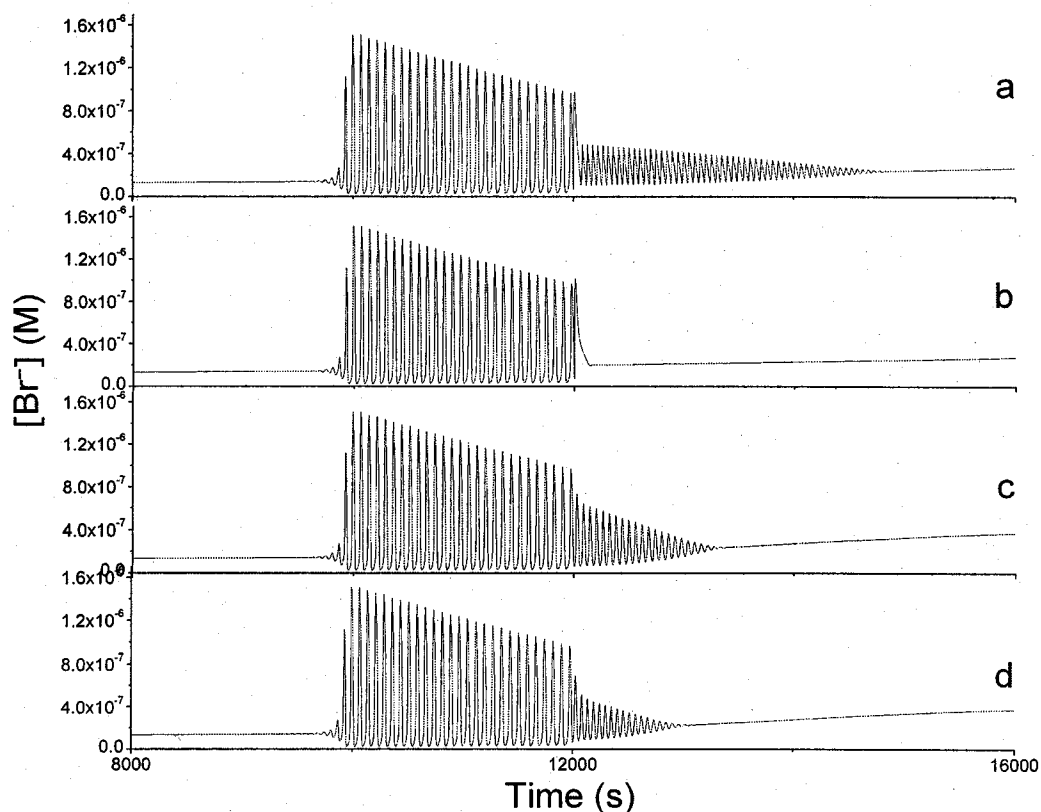


Figure 3.45 Simulation of ethanol perturbation by controlling the reaction $R14$ $BrO_2^* \rightarrow \text{final product A}$ and $R15$ $HQ^* \rightarrow \text{final product B}$, (a) $k_{14} = 30 \text{ M}^{-1}\text{s}^{-1}$, (b) $k_{14} = 70 \text{ M}^{-1}\text{s}^{-1}$, (c) $k_{15} = 1 \times 10^5 \text{ M}^{-1}\text{s}^{-1}$, (d) $k_{15} = 1 \times 10^6 \text{ M}^{-1}\text{s}^{-1}$.

All above simulations indicate that the model proposed in Table 3.3 is quite reasonable. It is especially successful for the reproduction of the influence of the light intensity. However, it's not yet perfect. The results in the following simulations about the influence of $[H^+]$, $[NaBrO_3]$ and $[Q]$ are partially inconsistent with the true experimental results. The simulation in Figure 3.46 reflects the increase of the oscillation amplitude

and the decrease of the induction time when $[H^+]$ is decreased, and the vanishment of the oscillation at very high $[H^+]$. The increase of the oscillation time conflicts with the experimental results.

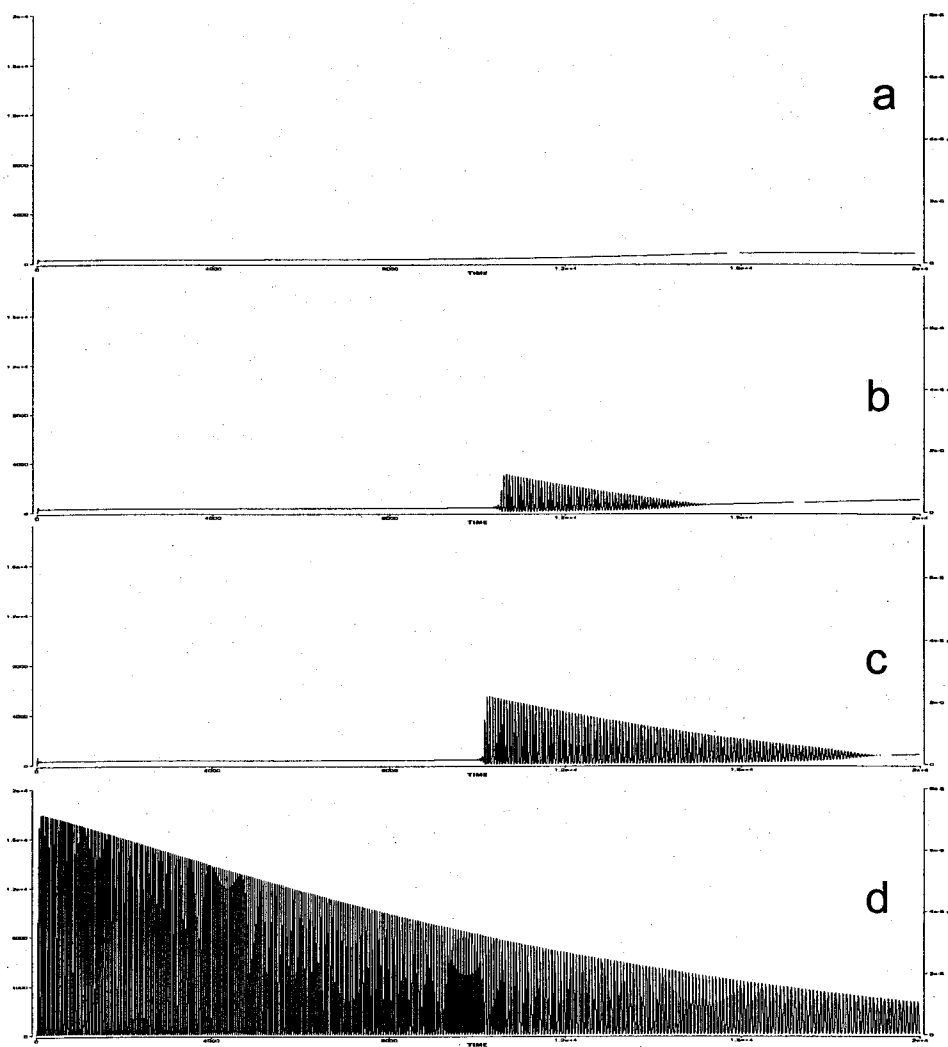


Figure 3.46 Simulations of Q-bromate oscillation under different $[H_2SO_4]$ (a) 2.0M, (b)

1.8M, (c) 1.6M, (d) 1.4M. The other reaction conditions are $[Q] = 0.02\text{M}$, $[\text{NaBrO}_3] = 0.05\text{M}$.

Simulations in Figure 3.47 characterize the influence of $[\text{NaBrO}_3]$. The calculated results such as the reduction of the induction time and the increase of the oscillation amplitude as $[\text{NaBrO}_3]$ decreases and the disappearance of oscillation at high concentration of BrO_3^- agree well with the experiments. Yet the variation in the length of the oscillatory window doesn't agree with experiments. The above discrepancies between simulations and experiments suggest that some of the reaction steps and rate constants need to be refined in the future study.

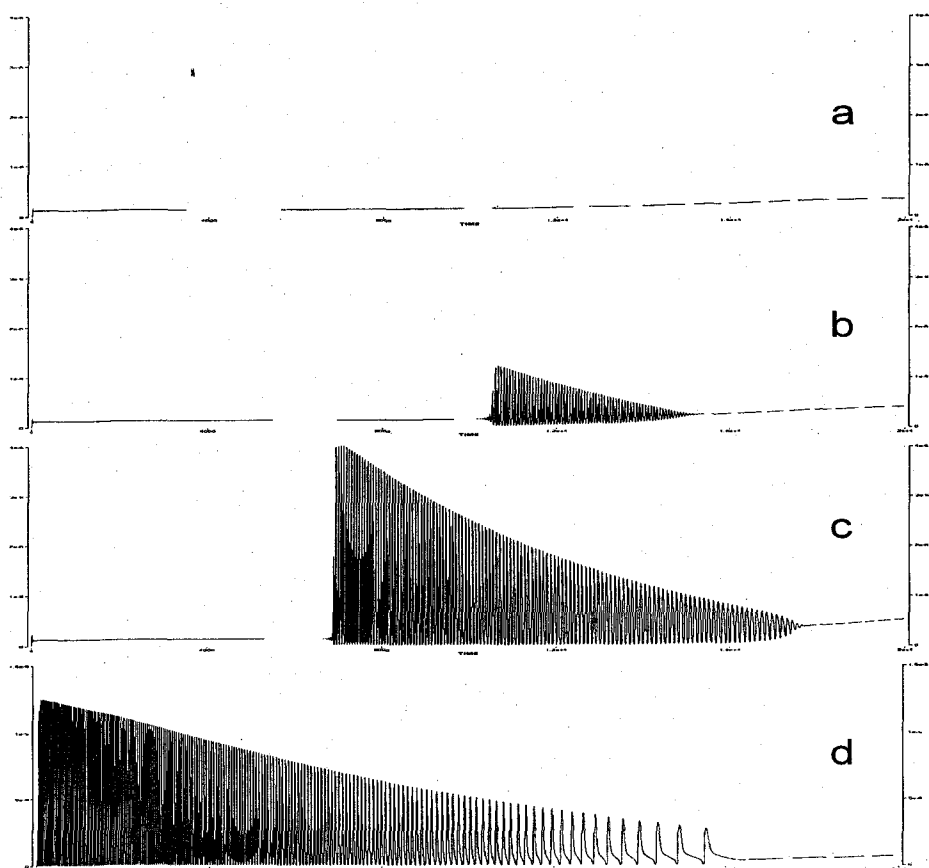


Figure 3.47 Simulation of Q-bromate oscillation under different $[\text{NaBrO}_3]$ (a) 0.06M, (b) 0.05M, (c) 0.04M, (d) 0.03M. The other reaction conditions are $[\text{Q}] = 0.02\text{M}$, $[\text{H}_2\text{SO}_4] = 1.8\text{M}$.

3.8 Conclusions

The 1,4-Benzoquinone-bromate reaction investigated in this chapter is a brand new and very novel oscillator that only exists under the proper illumination. There are several

controlling factors existed both internally and externally in this oscillatory system. The experiments indicate that it has some common character with the conventional bromate-driven oscillators which take bromide ion as a control factor. The study with spectrophotometer demonstrates that new species are generated in the system under illumination and supports the assumption of the reaction

$Q + 2H^+ \xrightarrow{h\nu} H_2Q$ (R13). pH is another factor that significantly influences the oscillatory behavior. The light intensity and wavelength should be the most critical external factor that determines the oscillation behavior. The primary study suggests that the wavelength between 300nm~400nm may be responsible to the photochemical reaction in this system. The demanding light intensity may be due to the inhomogeneous distribution of the spectra of the light source. The quenching phenomena observed by adding ethanol indicates that the free radicals are involved in the reaction. The revival of oscillation due to the addition of Q implicates the disappearance of the oscillation is owing to the depletion of Q. The influences of other variables such as $[NaBrO_3]$, temperature, stirring rate and the presence of oxygen have also been investigated.

In the mechanistic study, the proposed model successfully simulated several experimental phenomena, such as the light intensity dependence, Bromide perturbation, oscillation revival with additional Q, and quenching by ethanol.

In summary, this study demonstrates the feasibility of achieving light-induced formation of 1,4-hydroquinone. The reaction can take place in such a degree that a new photo-controlled chemical oscillators could be established. As discussed earlier, without

illumination no reactions take place in this new system. Such a unique property in reaction kinetics opens a avenue to explore novel reaction behavior in perturbed nonlinear systems. On the other hand, the protocol presented in this study could be used as a new, efficient method to prepare bromo-1,4-benzoquinone from 1,4-benzoquinone or 1,4-hydroquinone because brominated 1,4-benzoquinone species is produced during the above process.

For the future study, more research could be conducted in the CSTR system. The mechanistic study could be implemented by improving light source, using more accurate narrow band filter and introduce mass spectroscopy, EPR and NMR to characterize the composition of the oscillation system. Some color indicators or catalysts should be introduced so that the oscillator may be applied in the reaction-diffusion system. Moreover, new oscillators could be developed by replacing 1,4-benzoquinone with other quinones and replacing sulfate acid with other acid such as nitrate acid or phosphate acid using other oxidant i.e. hydrogen peroxide. The simulated model needs to be refined in order to fit the reaction response to the variation of $[H_2SO_4]$ and $[NaBrO_3]$.

Chapter 4. Summary and Perspectives

This thesis investigated nonlinear dynamics in the oxidations of 1,4-CHD and its derivatives by acidic bromate. Due to the absence of gas production, which is an advantage in the study of pattern formation in reaction-diffusion media, the 1,4-CHD-bromate reaction has attracted increasing attention in the last decade. Our study demonstrates that, in addition to the compositions of the reaction solution, oscillations in the 1,4-CHD-bromate system are also sensitive to mechanical mixing, in which various complex oscillations have been induced by simply varying the mixing rate. Experiments implicate that the observed stirring sensitivity may arise from hydroquinone, which is an intermediate product involved in the autocatalytic reaction process. Numerical simulations show that the stirring effect could be explained by the dependence of fast disproportionation of hydroquinone radicals onto the transportation.

Investigations on the photosensitivity of the 1,4-CHD-bromate reaction led to the discovery of both light-induced and light-quenched oscillatory behavior in such a system. Mechanistic studies suggest that the unique photosensitivity of the 1,4-CHD-bromate reaction may be due to the photo-reproduction of hydroquinone from 1,4-benzoquinone. This conclusion leads us to construct a new photo-mediated chemical oscillator, which is the reaction between 1,4-benzoquinone and bromate in acidic environment.

Our preliminary investigations on the newly discovered light-mediated 1,4-benzoquinone-bromate oscillator indicate that the new oscillatory system is not only

controlled by bromide ion, where successful quenchings have been obtained in both a batch and a CSTR system, it is also radical-controlled, in which the presence of a radical scavenger significantly affects the oscillatory behavior. Indeed, the amplitude of oscillation can be manipulated conveniently through adding a proper amount of ethanol, a radical scavenger used in this research. Experiments conducted in a CSTR illustrate that this new chemical oscillator is also capable of exhibiting various complex dynamics as the flow rate is adjusted systematically. More research can be pursued along this direction to explore novel interactions of intrinsic dynamics and external forcing, in which reaction conditions can be maintained at a stable, yet far from thermodynamic equilibrium with the continuous supply of fresh chemicals.

A model consisting of 13 reaction steps is proposed here to qualitatively account for the nonlinear behavior seen in the light-mediated 1,4-benzoquinone-bromate reaction. Which most of the experimental results have been successfully reproduced by the model, effects of the acid concentration on the reaction behavior do not agree with experiments. Such a discrepancy may arise from the simplified considerations of photo-reproduction of hydroquinone, which is known to depend on acid concentrations. Further improvement of the model can be pursued along such a direction as well as characterizing individual reaction steps.

Appendix

1. Code of simulation in Table 2.1

METHOD Stiff

STARTTIME = 0
STOPTIME=40000
DTMIN=1e-10
DTMAX=1
TOLERANCE=1e-12
DTOUT=0
DT=0.0001

init Br=1e-8
init Br2=1e-8
init HOBr=1e-8
init HBrO2=1e-8
init BrO2r=1e-8
init BrO3=0.14
init H2BrO2=1e-8
init Br2O4=1e-8
init H2Q=0.03
init HQR=1e-8
init Q=1e-8
init CHD=0.06
init CHDE=1e-8
init BrCHD=1e-8
init CHED=1e-8

H=1.8
H2O=55

k1f=8e9
k1r=80
k2f=2.5e6
k2r=2e-5
k3f=1.2
k3r=3.2
k4f=2e6
k4r=1e8
k5f=1.7e5
k6f=48
k6r=3200
k7f=75000
k7r=1.4e9
k8f=8e5
k9f=8e9
k10f=8.8e8
k10r=0.00077
k11f=0.0007
k11r=520
k12f=2.8e9
k13f=2.8e9

k14f=5e-5
 k15f=0.000194
 k16f=30000
 k17f=0.02
 k18f=6e5
 k19f=1e-5
 k20f=0
 k20r=0

$$d/dt(\text{Br})=-(K1f*\text{Br}*\text{HOBr}*\text{H}-K1r*\text{Br}2*\text{H}2\text{O})-(k2f*\text{Br}*\text{HBrO}2*\text{H}-k2r*\text{HOBr}*\text{HOBr})-(k3f*\text{Br}*\text{BrO}3*\text{H}*\text{H}-k3r*\text{HOBr}*\text{HBrO}2)+(k12f*\text{CHDE}*\text{Br}2)+(k14f*\text{BrCHD})+2*(k16f*\text{H}2\text{Q}*\text{Br}2)+k18f*\text{H}2\text{Q}*\text{HOBr}$$

$$d/dt(\text{Br}2)=K1f*\text{Br}*\text{HOBr}*\text{H}-K1r*\text{Br}2*\text{H}2\text{O}-(k12f*\text{CHDE}*\text{Br}2)-(k16f*\text{H}2\text{Q}*\text{Br}2)$$

$$d/dt(\text{HOBr})=-(K1f*\text{Br}*\text{HOBr}*\text{H}-K1r*\text{Br}2*\text{H}2\text{O})+2*(k2f*\text{Br}*\text{HBrO}2*\text{H}-k2r*\text{HOBr}*\text{HOBr})+(k3f*\text{Br}*\text{BrO}3*\text{H}*\text{H}-k3r*\text{HOBr}*\text{HBrO}2)+(k5f*\text{HBrO}2*\text{H}2\text{BrO}2)-(k13f*\text{CHDE}*\text{HOBr})-(k18f*\text{H}2\text{Q}*\text{HOBr})$$

$$d/dt(\text{H}2\text{BrO}2)=k4f*\text{HBrO}2*\text{H}-k4r*\text{H}2\text{BrO}2-(k5f*\text{HBrO}2*\text{H}2\text{BrO}2)$$

$$d/dt(\text{HBrO}2)=-(k2f*\text{Br}*\text{HBrO}2*\text{H}-k2r*\text{HOBr}*\text{HOBr})+(k3f*\text{Br}*\text{BrO}3*\text{H}*\text{H}-k3r*\text{HOBr}*\text{HBrO}2)-(k4f*\text{HBrO}2*\text{H}-k4r*\text{H}2\text{BrO}2)-(k5f*\text{HBrO}2*\text{H}2\text{BrO}2)-(k6f*\text{HBrO}2*\text{BrO}3*\text{H}-k6r*\text{Br}2\text{O}4*\text{H}2\text{O})+(k8f*\text{H}2\text{Q}*\text{BrO}2r)+(k9f*\text{HQR}*\text{BrO}2r)+(k17f*\text{H}2\text{Q}*\text{BrO}3*\text{H})+(k19f*\text{CHD}*\text{BrO}3*\text{H})$$

$$d/dt(\text{BrO}3)=-(k3f*\text{Br}*\text{BrO}3*\text{H}*\text{H}-k3r*\text{HOBr}*\text{HBrO}2)+(k5f*\text{HBrO}2*\text{H}2\text{BrO}2)-(k6f*\text{HBrO}2*\text{BrO}3*\text{H}-k6r*\text{Br}2\text{O}4*\text{H}2\text{O})-(k17f*\text{H}2\text{Q}*\text{BrO}3*\text{H})-(k19f*\text{CHD}*\text{BrO}3*\text{H})$$

$$d/dt(\text{Br}2\text{O}4)=k6f*\text{HBrO}2*\text{BrO}3*\text{H}-k6r*\text{Br}2\text{O}4*\text{H}2\text{O}-(k7f*\text{Br}2\text{O}4-K7r*\text{BrO}2r*\text{BrO}2r)$$

$$d/dt(\text{BrO}2r)=2*(k7f*\text{Br}2\text{O}4-K7r*\text{BrO}2r*\text{BrO}2r)-(k8f*\text{H}2\text{Q}*\text{BrO}2r)-(k9f*\text{HQR}*\text{BrO}2r)$$

$$d/dt(\text{H}2\text{Q})=-(k8f*\text{H}2\text{Q}*\text{BrO}2r)+(k10f*\text{HQR}*\text{HQR}-k10r*\text{H}2\text{Q}*\text{Q})+(k15f*\text{CHED}*\text{H})-(k16f*\text{H}2\text{Q}*\text{Br}2)-(k17f*\text{H}2\text{Q}*\text{BrO}3*\text{H})-(k18f*\text{H}2\text{Q}*\text{HOBr})+(k19f*\text{CHD}*\text{BrO}3*\text{H})+k20f*\text{Q}*\text{H}^2-k20r*\text{H}2\text{Q}$$

$$d/dt(\text{HQR})=k8f*\text{H}2\text{Q}*\text{BrO}2r-(k9f*\text{HQR}*\text{BrO}2r)-2*(k10f*\text{HQR}*\text{HQR}-k10r*\text{H}2\text{Q}*\text{Q})$$

$$d/dt(\text{Q})=(k9f*\text{HQR}*\text{BrO}2r)+(k10f*\text{HQR}*\text{HQR}-k10r*\text{H}2\text{Q}*\text{Q})+(k16f*\text{H}2\text{Q}*\text{Br}2)+(k17f*\text{H}2\text{Q}*\text{BrO}3*\text{H})+(k18f*\text{H}2\text{Q}*\text{HOBr})-k20f*\text{Q}*\text{H}^2+k20r*\text{H}2\text{Q}$$

$$d/dt(\text{CHD})=-(k11f*\text{CHD}*\text{H}-k11r*\text{CHDE}*\text{H})-(k19f*\text{CHD}*\text{BrO}3*\text{H})$$

$$d/dt(\text{CHDE})=(k11f*\text{CHD}*\text{H}-k11r*\text{CHDE}*\text{H})-(k12f*\text{CHDE}*\text{Br}2)-(k13f*\text{CHDE}*\text{HOBr})$$

$$d/dt(\text{BrCHD})=(k12f*\text{CHDE}*\text{Br}2)+(k13f*\text{CHDE}*\text{HOBr})-(k14f*\text{BrCHD})$$

$$d/dt(\text{CHED})=(k14f*\text{BrCHD})-(k15f*\text{CHED}*\text{H})$$

2. Code of the simulation in Table 3.3

METHOD Stiff

STARTTIME = 0
STOPTIME=60000
DTMIN=1e-10
DTMAX=1
TOLERANCE=1e-12
DOUT=0
DT=0.0001
H2O=1

{ 1: Br+HBr+H <--> Br2+H2O }

RXN1 = K1f*Br*HBr*H - K1r*Br2*H2O

K1f = 8e+009

K1r = 80

INIT Br = 1e-008

INIT Br2 = 1e-009

INIT H = 1.8

INIT HBr = 1e-008

d/dt(Br) = -RXN1-RXN2-RXN3+RXN16+RXN18+2*RXN20+RXN22

d/dt(Br2) = +RXN1-RXN16-RXN20

d/dt(H) = -RXN1-RXN2-2*RXN3+RXN5-RXN6+2*RXN16-RXN17+RXN18-2*RXN21

d/dt(HBr) = -RXN1+2*RXN2+RXN3+RXN5-RXN18

{ 2: Br+HBrO2+H <--> 2HBr }

RXN2 = K2f*Br*HBrO2*H - K2r*HBr^2

K2f = 2.5e+006

K2r = 0

INIT HBrO2 = 1e-008

d/dt(HBrO2) = -RXN2+RXN3-2*RXN5-RXN6+RXN8+RXN9+RXN17

{ 3: Br+BrO3+2H <--> HBr+HBrO2 }

RXN3 = K3f*Br*BrO3*H^2 - K3r*HBr*HBrO2

K3f = 1.2

K3r = 3.2

INIT BrO3 = 0.05

d/dt(BrO3) = -RXN3+RXN5-RXN6-RXN17

{ 4: 2HBrO2 <--> HBr+BrO3+H }

RXN5 = K5f*HBrO2^2 - K5r*HBr*BrO3*H

K5f = 3400

K5r = 0

{ 5: HBrO2+BrO3+H <--> 2BrO2+H2O }

RXN6 = K6f*HBrO2*BrO3*H - K6r*BrO2^2*H2O

K6f = 48

K6r = 6.4e7

INIT BrO2 = 1e-008

d/dt(BrO2) = +2*RXN6-RXN8-RXN9

{ 6: $\text{H}_2\text{Q} + \text{BrO}_2 \leftrightarrow \text{HQ} + \text{HBrO}_2$ }

$\text{RXN}_8 = \text{K}_{8f} \cdot \text{H}_2\text{Q} \cdot \text{BrO}_2 - \text{K}_{8r} \cdot \text{HQ} \cdot \text{HBrO}_2$
 $\text{K}_{8f} = 800000$
 $\text{K}_{8r} = 0$
 $\text{INIT H}_2\text{Q} = 0.0000000001$
 $\text{INIT HQ} = 1\text{e-}008$

$d/dt(\text{H}_2\text{Q}) = -\text{RXN}_8 + \text{RXN}_{10} - \text{RXN}_{16} - \text{RXN}_{17} - \text{RXN}_{18} + \text{RXN}_{21}$
 $d/dt(\text{HQ}) = +\text{RXN}_8 - \text{RXN}_9 - 2 \cdot \text{RXN}_{10}$

{ 7: $\text{HQ} + \text{BrO}_2 \leftrightarrow \text{Q} + \text{HBrO}_2$ }

$\text{RXN}_9 = \text{K}_{9f} \cdot \text{HQ} \cdot \text{BrO}_2 - \text{K}_{9r} \cdot \text{Q} \cdot \text{HBrO}_2$
 $\text{K}_{9f} = 8\text{e}+009$
 $\text{K}_{9r} = 0$
 $\text{INIT Q} = 0.02$

$d/dt(\text{Q}) = +\text{RXN}_9 + \text{RXN}_{10} + \text{RXN}_{17} + \text{RXN}_{18} - \text{RXN}_{21} + \text{RXN}_{22}$

{ 8: $2\text{HQ} \leftrightarrow \text{H}_2\text{Q} + \text{Q}$ }

$\text{RXN}_{10} = \text{K}_{10f} \cdot \text{HQ}^2 - \text{K}_{10r} \cdot \text{H}_2\text{Q} \cdot \text{Q}$
 $\text{K}_{10f} = 8.8\text{e}+008$
 $\text{K}_{10r} = 0$

{ 9: $\text{H}_2\text{Q} + \text{Br}_2 \leftrightarrow \text{QBr} + \text{Br} + 2\text{H}$ }

$\text{RXN}_{16} = \text{K}_{16f} \cdot \text{H}_2\text{Q} \cdot \text{Br}_2 - \text{K}_{16r} \cdot \text{QBr} \cdot \text{Br} \cdot \text{H}^2$
 $\text{K}_{16f} = 30000$
 $\text{K}_{16r} = 0$
 $\text{INIT QBr} = 1\text{e-}008$

$d/dt(\text{QBr}) = +\text{RXN}_{16} - \text{RXN}_{22}$

{ 10: $\text{H}_2\text{Q} + \text{BrO}_3 + \text{H} \leftrightarrow \text{Q} + \text{HBrO}_2 + \text{H}_2\text{O}$ }

$\text{RXN}_{17} = \text{K}_{17f} \cdot \text{H}_2\text{Q} \cdot \text{BrO}_3 \cdot \text{H} - \text{K}_{17r} \cdot \text{Q} \cdot \text{HBrO}_2 \cdot \text{H}_2\text{O}$
 $\text{K}_{17f} = 0.02$
 $\text{K}_{17r} = 0$

{ 11: $\text{H}_2\text{Q} + \text{HOBr} \leftrightarrow \text{Q} + \text{Br} + \text{H} + \text{H}_2\text{O}$ }

$\text{RXN}_{18} = \text{K}_{18f} \cdot \text{H}_2\text{Q} \cdot \text{HOBr} - \text{K}_{18r} \cdot \text{Q} \cdot \text{Br} \cdot \text{H} \cdot \text{H}_2\text{O}$
 $\text{K}_{18f} = 600000$
 $\text{K}_{18r} = 0$

{ 12: $\text{Br}_2 \leftrightarrow 2\text{Br}$ }

$\text{RXN}_{20} = \text{K}_{20f} \cdot \text{Br}_2 - \text{K}_{20r} \cdot \text{Br}^2$
 $\text{K}_{20f} = 0$
 $\text{K}_{20r} = 0$

{ 12: $\text{Q} + 2\text{H} \leftrightarrow \text{H}_2\text{Q}$ }

$\text{RXN}_{21} = \text{K}_{21f} \cdot \text{Q} \cdot \text{H}^2 - \text{K}_{21r} \cdot \text{H}_2\text{Q}$
 $\text{K}_{21f} = 2.2\text{e-}4$
 $\text{K}_{21r} = 0$

{ 13: $\text{QBr} \leftrightarrow \text{Q} + \text{Br}$ }

$\text{RXN}_{22} = \text{K}_{22f} \cdot \text{QBr} - \text{K}_{22r} \cdot \text{Q} \cdot \text{Br}$
 $\text{K}_{22f} = 3.5\text{e-}6$
 $\text{K}_{22r} = 0$

Reference:

- (1)Fechner, A. T. *Schweigg. J.* **1828**, 53, 61.
- (2)Ostwald, W. *Phys. Zeitsch.* **1899**, 8, 87.
- (3)Bray. W. C. *J. Am, Chem. Soc.* **1921**, 43, 1262.
- (4)Scott, S. K. *Oscillations, Waves, and Chaos in Chemical Kinetics*; Oxford University Press: Oxford, UK, **1994**.
- (5)Epstein, I.R.; Pojman, J.A. *An introduction to Nonlinear Chemical Dynamics*; Oxford University Press: Oxford, UK, **1998**.
- (6)Field, R. J.; Körös, E.; Noyes, R. M. *J. Am. Chem. Soc.* **1972**, 94, 8649.
- (7)Scott, S. K. *Chemical Chaos*; Oxford University Press: Oxford, UK, **1991**.
- (8)Noszticzius, Z; Gaspar, V; Foersterling, H. D. *J. Am. Chem. Soc.* **1985**, 107, 2314.
- (9)Rouff, P. J. *Phys. Chem.* **1984**, 88, 2851.
- (10)Forsterling, H. D. ; Mursinyi, S.; Noszticziusf, Z. *J. Phys. Chem.* **1990**, 94, 2915.
- (11)Farage, V. J.; Janjic, D. *Chem. Phys. Lett.* **1982**, 88, 301.
- (12)Farage, V. J.; Janjic, D. *Chem. Phys. Lett.*, **1982**, 93, 621.
- (13)Huh, D. S.; Choe, S. J.; Kim, M. S. *React. Kinet. Catal. Lett.* **2001**, 74, 11.
- (14)Kurin-Csörgei K.; Szalai ,I.; Körös, E. *React. Kinet. Catal. Lett.* **1995**, 54, 217.
- (15)Kurin-Csörgei, K.; Zhabotinsky, A. M.; Orban, M.; Epstein, I. R. *J. Phys. Chem.* **1996**, 100, 5393.
- (16)Szalai, I.; Körös, E. *J. Phys. Chem. A* **1998**, 102, 6892.
- (17)Szalai, I.; Körös, E.; Gyorgyi, L. *J. Phys. Chem. A* **1999**, 103, 243.

- (18)Kurin-Csorgei, K. ; Szalai, I; Molnar-Perl, I.; Koros, E. *React. Kinet. Catal. Lett.* **1994**, *53*, 115.
- (19)Szalai, I.; Kurin-Csoergei, K.; Epstein, I. R.; Orban, M. *J. Phys. Chem. A* **2003**, *107*, 10074.
- (20) Hamik, C. T.; Manz, N. and Steinbock O.; *J. Phys. Chem.* **2001**, *105*, 6144.
- (21)Bar-Eli, K and Haddad, S. *J. Phys. Chem.* **1979**, *83*, 2952.
- (22)Wang, J.; Hynne, F.; Sorensen, P. G.; Nielsen, K. *J. Phys. Chem.* **1996**, *100*, 17593.
- (23)Steinbock, O.; Hamik, C. Y.; Steinbock, B. *J. Phys. Chem. A* **2000**, *104*, 6411.
- (24)Naggy, G; Körös, E; Oftedal, N; Tjelflaat, K.; Ruoff, P. *Chem. Phys. Lett.* **1996**, *250*, 255.
- (25)Masia, M.; Marchettini, N.; Zambrano, V.; Rustici, M. *Chem. Phys. Lett.* **2001**, *341*, 285.
- (26)Kuhnet, L.; Agladze, K.; Krinsky, V. *Nature* **1990**, *337*, 224.
- (27)Hanazaki, I. *J. Phys. Chem.* **1992**, *96*, 5652.
- (28)Mori, Y.; Nakamichi, Y.; Sekiguchi, T.; Okazaki, N.; Matsumura, T.; Hanazaki, I. *Chem. Phys. Lett.* **1993**, *221*, 421.
- (29)Hanazaki, I.; Mori, Y.; Sekiguchi, T.; Rabai, G. *Physica D* **1995**, *84*, 228.
- (30)Kaminaga, A.; Hanazaki, I. *J. Phys. Chem. A* **1998**, *102*, 3307.
- (31)Sekiguchi, T.; Mori, Y.; Okazaki, N.; Hanazaki, I. *Chem. Phys. Lett.* **1993**, *211*, 1309.
- (32)Sorensen, P.G.; Lorenzen, T.; Hynne, F. *J. Phys. Chem.* **1996**, *100*, 19192.
- (33)Trendl, L; Knudsen, D.; Nakamura, T.; Inoue, T. M.; Jorgensen, K. B; Rouff, P. J. *Phys. Chem. A* **2000**, *104*, 10783.

- (34)Huh, D. S.; Kim, H. S.; Wang, J. C.; *Chem. Phys. Lett.* **2003**, *378*, 78.
- (35)Huh, D. S.; Kim, Y. J.; Kim, H. S.; Kang, J. K. and Wang, J., *Phys. Chem. Chem. Phys.* **2003**, *5*, 3188.
- (36)Wang, J.; Yadav, K.; Zhao, B.; Gao, Q. and Huh, D. *J. Chem. Phys.* **2004**, *121*, 10138.
- (37)Zhao, B.; Wang, J. *J. Phys. Chem. A* **2005**, *109*, 3647.
- (38)Steinbock, O.; Zykov, V.; Müller, S. C.; *Nature* **1993**, *336*, 322.
- (39)Epstein, I. R.; Showalter, K.; *J. Phys. Chem.* **1996**, *100*, 13132.
- (40)Epstein, I. R.; Sagués, F.; *Dalton Trans.* **2003**, 1201
- (41)Horvath, A. K.; Nagypal, I.; Epstein, I. R. *J. Am. Chem. Soc (Communication)*. **2002**, *124*, 10956
- (42)Kurin-Csörgei, K.; Epstein, I.R.; Orbán, M. *Nature*, **2005**, *413*, 139.
- (43)Kapral, K. and Showalter, K. *Chemical Waves and Patterns*, Kluwer Academic Publishers, Netherland, **1995**.
- (44) Luo, Y.; Epstein, I. R. *J. Chem. Phys.* **1986**, *85*, 5733.
- (45)Menzinger, M.; Jankowski, P. *J. Phys. Chem.* **1986**, *90*, 1217.
- (46)Ali, F.; Menzinger, M. *J. Phys. Chem.* **1991**, *95*, 6408.
- (47)Menzinger, M.; Jankowski, P. *J. Phys. Chem.* **1986**, *90*, 6865.
- (48)Vanag, V. K.; Melikhov, D. P. *J. Phys. Chem.* **1995**, *99*, 17372.
- (49)Lopez-Tomas, L.; Sagues, F. *J. Phys. Chem.* **1991**, *95*, 701.
- (50)Dutt, A. K.; Muller, S. C. *J. Phys. Chem.* **1993**, *97*, 10059.

- (51) Ruoff, P. *Chem. Phys. Lett.* **1982**, *90*, 76.
- (52) Roux, J. C.; DeKepper, P.; Boissonate, J. *Phys. Lett. A* **1983**, *97*, 168.
- (53) Menzinger, M.; Boukalouch, M.; DeKepper, P.; Boissonade, J.; Rous, J. C.; Saadaoui, H. *J. Phys. Chem.* **1986**, *90*, 313.
- (54) Menzinger, M.; Giraudi, A. *J. Phys. Chem.* **1987**, *91*, 4391.
- (55) Dutt, A. K.; Menzinger, M. *J. Phys. Chem.* **1990**, *94*, 4867.
- (56) Nagypal, I.; Epstein, I. R. *J. Phys. Chem.* **1986**, *90*, 6285.
- (57) Hlavacova, J.; Sevcik, P. *J. Phys. Chem.* **1994**, *98*, 6304.
- (58) Hlavacova, J.; Sevcik, P. *Chem. Phys. Lett.* **1993**, *201*, 242.
- (59) Li, R.-S.; Li, J. *Chem. Phys. Lett.* **1988**, *144*, 96.
- (60) Vanag, V. K.; Alfimov, M. V. *J. Phys. Chem.* **1993**, *97*, 1884.
- (61) Ali, F.; Menzinger, M. *J. Phys. Chem. A* **1997**, *101*, 2304.
- (62) Vanag, V. K. *J. Phys. Chem. A* **1997**, *101*, 8964.
- (63) Ruoff, P. *J. Phys. Chem.* **1992**, *96*, 9104.
- (64) Menzinger, Michael; Jankowski, Peter. *J. Phys. Chem.* **1990**, *94*, 4123.
- (65) Patonay, G.; Noszticzius, Z. *React. Kinet. Catal. Lett.* **1981**, *17*, 187.
- (66) Sevcik, P.; Adamcikova, L. *Chem. Phys. Lett.* **1988**, *146*, 419.
- (67) Sevcik, P.; Adamcikova, L. *Chem. Phys. Lett.* **1989**, *91*, 1012.
- (68) Pojman, J. A.; Dedeaux, H.; Fortenbery, D. *J. Phys. Chem.* **1992**, *96*, 7331.
- (69) Noszticzius, Z.; Bodnar, Z.; Garamszegi, L.; Wittmann, M. *J. Phys. Chem.* **1991**, *9*, 6575.

- (70) Ruoff, P. *J. Phys. Chem.* **1993**, *97*, 6405.
- (71) Ruoff, P.; Noyes, R. M. *J. Phys. Chem.* **1986**, *90*, 4700.
- (72) Resch, P.; Munster, A. F.; Schneider, F. W. *J. Phys. Chem.* **1991**, *95*, 6270.
- (73) Wang, J.; Sorensen, P. G.; Hynne, F. *J. Phys. Chem.* **1994**, *98*, 725.
- (74) John, B. R.; Scott, S. K.; Thompson, B. W. *Chaos* **1997**, *7*, 350.
- (75) Wang, J. *J. Phys. Chem. A* **2003**, *107*, 8774.
- (76) Görner, H. *J. Phys. Chem. A* **2003**, *107*, 11587.
- (77) Kruse, O.; Rupprecht, J.; Mussnug, J. H.; Dismukes, G. C. and Hankamer, B.; *Photochem. Photobiol. Sci.*, **2005**, *4*, 957.
- (78) Ka'da'r, S.; Amemiya, T. and Showalter K.; *J. Phys. Chem. A* **1997**, *101*, 8200.
- (79) Kurin-Csörgei, K.; Zhabotinsky, A. M.; Orbán, M. and Epstein, I.R.; *J. Phys. Chem. A* **1997**, *101*, 6827.
- (80) Ramesham, R.; Rose, M. F. *J. Mater. Sci. Lett.* **1997**, *16*, 799.
- (81) Roginsky, V. A.; Pisarenko, L. M.; Bors, W.; Michel, C. *J. Chem. Soc., Perkin Trans.* **1999**, *2*, 871.
- (82) Rodrigues, G. C.; Jansen, M. A. K.; Noort, M. E. v. d.; van Rensen, J. J. S. *Plant Science.* **2006**, *170*, 283.
- (83) Cramer, W A; Zhang, H; Yan, J; Kurisu, G; *Biochem. Soc. Tran.* **2005**, *33*, 921.

Vita Auctoris

Name: Bei Zhao

Place of Birth: Qingdao, Shandong, China

Year of Birth: 1980

Education: Ocean University of China, Qingdao, China
1999-2003 B.S.
University of Windsor, Canada
2003-2006 M.Sc

Publication and Presentations

(2003-2006)

Publications:

1. Jichang Wang*, Krishan Yadav, **Bei Zhao**, QingYu Gao, Do Sung Huh. "Photo-Controlled Oscillatory Dynamics in the Bromate-1,4- Cyclohexanedione Reaction" *J. Chem. Phys.* **2004**, *121*, 10138
2. **Bei Zhao**, Jichang Wang*. "Stirring-Controlled Bifurcations in the 1,4-Cyclohexanedione- Bromate Reaction" *J. Phys. Chem. A.* **2005**, *109(16)*, 3647
3. **Bei Zhao** and Jichang Wang*. "A Clock Reaction with the Photo Reproduction of 1,4-Hydroquinone" *J. Am. Chem. Soc.* **2006** (Submitted)
4. **Bei Zhao** and Jichang Wang*." Mechanistic study of the Photo- mediated 1,4-Benzoquinone-Bromate Reaction" *J. Phys. Chem. A.* A manuscript in preparation

Presentations:

1. Bei Zhao, Jichang Wang. Poster presentation: "Stirring Sensitivity in the 1,4-Cyclohexanedione-Bromate Reaction". *87th Canadian Chemistry Conference and Exhibition*, May 29th-June 1st, **2004**, London, Ontario, Canada
2. Jichang Wang*, Bei Zhao. Presentation: "Chemical Oscillations in the bromate-benzoquinone reaction." *Pacificchem* December, **2005**, Honolulu, Hawaii, USA